

Geophysical Logging for Hydrogeology

John H. Williams and Frederick L. Paillet



THE
GROUNDWATER
PROJECT

Geophysical Logging for Hydrogeology

The Groundwater Project

i

The Groundwater Project relies on private funding for book production and management of the Project.

Please consider [making a donation to the Groundwater Project](#) ↗ so books will continue to be freely available.

Thank you.

John H. Williams

*Groundwater Specialist
United States Geological Survey
Northbridge, Massachusetts, USA*

Frederick L. Paillet

*Emeritus Scientist
United States Geological Survey
Fayetteville, Arkansas, USA*

*Adjunct Professor
Department of Geosciences, University of Arkansas
Fayetteville, Arkansas, USA*

*Geophysical Logging for
Hydrogeology*

*The Groundwater Project
Guelph, Ontario, Canada
Version 3, January, 2024*

This GW-Project original publication is not protected by copyright. Any part of this book may be reproduced in any form or by any means without permission in writing from the authors. However, commercial distribution and reproduction are strictly prohibited.

Note that most GW-Project books are copyrighted, and that is not permissible to make GW-Project documents available on other websites nor to send copies of the documents directly to others. Kindly honor this source of free knowledge that benefits you and all those who want to learn about groundwater.

Any use of trade, firm, or product names is for descriptive purposes only and does not imply endorsement by the U.S. Government.

Published by the Groundwater Project, Guelph, Ontario, Canada, 2023.

Geophysical Logging for Hydrogeology / John H. Williams and Frederick L. Paillet - Guelph, Ontario, Canada, 2023.

79 pp.

ISBN: 978-1-77470-082-2

DOI: <https://doi.org/10.21083/UQGA6966>.

Please consider signing up to the GW-Project mailing list to stay informed about new book releases, events, and ways to participate in the GW-Project. When you sign up to our email list, it helps us build a global groundwater community. [Sign up](#).

APA Style 7th Edition Citation:

Williams, J. H., & Paillet, F. L. (2023). *Geophysical Logging for Hydrogeology*. The Groundwater Project. <https://doi.org/10.21083/UQGA6966>.



Domain Editor: Kamini Singha

Board: John Cherry, Shafick Adams, Richard Jackson, Ineke Kalwij, Renée Martin-Nagle, Everton de Oliveira, Marco Petitta, and Eileen Poeter.

Cover Image: Image by John Williams in 2022. Left to right, stratigraphic picks from a gamma log; clay-bound, capillary-bound, and mobile water content estimated from a nuclear magnetic resonance log; and fractured zone imaged by an acoustic-televviewer log.

Dedication

To the memory of W. Scott Keys (1928-2008), who mentored an entire generation of hydrogeologists in their application of geophysical logging in groundwater studies. Scott was recognized as one of the leading experts in the field and author of many works including "Borehole Geophysics Applied to Ground-Water Investigations" (1990).

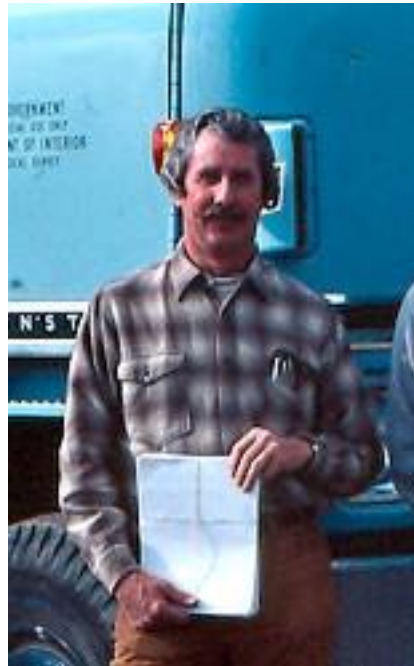


Table of Contents

DEDICATION	V
TABLE OF CONTENTS.....	VI
THE GROUNDWATER PROJECT FOREWORD	VIII
FOREWORD	IX
ACKNOWLEDGMENTS.....	X
1 INTRODUCTION	1
2 GEOPHYSICAL LOGGING METHODS AND EQUIPMENT	3
3 GEOPHYSICAL LOGS.....	5
3.1 DRILLING LOGS	7
3.2 DIRECT-PUSH LOGS	7
3.3 CONSTRUCTION LOGS	8
3.4 PETROPHYSICAL LOGS	9
3.4.1 <i>Gamma Logs</i>	9
3.4.2 <i>Acoustic Logs</i>	12
3.4.3 <i>Neutron logs</i>	13
3.4.4 <i>Electric Logs</i>	13
3.4.5 <i>Nuclear Magnetic Resonance (NMR) Logs</i>	16
3.5 IMAGE LOGS	17
3.6 FLUID-PROPERTY LOGS	19
3.7 FLOW LOGS	22
4 INTEGRATING GEOPHYSICAL LOGS AND OTHER BOREHOLE MEASUREMENTS.....	29
5 INTEGRATING GEOPHYSICAL LOGS AND SURFACE GEOPHYSICS	30
6 WRAP-UP	32
7 EXERCISES.....	33
EXERCISE 1	33
EXERCISE 2	34
EXERCISE 3	35
EXERCISE 4	36
EXERCISE 5	37
EXERCISE 6	39
EXERCISE 7	42
8 REFERENCES	43
9 BOXES.....	50
BOX 1 - CONE PENETRATION TESTING FOR GEOTECHNICAL INVESTIGATIONS	50
BOX 2 - NUCLEAR RANDOMNESS AND FILTERING OF GAMMA LOG DATA.....	51
BOX 3 - USE OF GAMMA LOGS FOR DEFINING LITHOLOGY AND STRATIGRAPHY	53
BOX 4 - USE OF GAMMA LOGS FOR MONITORING-WELL COMPLETION IN UNCONSOLIDATED AQUIFERS	55
BOX 5 - GEOPHYSICAL LOG ANALYSIS OF AN APPALACHIAN BASIN BOREHOLE.....	56
<i>Box 5.1 Data Collected at the Site</i>	56
<i>Box 5.2 Data Analysis</i>	58
<i>Box 5.3 The Huntley Mountain Formation Flow Zones</i>	59
<i>Box 5.4 The Catskill Formation Flow Zones</i>	60
<i>Box 5.5 Case Study: Formation Water Salinity in the Huntley Mountain and Catskill Formations</i>	60

BOX 6 - USE OF GAMMA, ELECTRIC, AND INDUCTION LOGS FOR DEFINING LITHOLOGY AND SALINITY..... 62

BOX 7 - USE OF FLOW LOGS FOR HYDRAULIC PROPERTY ANALYSIS 64

BOX 8 - RELATING GAMMA LOG AND CORE POROSITY 67

10 EXERCISE SOLUTIONS 68

SOLUTION EXERCISE 1 68

SOLUTION EXERCISE 2 68

SOLUTION EXERCISE 3 69

SOLUTION EXERCISE 4 70

SOLUTION EXERCISE 5 71

SOLUTION EXERCISE 6 74

SOLUTION EXERCISE 7 75

11 NOTATIONS 76

12 ABOUT THE AUTHORS 77

MODIFICATIONS TO ORIGINAL RELEASE A

The Groundwater Project Foreword

At the United Nations (UN) Water Summit held in December 2022, delegates agreed that statements from all major groundwater-related events will be unified in 2023 into one comprehensive groundwater message. This message was released at the UN 2023 Water Conference, a landmark event that brought attention at the highest international level to the importance of groundwater for the future of humanity and ecosystems. This message brought clarity to groundwater issues to advance understanding globally of the challenges faced and actions needed to resolve the world's groundwater problems. Groundwater education is key.

The 2023 World Water Day theme *Accelerating Change* is in sync with the goal of the Groundwater Project (GW-Project). The GW-Project is a registered Canadian charity founded in 2018 and committed to the advancement of groundwater education as a means to accelerate action related to our essential groundwater resources. To this end, we create and disseminate knowledge through a unique approach: the democratization of groundwater knowledge. We act on this principle through our website gw-project.org/, a global platform, based on the principle that

“Knowledge should be free, and the best knowledge should be free knowledge.” Anonymous

The mission of the GW-Project is to promote groundwater learning across the globe. This is accomplished by providing accessible, engaging, and high-quality educational materials—free-of-charge online and in many languages—to all who want to learn about groundwater. In short, the GW-Project provides essential knowledge and tools needed to develop groundwater sustainably for the future of humanity and ecosystems. This is a new type of global educational endeavor made possible through the contributions of a dedicated international group of volunteer professionals from diverse disciplines. Academics, consultants, and retirees contribute by writing and/or reviewing books aimed at diverse levels of readers from children to high school, undergraduate and graduate students, or professionals in the groundwater field. More than 1,000 dedicated volunteers from 127 countries and six continents are involved—and participation is growing.

Hundreds of books will be published online over the coming years, first in English, and then in other languages. An important tenet of GW-Project books is a strong emphasis on visualization with clear illustrations to stimulate spatial and critical thinking. In future, the publications will also include videos and other dynamic learning tools. Revised editions of the books are published from time to time. Users are invited to propose revisions.

We thank you for being part of the GW-Project Community. We hope to hear from you about your experience with the project materials, and welcome ideas and volunteers!

The GW-Project Board of Directors, January 2023

Foreword

Nearly all groundwater investigations in the field involve drilling boreholes for the purpose of determining subsurface conditions. The goal is to learn about geology and the water hosted by the geologic media. In the process of drilling the hole, information is obtained about the geologic materials; however, the value of this information is strongly dependent on the drilling method.

Typically, the bit at the bottom of the drill rod cuts the geologic materials into small chips that are brought to the surface by water or mud pumped into the hole at the bottom as the drilling proceeds. The geologic information gleaned from the chips is generally imprecise; further, nothing is learned about the water contained in the geologic media prior to drilling. A substantially more costly and more technically demanding form of drilling involves collection of continuous geologic cores. In some cases, water extracted from the core can be suitable for some analyses.

Geological and hydrological information obtained from samples collected while drilling can be greatly enhanced by collecting geophysical logs. Borehole geophysics involves lowering a measurement device down a borehole. The past 70 years have produced major advances in both the capabilities of the measurement devices and procedures for converting the measurements into useful information for understanding geology and groundwater conditions close to the borehole. The challenge to the hydrogeologist is not whether to do geophysical logging but in the selection of the particular geophysical logging tools suitable for the circumstances of each investigation. Most of the methods presented here are readily available in many countries from qualified contractors while others are still in the research and development mode. For little additional cost, relative to that of drilling boreholes, practicing hydrogeologists can be confident that including geophysical logging in their project will be beneficial in their groundwater investigations.

This book presents an overview of geophysical logging tools and explains the relevant hydrogeological information that can be gained from each tool. As scientists with the US Geological Survey, John Williams and Frederick Paillet have been immersed in geophysical logging across a wide spectrum of methods and site conditions. The authors' deep expertise is evident in this book, which provides hydrogeologists with up-to-date knowledge that will enhance their ability to choose and use the appropriate tools for generating geophysical logging data for their project. Given recent major technological and conceptual advances in geophysical logging, this is a timely addition to the GW-Project library that will benefit new and established practitioners in the field.

John Cherry, The Groundwater Project Leader

Guelph, Ontario, Canada, October 2023

Acknowledgments

We greatly appreciate the thorough reviews of this book by:

- ❖ Kamini Singha, Colorado School of Mines, Golden, Colorado, USA;
- ❖ Carole Johnson, US Geological Survey, Storrs, Connecticut, USA;
- ❖ Heather Crow, Geological of Survey, Ottawa, Ontario, Canada;
- ❖ Roger Morin, US Geological Survey (retired), Friendship, Maine, USA;
- ❖ Everton de Oliveira, Hidroplan and Instituto Água Sustentável (Sustainable Water Institute), Brazil;
- ❖ Matthys Dippenaar, Associate Professor, Engineering Geology and Hydrogeology, University of Pretoria, South Africa; and
- ❖ John Greenhouse, Tobermory, Ontario, Canada.

Special thanks to Carole Johnson for her contributions to the exercises. We are grateful for Amanda Sills and the Formatting Team of the Groundwater Project for their oversight, formatting, and copyediting of this book.

We thank Eileen Poeter (Colorado School of Mines, Golden, Colorado, USA) for reviewing, editing, and producing this book.

1 Introduction

Understanding subsurface parameters is critical for hydrogeologic studies as this knowledge informs exploration, remediation, and conformation to environmental regulations. Without understanding of subsurface conditions, this work would be difficult—if not impossible. Geophysical logging is one of the primary methods of collecting subsurface information for groundwater studies.

In this book, geophysical logging is defined as the measurement and analysis of electrical, acoustic, nuclear, and other physical properties in a borehole. Geophysical logs (a series of geophysical responses paired with their measurement depths) provide continuously generated high-resolution data that are repeatable and synergistic. These logs are useful to hydrogeologists because they can be interpreted to define the aquifer and confining unit framework and estimate or infer hydraulic properties and water quality.

Analysis of geophysical logs is most powerful when integrated with other subsurface information such as drill cores, drill cuttings, hydraulic tests, and groundwater samples. Logs can provide the ground truth needed for interpretation of surface-geophysical surveys, most directly for those that measure the same geophysical property.

Characterization of groundwater flow and contaminant movement is a primary objective for many aquifer studies. Effective use of modeling techniques to meet that objective depends on the ability to specify subsurface conditions including aquifer and confining unit distribution and properties. Geophysical logs provide one of the primary means of obtaining that subsurface information. In addition, the continuous and controlled-depth scale provided by logs creates a template on which to include discontinuous information such as that derived from water samples, segments of core, and straddle-packer hydraulic tests.

The depth-dependent data may be especially useful for constraining the inversion of surface geophysical data such as those given by seismic and resistivity surveys. Quality-control steps are needed to ensure depth errors are not incurred when collecting logs; procedures for resolving depth discrepancies between data sets are an important part of geophysical logging. These steps and procedures are described in detail in the sections that follow.

One of the most valuable attributes of geophysical logs is the complementary nature—the synergy—of the different types of physical measurements (e.g., nuclear, acoustic, electrical, optical) that can be obtained during a single logging session. Most geophysical interpretations involve multiple unknown parameters of interest such as clay content, water salinity, porosity, and permeability. In hydrogeology, log interpretations are commonly made graphically by overlaying log traces to identify where data sets vary in unison in response to one variable and where they diverge when another variable comes

into play. An important technique available for log analysis is the regression of geophysical log measurements against data from other logs, core, water samples, and hydraulic tests (Keys, 1990).

The different types of geophysical logs and equipment used in hydrogeologic investigations are reviewed herein. Analytical methods are illustrated using specific examples in both unconsolidated material and bedrock settings. Hands-on exercises and solutions are provided at the end of the book for readers to evaluate their learning.

2 Geophysical Logging Methods and Equipment

The most common geophysical logging method involves collecting logs with one or more sensors housed in a probe that is connected to a *wireline*—a cable used to raise and lower the probe and to transmit electrical signals and data (Figure 1a). The wireline geophysical logging system includes a winch and cable, logging computer, depth controls, and one or more probes. The logging system may be self-contained in a dedicated truck or, in the case of systems with shallower depth capability, they may be portable systems (Figure 2).

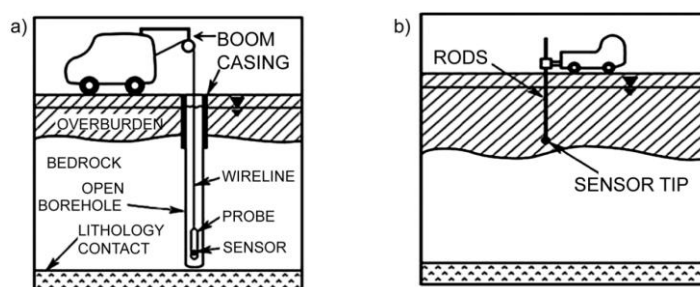


Figure 1 - Schematic of geophysical logging methods: a) conventional wireline logging of a drilled borehole and b) direct-push technology where sensors on the tip of rigid rods are pushed into the subsurface (Paillet & Ellefsen, 2005).

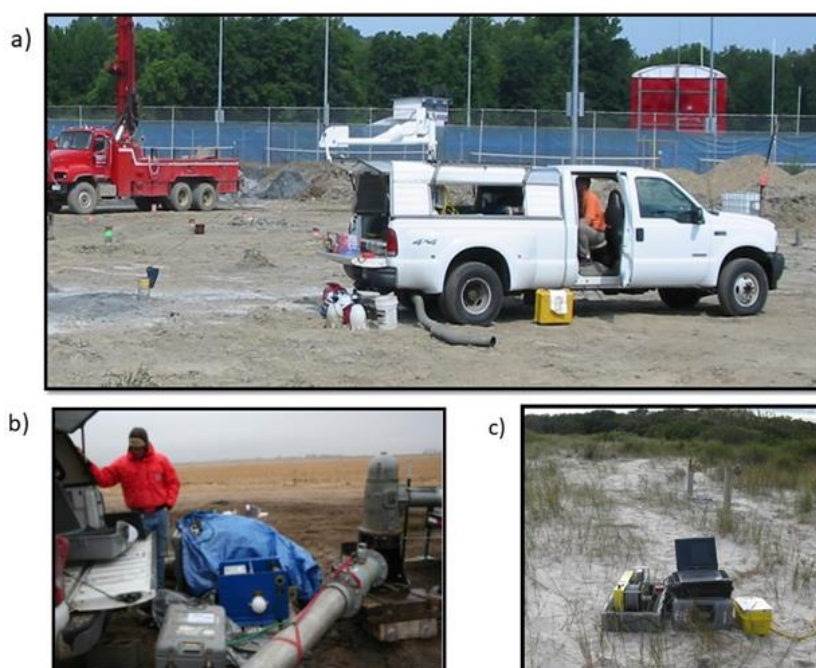


Figure 2 - Geophysical logging equipment: a) self-contained logging truck equipped with power supply, boom; winch, 1,200 m of wireline, uphole electronics, and a computer collecting geophysical logs in a geothermal wellfield; b) transportable logging system with winch, 300 m of wireline, uphole electronics, and a computer collecting flowmeter logs from a production test well; and c) portable logging system with winch, 200 m of wireline, uphole electronics and a computer collecting gamma and electromagnetic induction logs from a monitoring well (photographs by US Geological Survey).

Depth control is provided by a measuring wheel such that friction of the logging cable on the wheel generates pulses that can determine the rate of movement of the probe along the borehole. Slip rings on the winch allow power supply to the probe and communication of data streams to the logging computer via the wireline. The logging cable is run through a sheave or grooved wheel attached to the wellhead or suspended above it on a tripod or truck boom.

Measurement-while-drilling (MWD) methods record geophysical measurements as the borehole is drilled. MWD methods include drill parameter recorder (DPR) and direct-push technologies. In DPR technology, a computerized recorder installed on a drilling rig takes pressure, penetration rate, and other measurements related to the drilling process and conditions as the borehole is advanced, information that typically is only qualitatively captured by the driller's notes (Lindenbach, 2016). In direct-push technology, measurements are made with one or more sensors at the tip of a rod as it is pushed into the subsurface (Figure 1b).

Geophysical logging probes commonly contain—or can be coupled vertically (i.e., stacked) to include—more than one sensor to make multiple geophysical measurements at one time. Depending on measurement type and design, bowsprings or spring-loaded arms are used to centralize a probe with its sensors positioned near the center of the borehole or decentralize a probe with its sensors pressed against the borehole wall. Many geophysical probes measuring physical properties of the formation including electrical and nuclear properties are designed with sensors whose response is derived from an approximately spherical region surrounding the nominal depth position of the sensor.

The sphere is defined by the sampled volume that contributes about 90 percent of the total measured response. The diameter of the sample volume determines the vertical resolution of the log. For example, normal resistivity probes commonly are designed with electrodes spaced 41 and 163 cm (16 and 64 inches) apart; the longer electrode spacing samples a larger volume than the shorter electrode spacing. Hence, the long-normal log has lower vertical resolution than the short-normal log.

The sample volume of geophysical logging equipment is typically designed to provide an effective compromise between the need to minimize the effects of the borehole environment on the measurement and the need to maximize vertical resolution. That is, the volume of investigation needs to be large enough such that the borehole, casing, and annulus (if present) do not contribute in a disproportionate way to the bulk measurement and yet the investigated volume needs to be small enough to ensure effective resolution of thin beds. Standard geophysical logging probes are designed with sample volumes from two to four borehole diameters.

3 Geophysical Logs

Geophysical logs used in groundwater investigations may be grouped into the following major types: drilling, direct-push, construction, petrophysical, image, fluid property, and flow. The various types of logs, measured properties, borehole conditions, and the hydrogeologic information provided are summarized in Table 1.

Table 1 - Summary of geophysical logs used in groundwater investigations. VOCs are volatile organic compounds; DO is dissolved oxygen; m is meter

	Type of Log	Log Variation	Measured Property	Borehole Conditions	Hydrogeologic Information
	Drilling	Drill parameter recorder or manual	Rates, pressures, discharge	Measurements while drilling	Lithology, fractures, flow zone delineation
Direct Push	Cone penetrometer		Resistance, friction	Sediment (< 50 m depth)	Lithology, geotechnical properties
	Membrane interface		VOCs, hydrocarbons	Sediment (< 50 m depth)	Groundwater contamination
	Conductivity		Electrical conductivity	Sediment (< 50 m depth)	Lithology, salinity
	Permeameter	Hydraulic profiling tool	Pressure change from injected water	Sediment (< 50 m depth)	Hydraulic conductivity
Construction	Caliper	Single or multi-arm, acoustic	Hole diameter	Any conditions	Log corrections, cement volume, lithology, fractures
	Deviation	Magnetometer or gyroscope	Hole orientation and angle	No metallic casing for magnetometer	True spatial location, corrections to image logs
	Cement bond		Compressional wave velocity	Water- or mud-filled cemented casing	Cement seal integrity
	Casing collar locator				Correlate open-hole and cased logs
	Petrophysical				
Nuclear	Gamma	Gamma spectral	Gamma radiation from isotopes	Any conditions	Lithology and mineralogy
	Neutron	Thermal, epithermal, pulsed	Hydrogen content	Any conditions, optimum in uncased	Total porosity and lithology
	Gamma-gamma	Compensated (dual)		Any conditions, optimum in uncased	Density

	Type of Log	Log Variation	Measured Property	Borehole Conditions	Hydrogeologic Information
Elect- ric	Self potential		Electrical potentials	Water- or mud-filled open hole	Lithology and conductive pore fluids
	Single-point resistance	Differential	Electrical resistance	Water or mud-filled open hole	Lithology and fractures
	Normal resistivity	Focused or lateral	Electrical resistivity	Water or mud-filled open hole	Lithology and conductive pore fluids
Electromagnetic	Induction	Dual (medium and deep)	Electrical conductivity	Any condition except metallic casing	Lithology and conductive pore fluids
	Magnetic susceptibility		Magnetic susceptibility	Any condition except metallic casing	Magnetic minerals
	Nuclear magnetic resonance			Any condition except metallic casing	Total, free, and bound porosity; hydraulic conductivity
	Radar			Any condition except metallic casing	
	Acoustic	Acoustic waveform	Compressional wave velocity or slowness	Water- or mud-filled	Lithology and porosity, fractures
Image	Acoustic televiewer		Acoustic reflectivity of borehole wall	Water- or light mud-filled	Fractures, bedding, lithology
	Micro-electrical		Electrical resistivity of borehole wall	Water- or mud-filled	Fractures, bedding, lithology
	Optical televiewer		Optical image of borehole wall	Air or non-turbid water	Fractures, bedding, lithology
	Video		Fish-eye or sidewall view	Air or non-turbid water	Fractures, bedding, lithology, flow
Fluid Property	Fluid resistivity			Water- or mud-filled	Flow-zone location, log corrections
	Temperature			Any condition	Flow-zone location, log corrections
	Specific conductance		Temperature corrected fluid conductivity	Water-filled	Flow-zone location and water quality
	Specific ion and other	pH, DO, chloride, nitrate	Constituent concentration	Water-filled	Flow-zone location and water quality
	Nephelometer		Turbidity	Water-filled	Flow-zone location and water quality
	Flow			Water-filled	
	Spinner flowmeter		Vertical flow in borehole	Water-filled, centralized	Flow-zone hydraulics (higher velocities)
	Heat-pulse flowmeter		Vertical flow in borehole	Water-filled, centralized	Flow-zone hydraulics (lower velocities)
	Electromagnetic flowmeter		Vertical flow in borehole	Water-filled, centralized	Flow-zone hydraulics
	Tracer		Vertical flow in borehole	Water-filled	Flow-zone hydraulics

3.1 Drilling Logs

Drilling logs are logs collected during the drilling operation. Examples of drilling logs include drillers’ descriptions of drill cuttings and fluids, manual measurements of flow rate and specific conductance of surface discharge, and automated measurements through DPR technology. For example, Benoît and others (2004) used DPR technology to record penetration rate, torque, and pressures during the drilling of test boreholes to characterize bedrock fractures for application of in-situ bioremediation of organic contaminants.

3.2 Direct-Push Logs

Direct-push logs are logs collected during direct-push operations. A major advantage of direct-push logging over conventional wireline logging is that the direct-push sensor is surrounded by the formation so there is no influence of borehole fluid, annular space, or casing on the measurement. Commonly, direct-push log measurements are applied to classify soil-behavior types (SBTs) in geotechnical investigations and include tip resistance (pressure exerted on the cone as it is advanced), sleeve friction (friction on the sides of the rods), and pore pressure collected with a cone-penetration test (CPT) rig (Robertson, 1990). [Box 1](#) presents an example of the CPT method in SBT classification.

Christy and others (1994) introduced direct-push technology to measure formation electrical conductivity that has been applied to characterize subsurface lithology of sediments and delineate the freshwater-saltwater interface (Collins & Easley, 1999; Schulmeister et al., 2003). An example of logs collected using direct-push electrical conductivity and hydraulic profiling tools and their interpreted lithology and estimated hydraulic conductivity is shown in Figure 3.

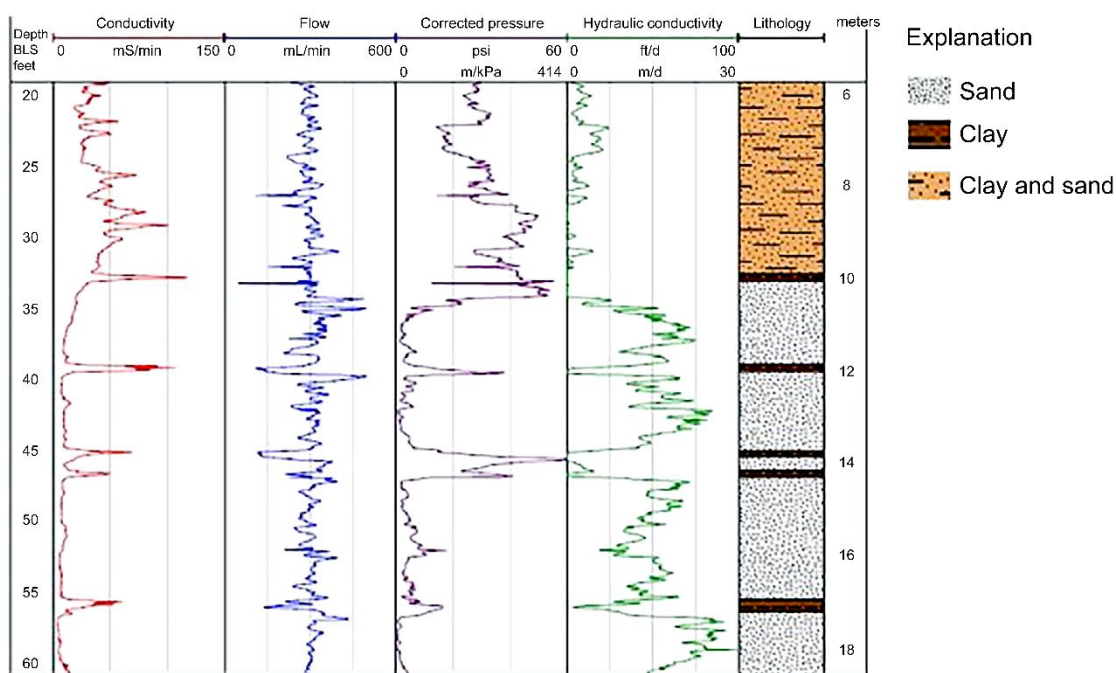


Figure 3 - Direct-push logs of electrical conductivity, flow, and corrected pressure, estimated hydraulic conductivity, and lithology in an alluvial aquifer (Modified from Adams, 2020; USGS, 2021a).

The direct-push method is widely used for shallow groundwater-contaminant investigations in unconsolidated sediments because it causes minimal surface and subsurface disruption compared to conventional drilling; and push rods can be equipped with membrane-interface probes that heat and mobilize organic contaminants for sampling (Christy, 1996). For example, McCall and others (2014) used a combined membrane-interface probe and hydraulic profiling tool to concurrently determine the distribution of VOCs and formation permeability in direct-push borings.

In [Exercise 1](#), CPT logs are analyzed to classify the SBTs of glaciolacustrine sediments penetrated by a boring.

3.3 Construction Logs

After a borehole is drilled, construction logs are collected using a conventional wireline logging system to characterize hole and well specifications. Caliper logs, which are measurements of borehole diameter with depth, are the most collected construction logs. The logs delineate enlargements of borehole diameter in open boreholes and are commonly used to determine borehole volume for well completion and for the interpretation of logs affected by changes in borehole diameter including nuclear, electrical, image, and flow logs, that are described in Sections 3.4 through 3.7.

Deviation logs measure borehole orientation, inclination angle, and provide true vertical depth. Boreholes will tend to deviate up dip (toward the perpendicular to the bedding) if the bedding is not steeply dipping (Brown et al., 1981). If the bedding is steeply dipping, borehole deviation tends to be downdip (parallel to the bedding). The path of a borehole determined from deviation-log analysis can be displayed in a three-dimensional cylinder (Figure 4). Deviation logs are needed to correct the orientation of bedrock fractures and bedding identified using oriented image logs.

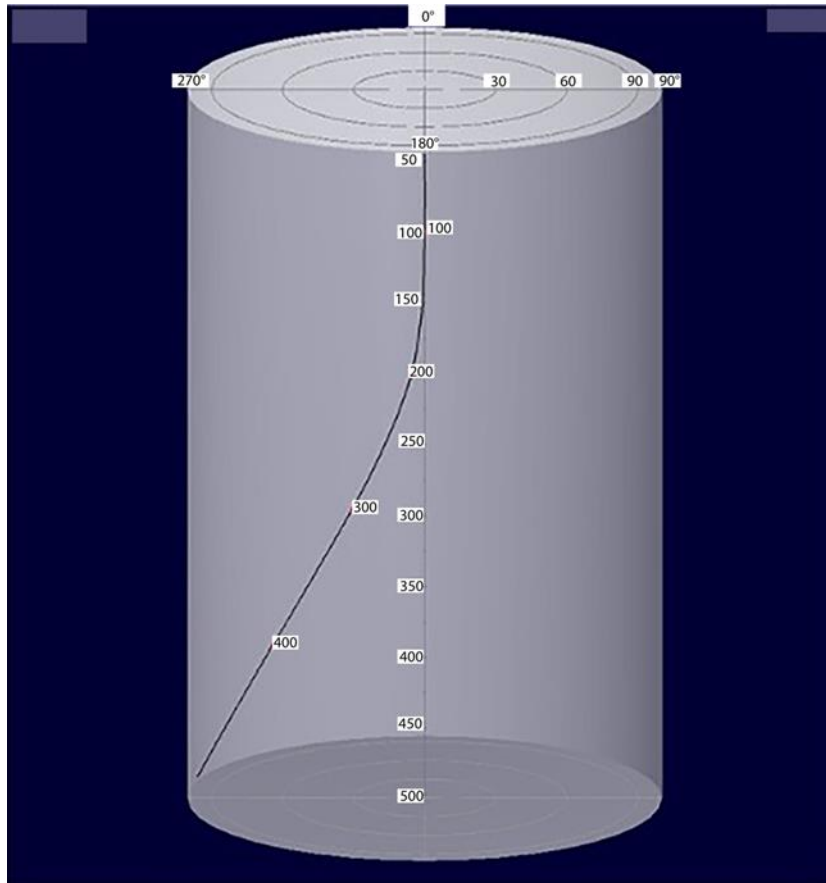


Figure 4 - Three-dimensional path determined from deviation log analysis of a borehole that penetrated gneiss with east dipping metamorphic fabric; the bottom of the borehole at total depth of ≈ 152 m (≈ 500 ft) below land surface deviated 20 degrees from vertical and was located \approx m (≈ 100 ft) to the west of the wellhead (Reynolds et al., 2015; USGS, 2021b).

Cement-bond logs are used to evaluate the degree of acoustic coupling of the cement between the casing and the formation. Casing collar locator logs, which are measured with a probe containing a coil-and-magnet arrangement, allow for correlation of cased and open-hole logs from the same borehole when combined with gamma logs.

3.4 Petrophysical Logs

Petrophysical logs measure the physical properties of geological formations and their interstitial fluids surrounding a borehole. Petrophysical logs that are widely used in groundwater investigations—gamma, electric, and induction conductivity—are discussed in this section. Acoustic- and neutron-porosity logging and state-of-the-art logging for hydraulic properties using nuclear magnetic resonance technology are also discussed.

3.4.1 Gamma Logs

Gamma logs are the most used petrophysical logs. Gamma logs can be collected over the full range of borehole conditions including open and cased holes (both steel or poly vinyl chloride-PVC) that are filled with air, water, or mud. The gamma log measures the total gamma emission produced by naturally occurring isotopes of potassium, thorium, and uranium. The gamma probe converts gamma rays emitted from the formation into

electronic pulses using a scintillator crystal. Scintillator crystals differ by size and age resulting in differences in sensitivities between probes. [Box 2](#) provides information on nuclear randomness and filtering of gamma log data.

Gamma emissions are recorded in counts per second (cps) that, in some cases, are expressed in standard API (American Petroleum Institute) units. An API unit is defined as 1/200th of the difference between the count rate recorded by a gamma probe in the middle of the radioactive bed and that recorded in the middle of the nonradioactive bed in a fabricated borehole maintained by API in Houston Texas.

Most multi-parameter probes include gamma detectors so that the gamma logs from separate runs can be used for depth correlation of all the logs. Gamma logs collected with different probes that are not recorded in standard API units may be normalized to a common response through comparison of the response in borehole intervals that were logged with the multiple probes as described by Johnson and others (2011).

In [Exercise 2](#), a gamma log from a monitoring well in the Long Island aquifer system, New York, USA, is plotted, filtered, and replotted.

The gamma activity in sedimentary formations is commonly assumed to be related to grain size: Gamma activity increases with clay content. In many sedimentary settings, lithologic and stratigraphic contacts are distinctly defined by a gamma log. [Box 3](#) presents an example of the use of gamma logs to delineate contacts in a classic sedimentary bedrock sequence.

However, exceptions to this generalization include glauconitic, phosphatic, and arkosic sands and sandstones, which display elevated gamma radiation due to their mineralogy. Additionally, sediments that contain sand to clay-sized grains that are dominated by a primary mineralogy—commonly quartz—with negligible clay alteration minerals display a reduced range of gamma response and overlap for the different grain sizes (Crow et al., 2017). A major application of gamma logs is stratigraphic correlation between boreholes in sedimentary rocks as shown in Figure 5 for a carbonate and shale bedrock sequence with key marker beds.

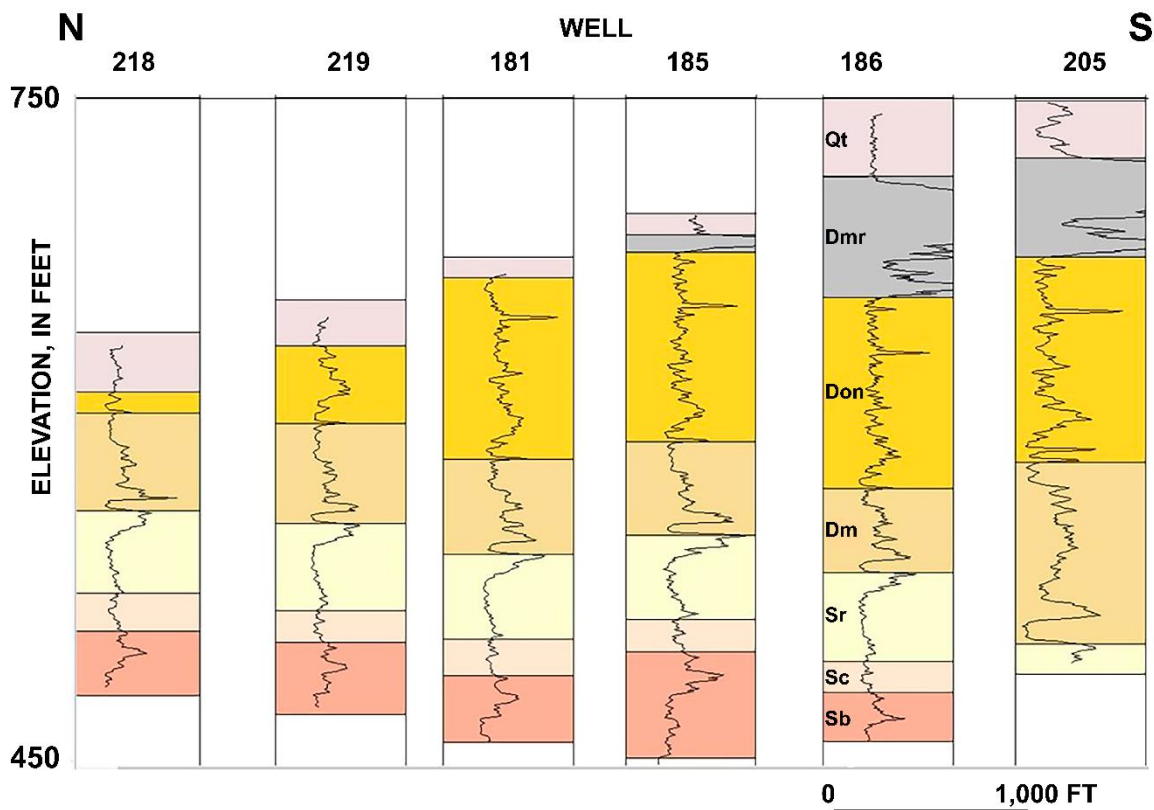


Figure 5 - Use of gamma logs for stratigraphic correlation between boreholes in Silurian and Devonian carbonate and shale bedrock. The stratigraphic units (shown on well 186) in ascending order are the Bertie Limestone (Sb), Cobleskill Limestone (Sc), Rondout Formation (Sr), Manlius Limestone (DM), Onondaga Limestone (Don), Marcellus Shale (Dmr), and Qt (till). Key marker beds include a phosphatic zone at the contact between Dmr and Don, the Tioga Ash Bed within the Don, and black organic-rich shales in the Dmr. The known depth of units and their characteristic geophysical log signature are used to identify the same units in other wells. The regional dip of bedding is about 5 degrees to the south. Repeated sections of the Dmr in well 205 indicates faulting (Eckhardt et al., 2011). The depth elevation ranges from 137 m to 228 m and 1,000 ft = 304.8 m.

In [Exercise 3](#), a gamma log is interpreted to delineate a major confining unit in the Long Island, New York, USA, aquifer system.

Generally, the gamma activity in crystalline rocks is a direct function of mineralogy and is not related to grain size. Mafic rocks such as basalt and diabase have characteristically low gamma emissions, while felsic rocks such as granite and pegmatite can have very high gamma emissions.

In unconsolidated sedimentary formations, where gamma activity can be assumed to be directly associated with radioisotopes in the clay minerals, the clay fraction (*CF*) can be regressed as the relative gamma value between minimum and maximum endpoints with *clean* (G_1) and *clay* (G_2) values for each gamma value (G) on the log as shown in Equation (1)

$$CF = (G - G_1)/(G_2 - G_1) \tag{1}$$

where:

CF = clay fraction

- G = gamma value
- G_1 = minimum gamma endpoint (clean)
- G_2 = maximum gamma endpoint (clay)

The clean and clay values are typically determined from intervals in the borehole where the end members are recognized but, in some cases, may be the best guess based on experience in the same or similar formation. For qualitative applications in many unconsolidated sedimentary aquifer systems, this relation can be used to estimate relative permeability of the sediments by assuming they are inversely related to the CF . [Box 4](#)↓ presents an example of the use of a gamma log to determine the placement of a monitoring well screen zone in an unconsolidated aquifer

In [Exercise 4](#)↓, gamma and driller logs are interpreted to delineate potential zones for screening a monitoring well in a glaciofluvial aquifer.

3.4.2 Acoustic Logs

Acoustic logs, also called sonic logs, measure the compressional-wave velocity of the rock surrounding an open, fluid-filled borehole. A piezoelectric transducer is used to generate acoustic waves in the fluid surrounding a centralized probe that, in turn, generate compressional and shear waves traveling along the borehole wall. These waves create a series of traveling seismic-waves that are detected at two or more receivers located at different distances along the borehole. Conventional acoustic probes record the first arrival of the signal (representing the compressional wave). Recorded arrival times at pairs of receivers are then differenced to remove *fluid delay* from the travel-time measurement.

Acoustic logs require that the tool be centralized in an uncased, fluid-filled borehole and are only effective in consolidated sedimentary or crystalline rocks at depths where confining pressure insures a consistent signal. Acoustic logs are typically analyzed to give the inverse of acoustic velocity, which is related to porosity as the volume-weighted average of the fluid and lithology travel times using the Wylie travel-time equation (White, 1983; Keys, 1990; Paillet & Cheng, 1991). This porosity estimate applies to intergranular porosity and can be compared to other estimates of total porosity to separate primary and secondary porosity in fractured or karst formations.

Full-wave form acoustic logs record the entire wave response (Paillet & Cheng, 1991) to determine shear wave travel-time and other parameters that can be related to rock properties. Specialized shear-wave probes (Chen, 1989) employ non-axisymmetric sources that excite mostly shear-wave energy propagating along the borehole wall. This can be used in shallow, poorly consolidated formations but is mostly of use in engineering and construction design applications. One other important application of acoustic logs in sedimentary aquifers is their use in providing a precise depth scale for surficial seismic soundings where the scale is given in two-way travel time rather than in vertical depth.

3.4.3 Neutron logs

Neutron logs, like gamma logs can be collected over the full range of borehole conditions. Traditionally, neutron logs have employed a radioactive source to generate neutron. Use of radioactive sources in freshwater aquifers has become less common in recent time because of safety concerns and associated regulations (US Nuclear Regulatory Commission (USNRC), 2013). This trend may change as a new generation of slim-hole neutron probes now exist that employ a neutron generator contained in the probe rather than a radioactive source.

Neutron porosity logs measure total porosity and do not distinguish between the effective porosity and the non-effective porosity attributed to clay-bound water. Effective porosity is of greater interest to hydrologists. This limitation needs to be accounted for when using porosity and resistivity logs to estimate formation water resistivity through the application of Archie's (1942) Equation. [Box 5](#)  presents the use of a neutron porosity log as input to Archie's Equation to estimate salinity levels in an Appalachian basin borehole in the USA. The relationship between the neutron response and clay content can also be used to identify lithology in formations where the gamma response and clay content are not related due to mineralogy.

3.4.4 Electric Logs

Electric logs measure the electrical properties of the formation and fluids surrounding the borehole. They include measurement of spontaneous potential, single-point resistance, and normal resistivity. Electric logs are collected in open boreholes filled with water or mud and used to identify lithology and salinity. Spontaneous-potential logs record voltages developed between the borehole fluid and the surrounding rock and fluids. Salinity differences between the borehole and formation fluids are necessary to use spontaneous potential logging for lithology and water quality evaluation.

Single-point resistance logs—which measure the electrical resistance between an electrode at the surface and an electrode on the probe downhole—are useful for delineating fractures in addition to lithology. However, they do not provide a quantitative measurement and are significantly affected by conductive borehole fluids. Normal-resistivity probes have electrodes at multiple spacings analogous to a scaled-down, surface-geophysical Schlumberger DC array. The most common electrode spacings are 41 and 163 cm (16 and 64 inches) but some probes have additional spacings of 20 and 81 cm (8 and 32 inches). Normal-resistivity measurements made with shorter electrode spacings are more affected by the borehole fluid than those made with longer spacings, but measurements with longer spacings can provide incorrect resistance values and thicknesses for thin beds.

Induction-conductivity logs measure the electrical conductivity of a donut-shaped volume of the formation and fluids surrounding the borehole. Induction-conductivity logs can be collected in open and PVC-cased boreholes that are filled with air, water, or mud.

Induction-conductivity probes use a transmitter coil that emits an electromagnetic signal to produce a primary field that, in turn, produces a secondary field that is sensed by the receiver coil. The strength of the secondary field is a function of the formation conductivity. Induction probes are designed to provide high-resolution vertical measurements of a formation that minimize the effect of borehole fluid.

Slim-hole induction probes commonly used in groundwater studies emit a 40 to 100 kHz electromagnetic signal, have a 50 cm (20 in) intercoil spacing, and are not significantly affected by the conductivity of the borehole fluid in boreholes < 20 cm (8 inches) in diameter. In their evaluation of a typical slim-hole induction probe, Taylor and others (1989) showed that an abrupt change in conductivity would be smoothed over a 1 m (3.3 ft) interval, such that the apparent conductivity of 0.5 m (1.6 ft) thick conductive bed would have a value relative to the surrounding formation that is only half of the true conductivity difference between the tin layer and the surrounding material.

Dual-induction probes typically have an additional intercoil spacing of 80 cm (31 in) to provide for both medium and deep conductivity measurements. Two depths of investigation are useful in evaluating the zone of invasion, which is the area surrounding a borehole where formation fluids are displaced by drilling fluid. Induction logs are useful for identifying lithology and conductive pore fluids (e.g., saltwater- or leachate-impacted groundwater) surrounding a borehole.

In many applications, collection of gamma logs and normal-resistivity or induction logs allows for distinguishing between lithologic and salinity effects on formation conductivity. Box 5 and [Box 6](#) present examples of such applications. As shown in Figure 6, in sandy aquifers with minimal clay content, induction conductivity correlates directly with formation water conductivity. Statistical relations have been developed between induction conductivity and specific conductance of water samples taken from discrete depths within conductive plumes in glaciofluvial aquifers. Statistical relations have also been developed between induction conductivity and specific conductance of water samples obtained by filter-pressing samples from, and by sampling at discrete depths within, coastal aquifers impacted by saltwater intrusion (Williams et al., 1993; Stumm & Como, 2017).

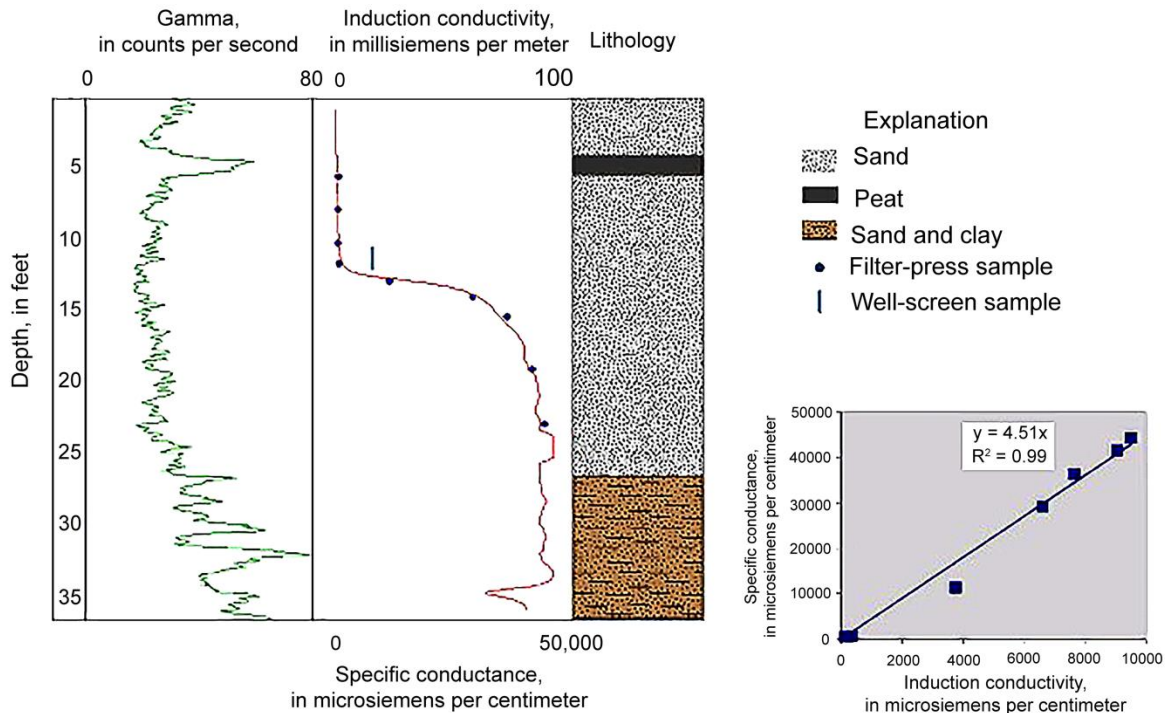


Figure 6 - Gamma, electromagnetic induction conductivity, and lithologic logs presented along with specific conductance of water obtained by filter-pressing samples and or extracted from discrete intervals within a 2-inch (5.1-cm) diameter monitoring well with polyvinyl chloride (PVC) casing and screen in a barrier-beach glaciofluvial aquifer. 35 feet is approximately 10.7 m. The regression line relating induction conductivity and specific conductance of filter-press samples is shown in the lower right (Modified from Schubert, 2010).

Although gamma logs are by far the most widely used logs for lithologic interpretation, normal resistivity and induction logs provide better information on sand and clay content in freshwater aquifers that do not display a straightforward relation between gamma and grain size. One important limitation of induction logs is the inability to measure contrasts in lithology or water conductivity in very resistive freshwater aquifers. In such aquifers, minor differences in calibration values applied between periodic measurements can be misidentified as changes in water quality. Normal resistivity logs may provide the most useful measurements in these environments.

In [Exercise 5](#), lithology is independently defined based on a gamma log and an induction log and the two interpretations are compared.

A variation of induction logs is the magnetic susceptibility log that measures the ratio between the primary magnetic field and the in-phase component of the magnetic field caused by the presence of magnetic minerals. Although traditionally used for mineral exploration, magnetic susceptibility logs can be useful for lithologic identification in groundwater studies in certain settings. For example, Crow and others (2017) observed that in sediments derived from the Canadian Shield (mainly granitic bedrock), the log response inversely mirrored induction conductivity as well as the gamma logs. This occurred because the coarse-grained fraction contained a higher percentage of heavier magnetic minerals than the fine-grained fraction. They also observed that magnetic susceptibility generally remained low regardless of grain size for sediments derived from carbonate and shale bedrock.

3.4.5 Nuclear Magnetic Resonance (NMR) Logs

Unlike other petrophysical logs that respond to the rock matrix, nuclear magnetic resonance (NMR) logs respond to the rate of decay of field-induced precession of the hydrogen protons in the formation fluid (water, gas, or oil), thus providing direct measurements of porosity. The relaxation time, or T_2 , is the time it takes for the hydrogen atoms to decay their coherent precession signal after being exposed to a radiofrequency pulse.

In groundwater investigations, NMR logs are used to determine water content (equivalent to porosity in the saturated zone) and pore size distribution (bound versus mobile water), and to estimate hydraulic conductivity (Figure 7). The distribution of water content, pore size distribution, and hydraulic conductivity with depth is important for hydrogeologic evaluations.

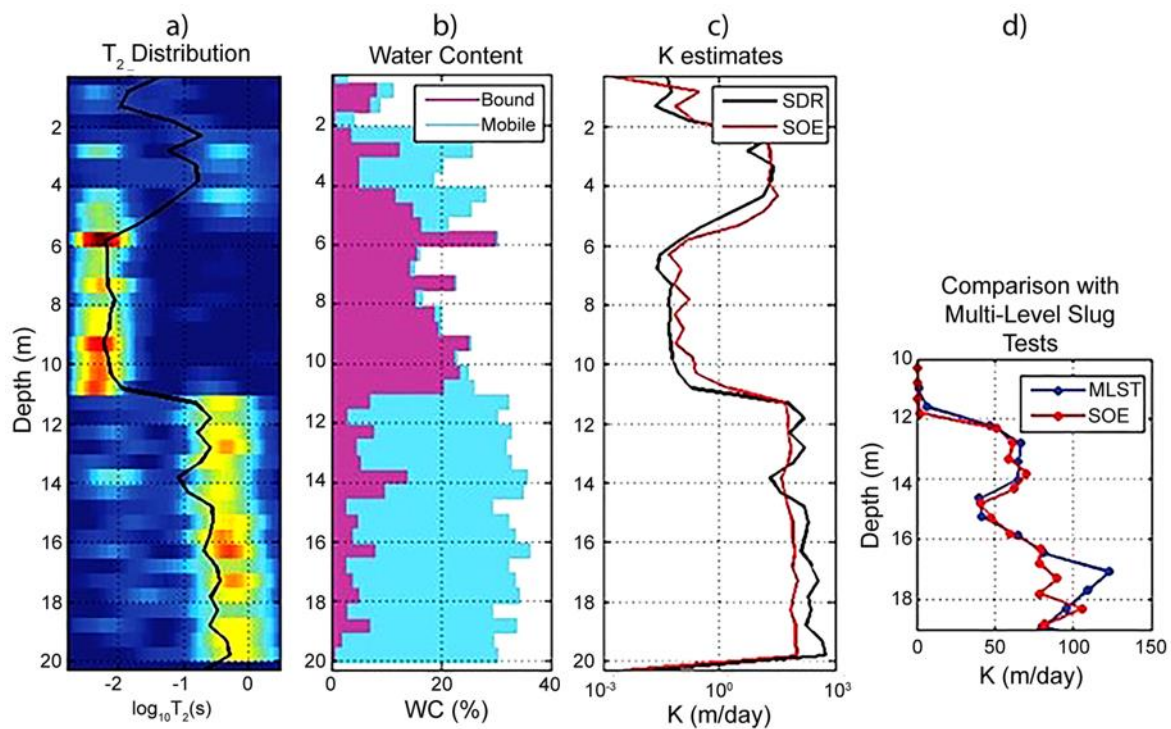


Figure 7 - Nuclear magnetic resonance (NMR) log collected from a 4-inch diameter PVC-cased and screened well in an alluvial aquifer: a) T_2 distribution, b) mobile and bound water content determined from the T_2 distribution, c) hydraulic conductivity (K) estimated from the NMR log using the Schlumberger-Doll Research (SDR) and sum-of-squared echoes (SOE) equations, and d) comparison of hydraulic conductivity values estimated from the NMR log using the SOE equation with site-specific regression-derived constants and values estimated from multi-level slug tests (Walsh et al., 2013).

Like most other logging technologies, NMR probes were first developed and widely used by the petroleum industry; they were later modified into slim-hole tools for groundwater investigations (Walsh et al., 2013). NMR probes collect measurements from a thin cylinder-shaped zone or shell surrounding the probe. The diameter of the measurement zone varies from 15 to 50 cm (6 to 20 in) depending on the design of the probe.

Proper probe selection is critical to ensure that the measurement zone is within the zone undisturbed by drilling (Spurlin et al., 2019). As NMR probes use strong magnets, the tools can be difficult to lower through metal-cased borehole intervals. Magnetic minerals (primarily magnetite) in sediments or bedrock can interfere with NMR measurements and, where present, need to be considered in probe selection, logging operation, and analysis.

The physical principle of NMR logging is the same principle underlying magnetic resonance imaging technology used in medicine. The NMR logging probe measures the response of the hydrogen spins in pore fluids to a generated magnetic field perturbation. The spin-echo decay time—referred to as the T_2 curve—is related to total water content (porosity in saturated conditions). Water bound in smaller pores exhibits shorter T_2 ; mobile water in larger pores exhibits longer T_2 .

Hydraulic conductivity can be estimated from NMR-derived porosity, T_2 decay parameters, and/or pore size distribution using equations based on the Kozeny-Carman relation (Carman, 1956). For example, Dunn and others (2002) describe the petrophysical and logging applications of NMR including its use in the estimation of formation permeability. Dlubac and others (2013) upscaled the NMR-derived hydraulic-conductivity estimates from a test well in the High Plains aquifer. The estimates were based on the Schlumberger-Doll Research (SDR) and Timur-Coates equations of the petroleum industry—which use empirical constants determined for consolidated rocks—to match those estimates with the site aquifer-test and flowmeter-log analyses.

Walsh and others (2013) derived hydraulic-conductivity estimates using the sum-of-squared echoes equation with a site-specific constant determined by regression with slug-test results for a shallow alluvial aquifer in Kansas, USA (Figure 7). Knight and others (2015) and Maurer and Knight (2016) determined optimum empirical constants for the SDR equation to estimate permeability for unconsolidated alluvial aquifers at research sites in Kansas and Washington, USA, using direct-push technology to perform hydraulic tests with a permeameter and an NMR probe in PVC-cased direct-push holes.

3.5 Image Logs

Image logs include oriented 360-degree images of the borehole wall, which are provided by acoustic (Zemanek et al., 1970) and optical methods (Williams & Johnson, 2004). Acoustic-televiwer (ATV) logs are collected in water- or light, mud-filled, open boreholes with an ultrasonic (500 kHz to 1.25 MHz) pulse source. Acoustic-televiwer tools produce amplitude and travel time logs of the emitted sonic pulses as they reflect off the borehole wall and travel back to the sensor.

The travel time log can be used to calculate a 360-degree *acoustic caliper* of the borehole wall, and the amplitude log is useful for fracture, bedding, and lithologic characterization (Figure 8). Multi-echo systems, which were first described by Broding (1982), record the full wave train of the reflected acoustic signal and are capable of imaging

behind plastic casing. This is useful for imaging poorly competent intervals that will not stay open without being cased and for inspecting annular grout seals.

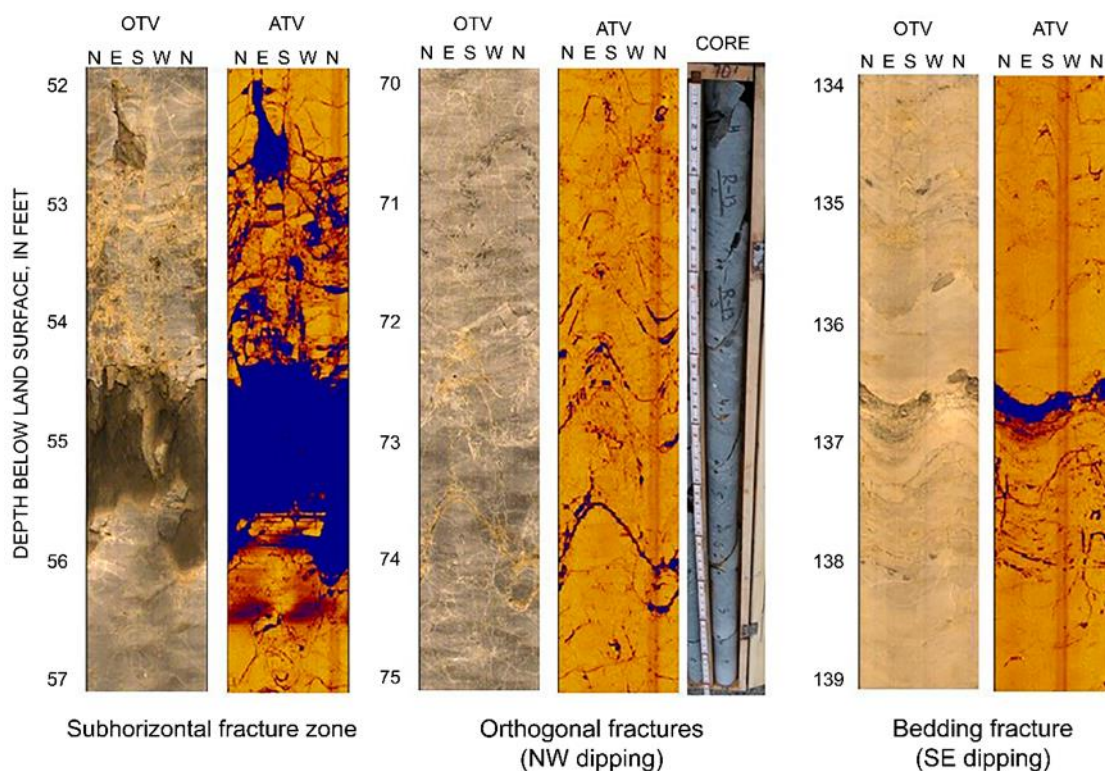


Figure 8 - Acoustic (ATV) and optical-televiwer (OTV) logs and core collected from a core hole in fractured and solutioned marble (Williams, 2008). Fracture dip direction is indicated by the cardinal direction corresponding to the trough of the sinusoidal curve of the fracture trace. On the depth scale, 52 ft \cong 16 m, 70 ft \cong 21 m, 134 ft \cong 41 m and the 5 ft interval is \cong 1.5 m; N E S W N indicates North, East, South, West, and North, respectively.

Optical-televiwer (OTV) logs are collected from borehole intervals filled with clear water or air with a camera and conical or hyperbolic reflector. In clear, water-filled, open bedrock boreholes, the images obtained from OTV and ATV logs together are highly complementary. While the relation between lithologic and structural features is not always clear on ATV logs, in darker rocks, fractures that are readily apparent on acoustic images are difficult to distinguish from dark-colored zones on optical images. Iron staining, other chemical precipitation, and bacterial growth that may be indicative of groundwater flow and (or) contamination are readily apparent on OTV logs.

Image logs can be interpreted to determine strike and dip of planar features including fractures, foliation, and bedding (Figure 9). Box 5 presents the distribution and orientations of bedding and fractures and that of breakouts related to tectonic stress as determined from the integrated analysis of ATV and OTV in an Appalachian basin borehole.

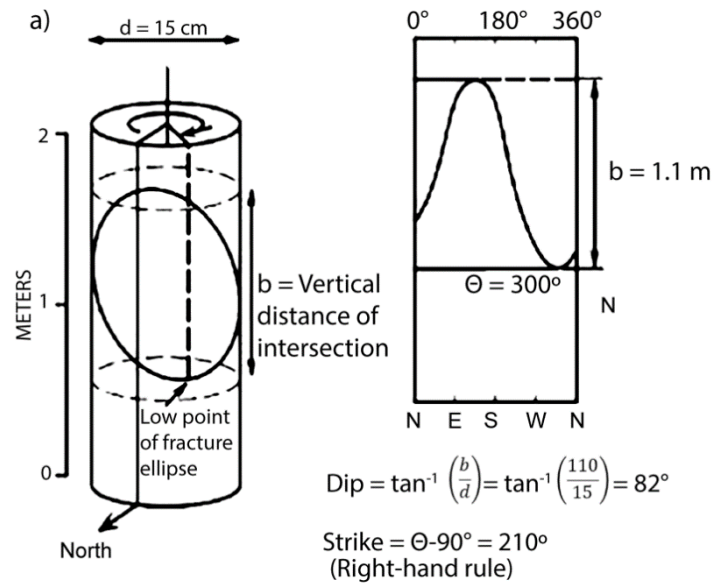


Figure 9 - Strike and dip of a planar feature such as a fracture or bed contact intersecting a borehole determined from analysis of a televiewer log (Paillet & Ollila, 1994).

A limitation of borehole imaging is the lack of borehole wall penetration. Image data apply to the highly local conditions at the borehole wall, and represent the formation as affected by drilling damage and contact with borehole fluids. For example, local measurements of fracture strike, dip, and aperture may not be indicative of fracture or fault properties over larger and more representative sections of the same subsurface feature. However, the fine-scale detail of image logs can be integrated with other log data to provide an enhanced interpretation of formation properties (Paillet, 2000).

3.6 Fluid-Property Logs

Fluid-property logs measure the physical and chemical properties of the fluid column in the borehole. The most common fluid-property probes measure fluid resistivity and temperature, but other specialized probes measure specific conductance, pH, dissolved oxygen, and specific ions such as chloride and nitrate. Fluid-property logs are commonly collected in water-filled, open holes under ambient conditions. However, comparison of fluid-property logs under differing hydraulic conditions provides additional information for flow-zone characterization.

Fluid-property logs are a simple and quick way to identify possible flow conditions and are an important step in the logging program whenever water quality and flow are of interest. Box 5 presents an example of repeated fluid-property logs collected over several months following completion of an open borehole that penetrated fresh and saline water zones. Figure 10 presents an example of fluid-property logs collected under ambient conditions that are repeated under pumping conditions to reveal changes in the fluid column. This served as a guide for depth-dependent, water-quality sampling. The results of the fluid property logging and depth-dependent sampling indicated that the shallow fracture zone penetrated by the well was impacted by road salt.

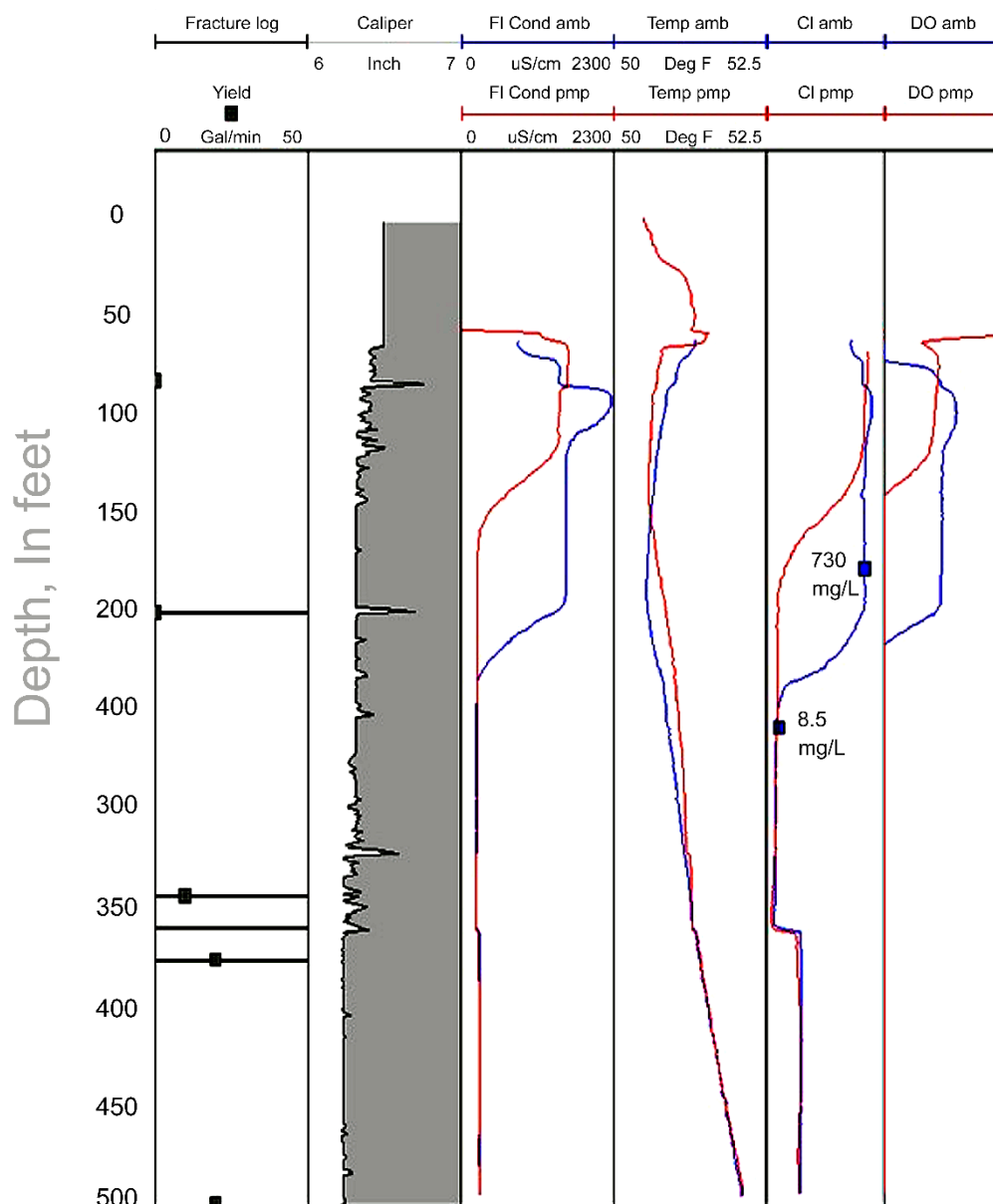


Figure 10 - Fluid-property logs and depth-dependent samples collected under ambient and pumped conditions along with driller-reported fractures and well yield for an open borehole in fractured bedrock. Scale conversions: 500 ft \cong 152 m; 50 Gal/min \cong 0.2 cubic meters per minute; 52.5 °F \cong 11.4 °C. Abbreviations: amb = ambient conditions; pmp = pumped conditions; FI Cond = fluid conductivity; Cl = chloride; DO = dissolved oxygen. Discrete depth samples are indicated with blue squares (Reynolds et al., 2015).

Temperature logs collected in boreholes under ambient conditions that have temperature gradients less than the geothermal gradient indicate the possible presence of vertical flow in the borehole. Isothermal gradients indicate vertical borehole flow of sufficient magnitude that the temperature of the fluid column is not in equilibrium with that of the surrounding formation. Pehme and others (2007, 2010) and Pehme (2012) collected repeated temperature logs in boreholes lined with an impermeable flexible sleeve under ambient conditions. This was done following heating of the borehole fluid to reveal flow zones that were masked by borehole flow in the open-hole logs.

The dilution-logging method involves collection of repeated specific-conductance or fluid-resistivity logs following replacement of the borehole fluid column with saline

water (West & Odling, 2006; Maurice et al., 2011) or distilled water (Tsang et al., 1990). Paillet and others (2012) presented an example of the application of dilution logging for the delineation of flow zones in an open borehole in fractured granite (Figure 11). The discrete depth locations where fresh formation water enters the borehole under ambient and pumped conditions are indicated by steps in the fluid-resistivity profiles. Ambient flow rates in the borehole estimated using the fluid column modeling program of Paillet (2012) compared favorably with those measured using a heat-pulse flowmeter.

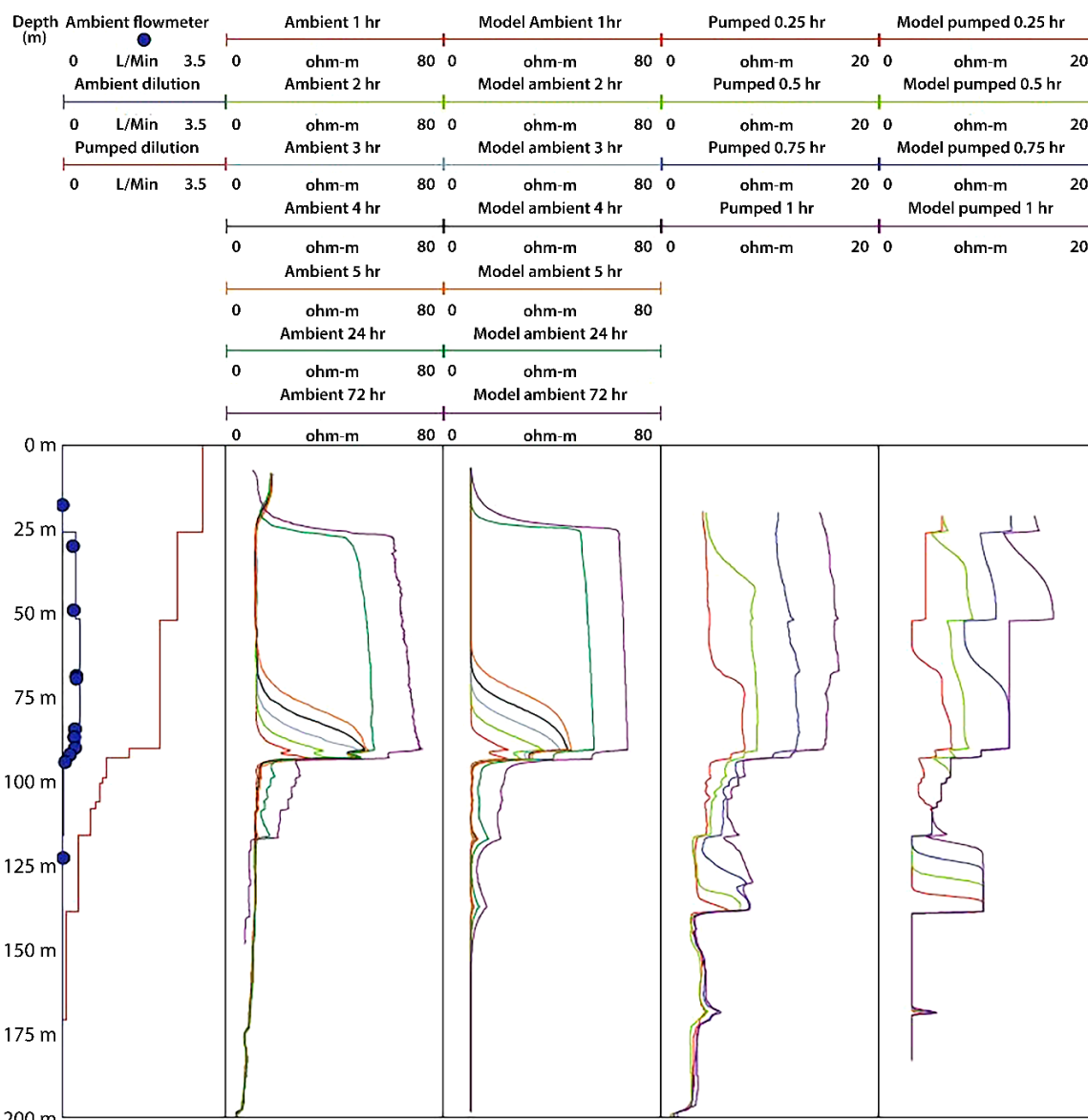


Figure 11 - Measured and modeled ambient and pumped dilution logs, ambient and pumped flows estimated from dilution-log analysis, and ambient flow measured with a heat-pulse flowmeter for an open borehole in fractured granite (Paillet et al., 2012).

In a closely related form of fluid column logging, dye tracing can be used to measure borehole flow. Methods involve downhole emplacement of dye accompanied by either downhole or uphole measurement. Izbicki and others (1999, 2005) used dye tracing to measure flow contributions under pumping conditions in large-diameter production wells.

Fluid column profile models used for saline- and distilled-water dilution logging can be applied to the analysis of dye-tracing logs.

3.7 Flow Logs

Flow logs provide direct measurements of borehole hydraulics from which aquifer properties of transmissivity, hydraulic conductivity, and hydraulic head may be estimated. Flow logs commonly are collected using one of three types of flowmeters: spinner, heat-pulse, and electromagnetic.

1. *Spinner flowmeters.* Flow is measured by recording the rotation rate of a 3- or 4-bladed impeller mounted with adjustable needle bearings on a freely rotating shaft. The borehole flow turns the blades, which rotates the shaft, and magnetic or optical sensors detect the rotation of the shaft. The impeller is housed in a protective cage or basket; impellers and baskets of different diameters are available. Frictional forces associated with shaft rotation must be overcome; the tool does not respond below the threshold velocity required to initiate rotation.

Maximum impeller and cage diameter for the borehole and use of lightweight impellers, jeweled bearings, and magnetic forces to reduce contact pressures are used to increase tool sensitivity (Young & Pearson, 1995). The threshold velocity (stall speed) of a typical spinner flowmeter is about 1.5 m/min (≈ 5 ft/min), which limits its use to higher flow conditions. Spinner flowmeters have been used to measure flows of more than 3,800 L/min (1,000 gal/min) in large-diameter production wells (Hanson & Nishikawa, 1996).

2. *Heat-pulse flowmeters* (Hess, 1986). Flow is measured at stationary points by recording the rate at which a small parcel of heated water generated by a wire grid moves up or down to a temperature sensor (thermistor) under the influence of borehole flow. The flow measurement range of the most widely used heat-pulse flowmeter that is equipped with a diverter fitted to channel flow through the probe throat is 3.8 to 56 L/min (0.01 to 1.5 gal/min). A heat-pulse flowmeter designed to be used without a diverter has a measurement range of 0.9 to 3 m/min (0.3 to 10 ft/min).
3. *Electromagnetic flowmeters* (Molz & Young, 1993; Young et al., 1998). Flow is measured by the voltage gradient generated by electrically conductive water moving through an EM coil. Based on Faraday's Law, the generated voltage is proportional to the flow velocity. The flow measurement range of the electromagnetic flowmeter with a fitted diverter is 0.2 to 38 L/min (0.05 to 10 gal/min).

Commonly, flowmeters are used with centralizers so that the axis of maximum borehole flow in the parabolic flow profile (highest velocity in the center of the borehole decreasing to zero at the borehole wall) coincides with the axis of the flow measurement section on the flowmeter. Some spinner flowmeters can be stacked with a three-arm caliper

tool with the caliper arms providing centralization. Some spinner flowmeters have spring-loaded centralizers for use in boreholes where the casing is a smaller diameter than the open or screened interval.

Diverter commonly are attached to flowmeters to concentrate flow through the flow-measurement throat of the tool. For some applications, diverters may also be purposely underfitted to the nominal borehole diameter, so a portion of the flow bypasses the throat to extend the upper measurement range of the flowmeter and (or) suppress the effects of diameter variations on logging logs (Paillet, 2004). The heat-pulse flowmeter equipped with an underfit flow diverter has been shown effective at flow rates over 75 L/m (20 gal/min; Paillet, 2004). The EM flowmeter may be used with an underfit diverter or without any diverter, expanding its upper measurement to more than 3,800 L/min (1,000 gal/min) in large-diameter production wells (Newhouse et al., 2005; Izbicki et al., 2005).

Flow measurements can be made in the stationary mode, with individual measurements at discrete depth stations, or in the logging mode, where the tool is moved along the borehole at a constant rate. Spinner and electromagnetic log data commonly are collected in both stationary and logging modes. Because of the time needed for capacitor recharge between measurements, it is impractical to use the heat-pulse flowmeter in logging mode.

Spinner-flowmeter measurements typically are made by logging the probe at a steady rate and then subtracting the effect of the probe motion from that of the borehole flow field. The best practice is to profile the borehole in the logging mode, and then collect stationary measurements at selected points.

Laboratory facilities consisting of a flow tube equipped with a flow metering device, and adjustable water source can be used to calibrate flowmeter response. However, spinner flowmeters typically are calibrated in the field by logging the tool in both up and down directions in casing or other no-flow interval at a range of constant speeds as measured by the depth encoder on the logging draw works. In some cases, calibration is done in the field as a linear proportion between a measured stationary response in casing under non-pumping conditions and a measured stationary response in casing under a known pumping rate.

In the case of heat-pulse and electromagnetic flowmeters, probe output is given in discharge based on calibration data obtained using controlled discharges in the laboratory and stored as calibration processing software in the probe. It is important to remember that borehole conditions in the field will be different than in the calibration facility, so the amount of flow bypassing flow diverters may vary considerably from calibration conditions. It is necessary to compare the calibrated probe response to the known discharge rate when flow is measured near the top of the borehole during pumping and adjust the calibration of the flow profile accordingly. Flow logs are typically adjusted by a bypass

factor to ensure that flow logs agree with known pumping or injection flows in casing when such measurements are available.

Flow logs are commonly collected under both ambient and stressed conditions to best characterize the well hydraulics. Depending on the distribution of head in zones where flow enters or exits the borehole and the transmissivity of those zones, zones with the lowest heads may not be identified if only ambient logs are collected. Also, these zones may not contribute to pumped waters depending on the pumping rate, an important consideration in wells used for groundwater-quality sampling. An example of ambient and pumped flow logs from a well with multiple screened zones in an unconsolidated aquifer where pumping reduced the downward ambient flow but did not reverse it is shown in Figure 12.

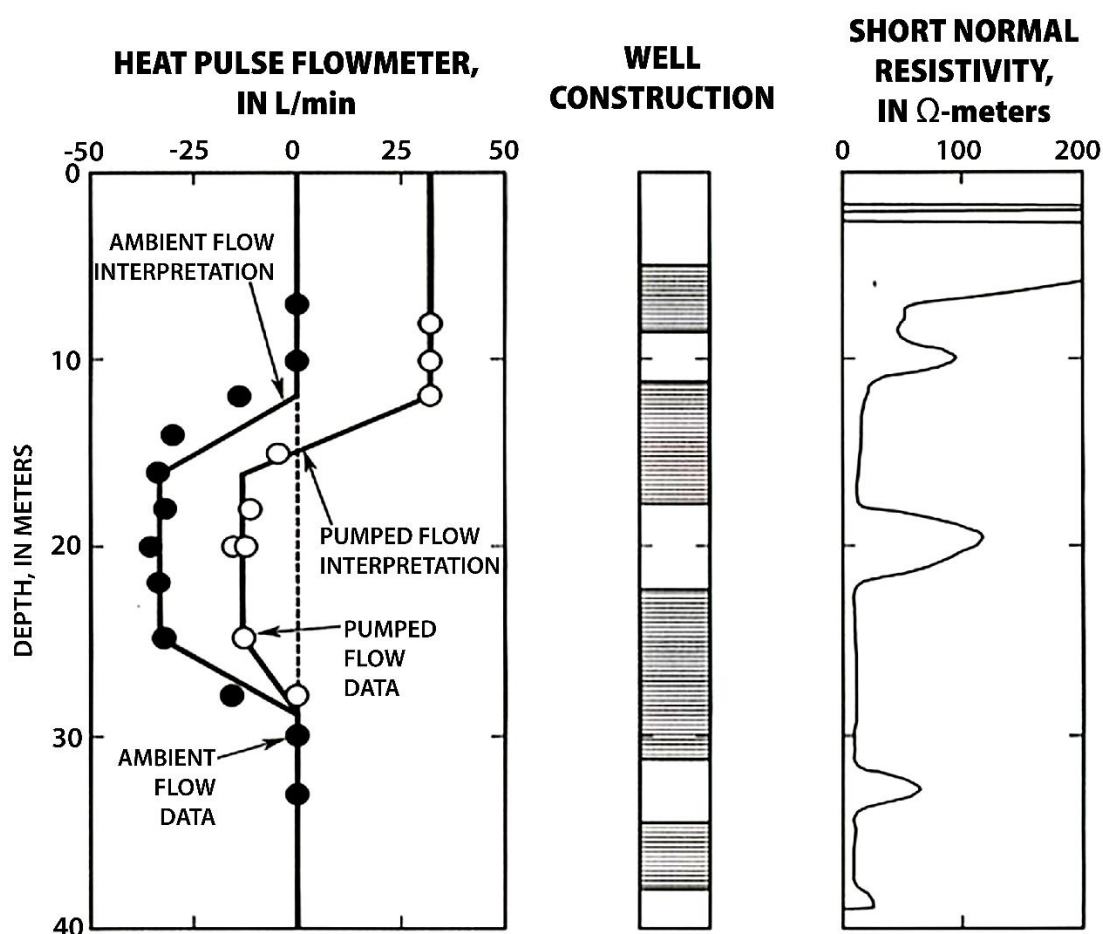


Figure 12 - Flow logs under ambient and pumping conditions in a PVC-cased observation well that is screened in an unconsolidated aquifer. The short normal resistivity log verified the screened intervals as zones of low resistivity. By convention, upward flows are expressed as positive values, downward flows are expressed as negative values, and screened intervals are indicated on well construction by a striped pattern (Paillet et al., 2000b).

Stressed-flow logs are typically collected under quasi-steady-state conditions (steady pumping or injection rate with nearly stabilized drawdown or recovery) so that shifts in the flow profile can be associated with specific flow zones. Considerable time can be lost in attempting to adjust the pumping rate to obtain a steady discharge in low-yielding

wells. In such cases, it may be simpler to instantaneously draw the water level down several meters and then measure flow during recovery. In subsequent calibration of the flow data, the discharge rate is calculated from the measured recovery rate and the known diameter of the borehole casing.

Methods commonly used for to estimate hydraulic properties of flow zones from flow-log data include proportion, analytical-solution, and numerical-model techniques (Molz & Young, 1993; Paillet, 1998, 2000; Rutledge, 1991; Halford, 2009; Day-Lewis et al., 2011). In the proportion method, ambient and stressed flow data are differenced to estimate the relative transmissivity of flow zones. [Box 7](#) presents an example of the proportion method. Analytical-solution and numerical-model methods use ambient and stressed flow-log data along with stress-rate and drawdown measurements to estimate flow-zone transmissivity and hydraulic head. The stress need not reverse the direction of ambient flow for the flow logs to be used for quantitative hydraulic analysis.

It is important to note the flow-log analysis method has been shown to generally detect and quantify the hydraulic properties of flow zones whose transmissivities are within two orders of magnitude of the most transmissive zone penetrated in a specific borehole (Paillet, 1998; Williams, 2008). An example of the quantitative analysis of ambient and pumped flow logs in an open-hole well that penetrated discrete flow zones in fractured sedimentary bedrock and comparison with discrete-interval hydraulic tests with a straddle-packer system is presented in Figure 13. The flow and other geophysical logs provided a synergistic data set that complimented the hydraulic test results in the characterization of flow and VOC transport at the site. [Box 5](#) presents an additional example of the quantitative analysis of flow logs and comparison with hydraulic test results.

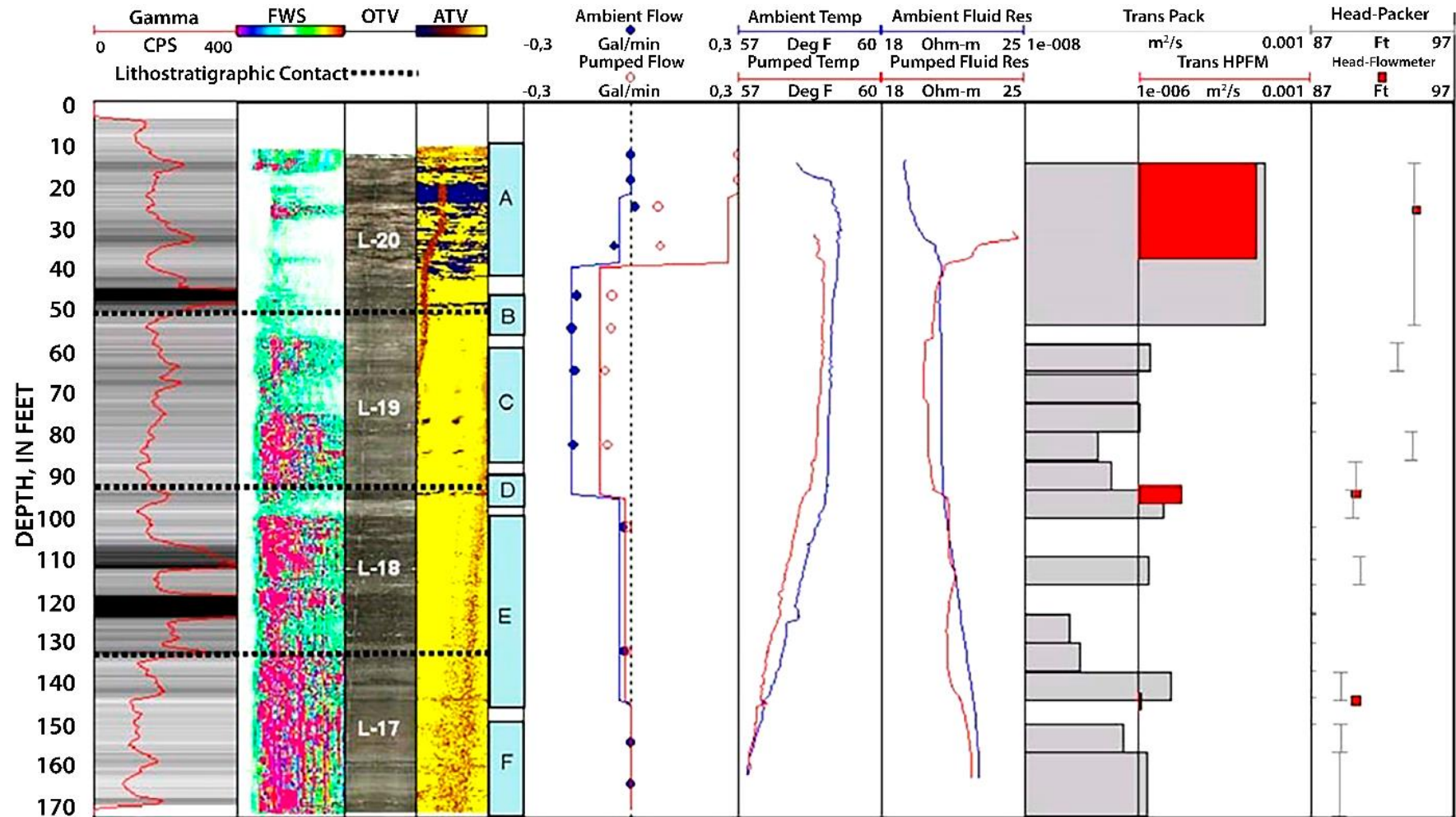


Figure 13 - Logs of gamma, full waveform sonic (FWS), optical televier (OTV), acoustic televier (ATV); along with flow, temperature, fluid resistivity under ambient (blue) and pumped (red) conditions; estimated transmissivity of flow zones (red rectangles) and hydraulic head of flow zones (red squares) from flowmeter analysis; estimated transmissivity (gray rectangles) and estimated head (gray lines) from discrete interval hydraulic test analysis (Williams et al., 2007). Dashed black lines indicate estimated locations of lithostratigraphic unit. Scale conversions: 170 ft \approx 52 m; 87 ft \approx 27 m; 97 ft \approx 30 m; 57 °F \approx 14 °C; 60 °F \approx 16 °C.

Analytical and numerical models provide the best means for the quantitative analysis of flow logs. Model output is simultaneously fit to ambient and stressed flow data to estimate transmissivity and hydraulic head for each identified flow zone. These analytical methods estimate the hydraulic-head differences between the flow zones that drive inflows and outflow.

Each hydraulic-head difference can be referenced to the ambient water-level measurement and converted to a water-level depth below the measurement point or a hydraulic-head elevation. Such hydraulic-head estimates provide more information on large-scale flow paths and connections than that provided by discrete estimates of transmissivity alone. An example of model analysis of ambient and pumped flow logs in an open borehole that penetrated discrete flow zones in carbonate bedrock is shown in Figure 14 and Table 2.

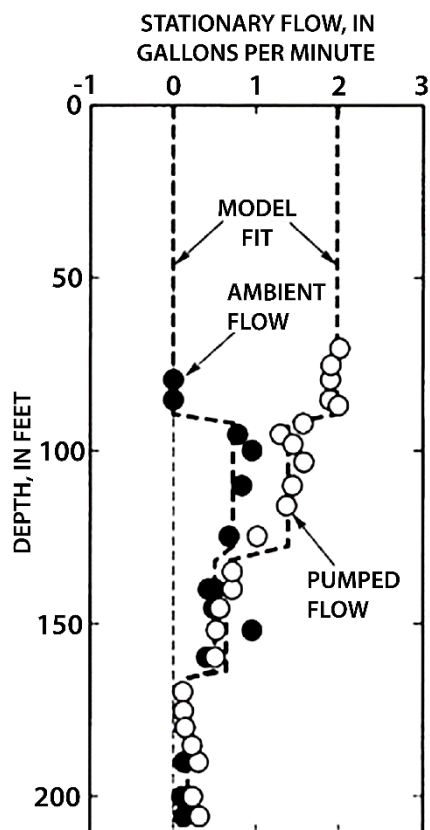


Figure 14 - Measured and modeled flow logs under ambient and pumped conditions for flow zones penetrated by an open borehole in a carbonate-bedrock aquifer at the Rochester site, southeastern Minnesota, USA (Paillet et al., 2000a). By convention, upward flow is expressed as a positive value and downward flow as a negative value. Scale conversions: 50ft \cong 15m; 200 ft \cong 61 m; -1 gal/min \cong -4 L/min; 3gal/min \cong 11L/min.

Table 2 - Model-estimated transmissivity and hydraulic head of flow zones penetrated by an open borehole in a carbonate-bedrock aquifer at the Rochester site, southeastern Minnesota, USA (Paillet et al., 2000a).

Zone	Depth (m)	Depth (ft)	Hydraulic head (m)	Hydraulic head (ft)	Water level ^a (m)	Water level ^b (ft)	Trans* (m ² /day)	Trans* (ft ² /day)
4	25–28	83–92	0	0	5.00	16.4	41	440
3	39–40	129–131	0.15	0.5	4.85	15.9	15	165
2	51	167	0.61	2	4.39	14.4	2.6	28
1	62–64	205–210	0.61	2	4.39	14.4	1.0	11

^a m below Top of Casing^b ft below Top of Casing

*Transmissivity

In Exercise 6⁷, flow-zone transmissivity and hydraulic head are estimated from ambient and pumped flow-log data using a spreadsheet program.

4 Integrating Geophysical Logs and Other Borehole Measurements

Geophysical logs provide a continuous profile of aquifer properties that reflect the variation of the penetrated formation(s) over the length of the borehole. This continuous profile can be related to point or interval measurements such as those from core analyses or hydraulic tests by comparing the two data sets.

Establishment of a relation between geophysical logs and other borehole measurements typically involves recognition of potential offset in the depth scales of the separate data sets, and the disparity in sample volume involved in collecting the data. The effects of both sample volume differences and depth offsets need to be considered whenever geophysical logs are compared with point or interval data. Logging cables stretch (in contrast to rigid drill string) so differences in reference depths are to be expected. Core samples represent measurements made over a scale much smaller than that of the geophysical log, while hydraulic tests involve measurements averaged over significantly larger depth intervals than those associated with each log data point. [Box 8](#) presents an example of issues involved with correlating log and core data.

In [Exercise 7](#), gamma and core porosity from a borehole in a sandstone aquifer are plotted and regressed.

5 Integrating Geophysical Logs and Surface Geophysics

An important application of geophysical logs is their integrated analysis with surface-geophysical measurements, commonly of the same physical property but with much higher depth resolution than is possible with surface measurements.

Integrated analysis is advantageous for two primary reasons:

1. to verify and adjust imprecise depth scales given by methods used to analyze the surface soundings, and
2. to verify the patterns of subsurface variation given by the specific model used to process the soundings.

Acoustic or sonic logs are routinely used in petroleum exploration to correct depth scales given on seismic sections developed from data generated using surficial seismic techniques. An example of this is given by Paillet and Ellefsen (2005) where a *synthetic seismogram* is constructed from a sonic log and the resulting diagram is overlain on the seismic section to provide a precise depth scale.

Electromagnetic soundings are commonly used to identify aquifer and confining units, map saltwater intrusion, or delineate electrically conductive contaminant plumes. Electromagnetic sounding measurements are inverted to produce geoelectric profiles that represent the subsurface as discrete layers of specified electrical resistivity or conductivity and thickness. Induction- or normal-resistivity logs can then provide useful verification of the sounding geometry.

Paillet and others (1999) and Fitterman and Prinos (2011) used an integrated analysis of transient-electromagnetic (TEM) surface soundings and induction logs in the investigation of saltwater intrusion in southern Florida. Selected TEM soundings were conducted in the vicinity of boreholes to help verify that the interpreted TEM results were effectively representing subsurface conditions. Figure 15 shows that resistivity values and bottom contact depths estimated from four soundings that surrounded three boreholes agree with the subsurface induction profiles obtained in the boreholes on the same date: April 28th, 2008.

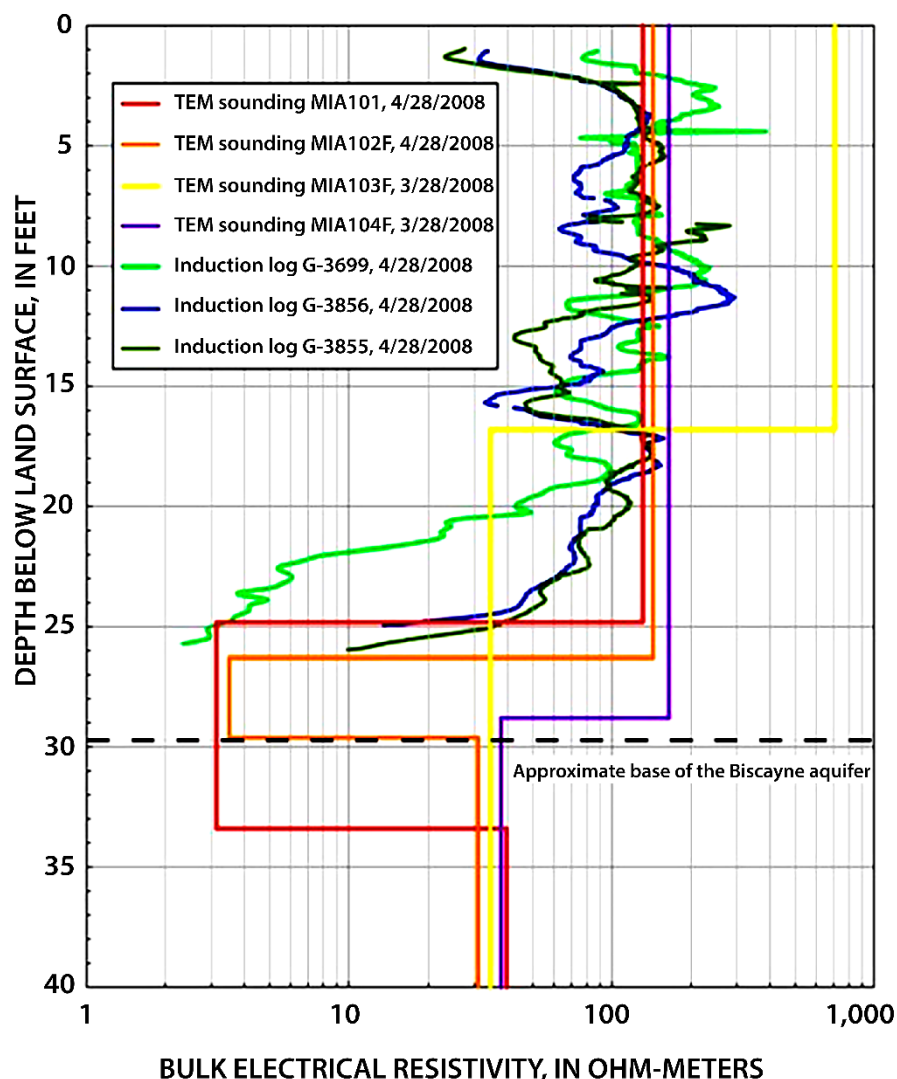


Figure 15 - Comparison of transient electromagnetic (TEM) soundings MIA101, MIA102, MIA103, and MIA104 with induction logs from Biscayne aquifer wells G-3699, G-3856, and G-3855 (Fitterman and Prinos, 2011). Well G-3699 is approximately 460 m east-northeast of sounding MIA101. Well G-3856 is 300 m east-northeast.

The TEM soundings were also used to investigate the variation in subsurface resistivity over distances up to 15 km (9.3 mi) between boreholes that had to be spaced considerable distances apart to investigate subsurface salinity over an entire region. Once these soundings were obtained along transects between several boreholes, two additional boreholes were drilled at accessible locations where the soundings showed local maxima and minima in deeper level resistivity.

Induction logs in the two boreholes verified the resistivity values and contact depth of the deeper layer inferred from the TEM soundings. This provided important additional verification of the TEM profile interpretation. It also supported the conclusion that an irregular pattern of deeper layer conductivity was related to flow of saline water upward through windows in underlying confining layers. A significant regional upward hydraulic gradient that could be driving this upflow was identified using borehole flowmeter methods in almost all boreholes drilled for the study.

6 Wrap-up

Geophysical logging can play an important role in any study where boreholes are drilled to explore the subsurface, and often serves as the scaffolding on which useful subsurface models are constructed. After the expense of drilling, an investigator has a surface casing sticking out of the ground, a descriptive driller's log, and perhaps some cuttings. Even when the project budget allows for the added expense of coring, often some samples are lost, and cores that are recovered are damaged by the drilling process.

When the subsurface is explored by drilling, well logs can provide a wealth of information at relatively little additional cost. For example, the precise depth at which inflow zones or marker beds intersect the borehole can be critically important information in contaminant-migration or water supply studies. The additional information gleaned from geophysical logs can be vital because of the unique properties of geophysical log data as listed in the following bullets.

- Geophysical logs provide a precise and continuous record of formation properties versus depth with no missing sections.
- Geophysical logs provide multiple, physically independent measurements of formation properties adjacent to the borehole that can be used to solve multi-variate interpretation inversions to address the non-uniqueness of the subsurface. Single geophysical measurements from surface seismic, electrical, or electromagnetic surveys cannot be uniquely related to a specific property of interest because signals from surficial surveys need to travel through multiple zones of differing characteristics, thus an effective property representing the entire section is produced.
- Geophysical logs provide measurements made in situ without damage from drilling or pressure release when established interpretation methods and control of the volume of investigation are used to minimize borehole diameter and fluid column influence on the data.

Our review of geophysical logging applications in hydrogeology is designed to demonstrate the powerful contributions made by this method over the range of groundwater applications. We have demonstrated these contributions with a series of instructive case histories encountered through several decades of personal logging experience.

7 Exercises

Exercise 1

As part of a geotechnical investigation in a landslide-prone area underlain by glaciolacustrine sediments, cone penetrometer (CPT) logs were collected from an 85 ft (25.9 m) deep direct-push (DP) boring.

The CPT logs included tip resistance (Q_t) and sleeve friction (F_s) logs in units of tons per square foot (tsf).

Data for this exercise, is provided in a spreadsheet within a [zip file that can be downloaded from the web page for this book](#)[↗]. The zip file is named *Geophysical-Logging-for-Hydrogeology-Exercise_Spreadsheets.zip*.

The spreadsheet for this exercise is named *GPloggingExercise1_CPT_SBT.xlsx*, and contains several worksheets.

- The worksheet named [*Intro*] describes the exercise.
- The worksheet named [*RawData*] contains the CPT logs with depth in feet with tip resistance and sleeve friction in tons per square foot.
- The worksheet named [*Work-Qt_Fs_and_SBT*] has a copy of the CPT data and provides a worksheet for this exercise.

In the worksheet named [*Work-Qt_Fs_and_SBT*]:

- a) Calculate and plot the friction ratio (R_f) log, where R_f is the ratio of the F_s to Q_t in percent.
- b) Plot R_f versus Q_t and overlay on Soil Behavior Type (SBT) chart.
- c) Use the overlay to assign SBTs to the reported lithologies penetrated by a nearby boring.

[Solution to Exercise 1](#) ↴

[Return to where text linked to Exercise 1](#) ↴

Exercise 2

Data for this exercise, is provided in a spreadsheet within a [zip file that can be downloaded from the web page for this book](#)[↗]. The zip file is named *Geophysical-Logging-for-Hydrogeology-Exercise_Spreadsheets.zip*.

The spreadsheet for this exercise is named *GPloggingExercise2_GammaFilter.xlsx* and contains several worksheets.

- The worksheet named [*Intro*] describes the exercise.
- The worksheet named [*RawData*] contains the gamma log with depth in feet and gamma emissions in cps.
- The worksheet named [*Work-Gamma&FilterPlots*] has a copy of the gamma data and provides a worksheet for plotting the data, filtering, and replotting.

View Grant Park well information including geological and geophysical logs by searching for USGS NWIS Site Number 403844073412701 on the [USGS GeoLog Locator website](#)[↗]. A one-minute video on the home page provides information on how to use the GeoLog locator.

- a) Plot gamma log data and
- b) Filter gamma log data
- c) Replot log using the filtered data.

[Solution to Exercise 2](#)[↓]

[Return to where text linked to Exercise 2](#)[↑]

Exercise 3

In this exercise, gamma data are plotted and interpreted to define the depth of a confining unit that separates two aquifers.

Data for this exercise, is provided in a spreadsheet within a [zip file that can be downloaded from the web page for this book](#)[↗]. The zip file is named *Geophysical-Logging-for-Hydrogeology-Exercise_Spreadsheets.zip*.

The spreadsheet for this exercise is named *GPloggingExercise3_GammaLithoStrat.xlsx* and contains several worksheets.

- The worksheet named [*Intro*] describes the exercise.
 - The worksheet named [*Work-PlotGam&StratPick*] contains the gamma log with depth in feet and gamma emissions in cps where the exercise can be undertaken.
- a) Plot a gamma log from 500 to 850 ft (152.4 to 259.1 m) in the worksheet [*Work-PlotGam&StratPick*].
 - b) Pick the bottom and top of the Raritan confining unit that separates the Lloyd aquifer below from the Magothy aquifer above in [*Work-PlotGam&StratPick*]. Based on the gamma log, where is the upper and lower contact of the confining unit?
 - c) Compare your gamma picks with the geologist log, which is provided on the far right side of [*Work-PlotGam&StratPick*] as a graphic image. You can select the image/graphic and move it over to your results for side-by-side comparison. If you downloaded the spreadsheet for the logs of 403844073412701 from the GeoLog Locator website while working on Exercise 2, the eleventh row of the first worksheet provides a link to view or download the lithology log for the site, a direct link is provided here:

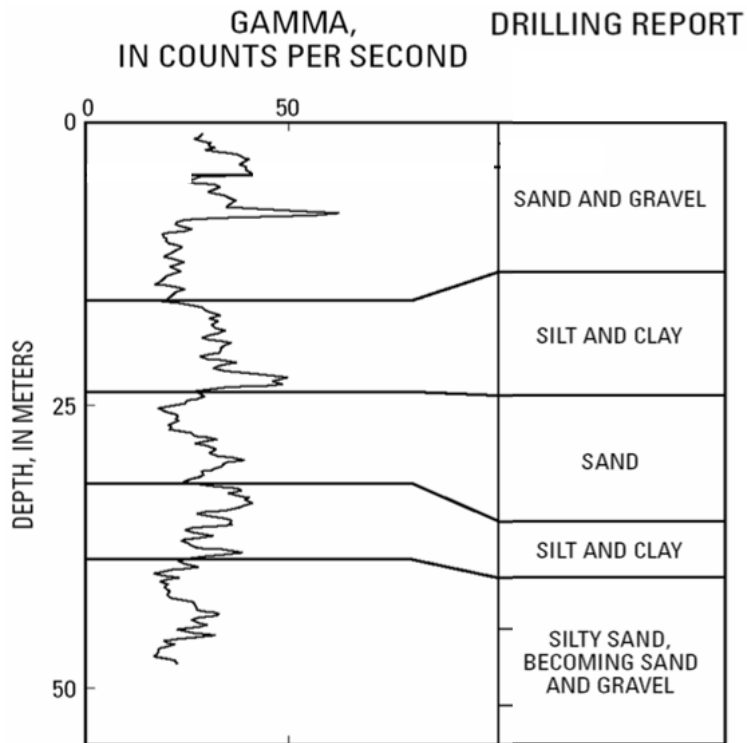
[https://txdata.usgs.gov/GeoLogArchiver/odata/Logs\(38195\)/LogFile](https://txdata.usgs.gov/GeoLogArchiver/odata/Logs(38195)/LogFile)[↗].

[Solution to Exercise 3](#)[↴]

[Return to where text linked to Exercise 3](#)[↴]

Exercise 4

Using the diagram below, identify potential zones to be fitted with well screen for a nested monitoring well installation, then compare your selected screen zones with the solution. Identify shallow, intermediate, and deep zones for screening the monitoring well.



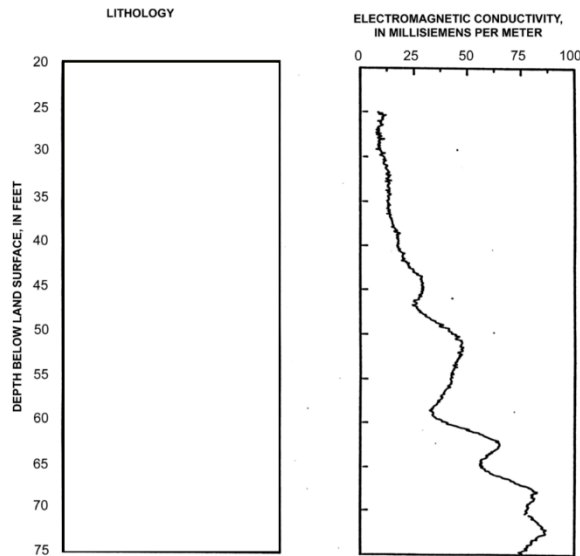
Gamma and driller logs at a nested monitoring well installation site.

[Solution to Exercise 4 ↓](#)

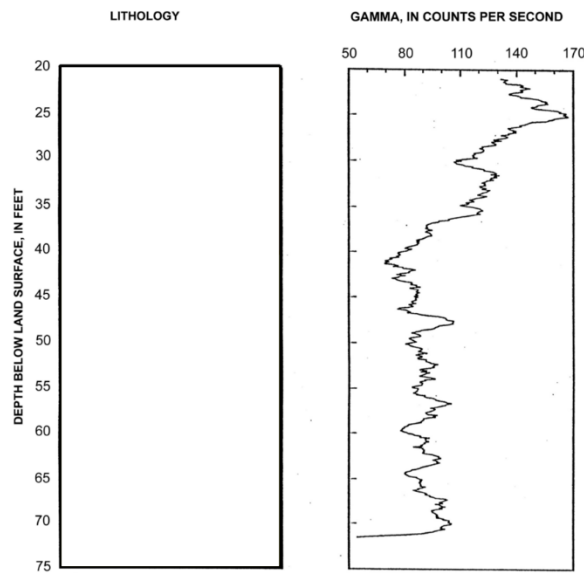
[Return to where text linked to Exercise 4 ↑](#)

Exercise 5

a) Define the lithology based on the typical relation with sand-clay content for electromagnetic conductivity and for gamma counts at the monitoring well in coastal-plain sediments in Virginia, USA. Assume the formation water is fresh. How do your two lithologic interpretations compare?



Electromagnetic conductivity of a monitoring well at the Explosive Experimental Area, Naval Surface Warfare Center, Dahlgren, Virginia, USA.



Gamma counts of a monitoring well at the Explosive Experimental Area, Naval Surface Warfare Center, Dahlgren, Virginia, USA.

Depth (ft)	Description Well EEA-M5 (54Q63).
18.5	Sand, greenish black (5GY 2/1), fine to very fine-grained, micaceous, very glauconitic
20.0–22.0	Sand, dark-greenish-gray (5GY 4/1). very-fine-to fine-grained, micaceous, glauconitic. Contains shell fragments. Contains quartz pebble (75 mm) at 21.5 ft (from above?).
25.0–27.0	Silty sand, dark-greenish-gray (5GY 4/1) to greenish-black (5GY 2/1), fine-grained, micaceous, glauconitic. Contains abundant bivalve fragments and whole shells (<i>Macrocallista</i> , <i>Cubitostrea</i>), some shells articulated.
30.0–32.0	Silty sand, dark-greenish-gray (SGY 4/1), fine-grained, micaceous, glauconitic. Contains bivalve fragments and whole shells (<i>Macrocallista</i> , <i>Cubitostrea</i>). Massively bedded.
35.0–37.0	Silty sand, dark-greenish-gray (5GY 4/1), fine-grained, micaceous, glauconitic. Contains bivalve fragments and whole shells (<i>Macrocallista</i> , <i>Cubitostrea</i>). Massively bedded.
40.0–42.0	Silty sand, dark-greenish-gray (5GY 4/1) to greenish-black (5GY 2/1), medium-to fine-grained, micaceous, very glauconitic Contains bivalves (<i>Macrocallista</i> , <i>Venericardia</i> , <i>Cubitostrea</i>). Massively bedded.
45.0–47.0	Silty sand, greenish-gray (5GY4/1) to greenish-black (5GY 2/1) very-fine-to medium-grained, micaceous, very glauconitic. Massively bedded. Sparsely fossiliferous (<i>Macrocallista</i> , <i>Venericardia</i>).
50.0–52.0	Silty sand, greenish-black (5GY 2/1), fine-grained, micaceous, very glauconitic. Massively bedded. Sparsely fossiliferous (<i>Venericardia</i>), shells chalky. Contains 3" diameter carbonate concretion at 51.7 ft.
55.0–57.0	Silty sand, greenish-black (5GY 2/1), fine-to very-fine-grained, micaceous, very glauconitic. Bioturbated. Moderately fossiliferous (<i>Venericardia</i> , <i>Macrocallista</i>).
60.0–62.0	Silty sand, dark-greenish-gray (5GY4/1), fine-to very-fine-grained, micaceous, glauconitic. Bioturbated. Sparsely fossiliferous (<i>Venericardia</i>).
65.0–67.0	Clayey silty sand, dark-greenish-gray (SGY 4/1) to greenish-black (5GY 2/1), fine-grained, micaceous, glauconitic. Bioturbated. Contains plant material. Fossiliferous (<i>Venericardia</i> , <i>Cubitostrea</i>).
70.0–72.0	Sandy silty clay, dark-greenish-gray (56Y 4/1), micaceous, glauconitic. Sand is very-fine-grained. Sparsely fossiliferous. Contains plant stem.
75.0–77.0	Silty sandy clay, dark-greenish-gray (5GY 4/1), micaceous, glauconitic. Sand is very-fine-grained. Contains sparse chalky shell fragments.

¹ Hammond and Bell (1995) at [USGS](#).

b) What might be affecting the gamma log response? *Hint*: consider [this information about glauconite](#) (Winterer, 2012).

[Solution to Exercise 5](#) ↓

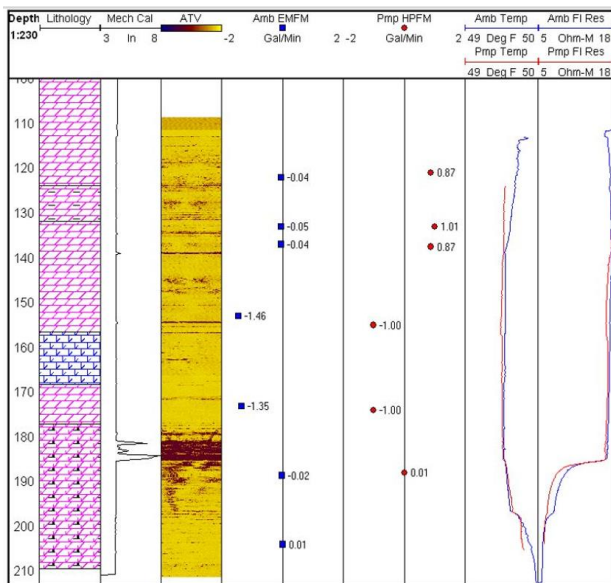
[Return to where text linked to Exercise 5](#) ↑

Exercise 6

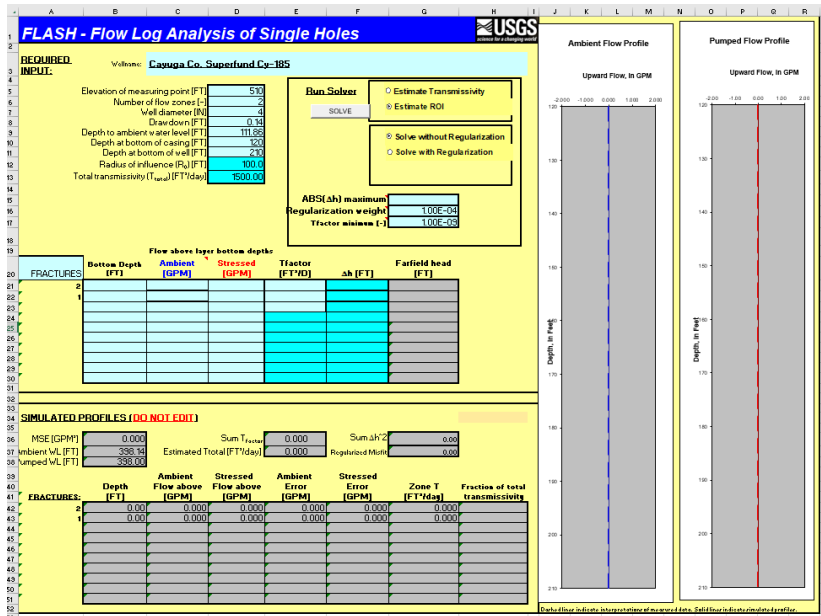
For this exercise, you will use the computer program FLASH (Flow-Log Analysis of Single Holes) to simulate or model wellbore flow and estimate zone transmissivity and hydraulic head. FLASH is coded in Microsoft Excel with Visual Basic for Applications.

Start by downloading FLASH.zip from <https://code.usgs.gov/water/esp/hgb/flash/>, unzip the file, and follow the installation directions found in Installation_README.pdf.

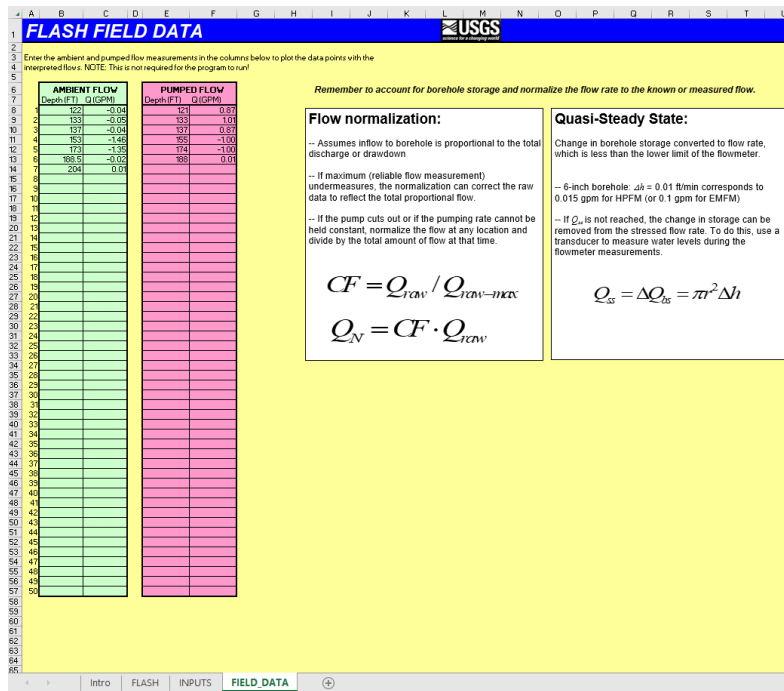
Geophysical logs including caliper, ATV, fluid, and flow logs were collected from an open-hole well completed in fractured carbonate bedrock. The well measuring point was 510 feet above land surface. The depth to the bottom of the well was 210 feet and the depth to the bottom of the casing was 120 feet. The well was 4-inches in diameter. The depth to the ambient water level was 111.86 feet. Fluid logs and stationary flowmeter measurements were made under ambient conditions. Fluid logs and stationary flowmeter measurements were repeated under steady-state drawdown of 0.14 feet while pumping at 1 gallon per minute for sampling. A total well transmissivity of 1500 ft²/d was estimated based on the well's specific capacity (pumping rate divided by drawdown). Flow and the other geophysical logs are presented below.



Using the information above and the program [FLASH], enter the measuring point elevation, number of fractures, well construction information, ambient water level, drawdown, and estimated total transmissivity into the worksheet named [INPUTS]. Enter an initial guess of 100 feet for the radius of influence (ROI), and in the Run Solver box, click on Estimate ROI. Your [INPUTS] worksheet should look like that below.



Next, enter the ambient and flow measurements in the [FIELD_DATA] worksheet as shown below.



Your [INPUTS] worksheet should now look like that below with the plotted flow measurements.

Exercise 7

In this exercise, gamma log data are compared with porosity values determined from core samples and a regression line is fit to the data.

Data for this exercise, is provided in a spreadsheet within a [zip file that can be downloaded from the web page for this book](#)[↗]. The zip file is named *Geophysical-Logging-for-Hydrogeology-Exercise_Spreadsheets.zip*.

The spreadsheet for this exercise is named *GPloggingExercise7_GammaCore.xlsx* and contains several worksheets.

- The worksheet named [*Intro*] describes the exercise.
- The worksheet named [*RawData*] provides porosity and gamma counts as a function of depth.
- The worksheet named [*Work-Plot&DepthAdj&Regress*] that includes the gamma counts as a function of depth, directions, and layout for undertaking the exercise.

Before performing the regression, you will want to be sure the depths of the porosity are aligned with the gamma log. There are three parts to the exercise, including plotting the data for the depth of interest, performing a depth shift on the core-porosity data, and then generating a regression. Be sure to consider the results and answer the question in part 3. The gamma data in the worksheet named [*RawData*] have already been filtered.

In [*Work-Plot&DepthAdj&Regress*], you will find a 3-part exercise. Each part has instructions at the top of the worksheet.

Part 1: Plot the Data

- a) Plot gamma log data as a scatter plot with straight lines.
- b) Plot core porosity data as a scatter plot with smooth lines and markers.
- c) Reverse porosity scale (with high percent on left and low percent on right).

Part 2: Perform a Depth Matching

- a) Visually/graphically adjust porosity depth scale to line up local maximums of gamma with minimums of porosity.
- b) Estimate depth offset and calculate the porosity depths accordingly. That is, adjust the depth log for the porosity plot and replot.

Part 3: Plot Depth Adjusted Data and Perform Regression

- a) Regress porosity on gamma and determine the linear relation (use the adjusted depth on the porosity). Cross plot the porosity and gamma in a scatterplot, then add linear regression line.
- b) Is this the expected relation between porosity in a sandstone aquifer? Explain why.

[Solution to Exercise 7](#)[↘]

[Return to where text linked to Exercise 7](#)[↗]

8 References

- Adams, R. F. (2020). *Money, Mississippi and Lake Poinsett Dam, Arkansas, grain-size analysis* [Data release]. US Geological Survey.
<https://www.sciencebase.gov/catalog/item/606f0315d34ef998701887ff>.
- Archie, G.E. (1942). The electrical resistivity log as an aid in determining some reservoir characteristics. *American Institute of Mining, Metallurgical, and Petroleum Engineers Transactions*, 146(1), 54–62. <http://doi.org/10.2118/942054-G>.
- Benoît, J., Sadkowski, S. S., & Bothner, W. A. (2004). Rock characterization using drilling parameters. In *Proceedings of the Second International Conference on Geotechnical and Geophysical Site Characterization ISC-2* (pp. 665–670). Millpress.
https://scholars.unh.edu/civeng_facpub/21/.
- Bradbury, K. R., & Rothschild, E. R. (1985). A computerized technique for estimating the hydraulic conductivity of aquifers from specific-capacity data. *Ground Water*, 23(2), 240–246. <https://doi.org/10.1111/j.1745-6584.1985.tb02798.x>.
- Broding, R. A. (1982). Volumetric scanning well logging. *The Log Analyst*, 23, 14–19.
- Brown, E. T., Green, S. J., & Sinha, K. P. (1981). The influence of rock anisotropy on hole deviation in rotary drilling—A review. *International Journal of Rock Mechanics and Mining Science*, 18, 387–401.
- Carman, P. C. (1956). *Flow of gases through porous media*. Academic Press.
- Chen, S. T. (1989). Shear-wave logging with quadrupole sources. *Geophysics*, 54(50), 590–597. <https://doi.org/10.1190/1.1442686>.
- Christy, C. D., Christy, T. M., & Wittig, V. (1994). A percussion probing tool for the direct sensing of soil conductivity. In *Proceedings of the 8th National Outdoor Action Conference* (pp. 381–394). National Ground Water Association. <http://www.ngwa.org/>.
- Christy, T. M. (1996). A drivable permeable membrane sensor of volatile compounds in soil. In *Proceedings of the 10th National Outdoor Action Conference* (pp. 169–177). National Ground Water Association. <http://www.ngwa.org/>.
- Collins, W. H., & Easley, D.H. (1999). Fresh-water lens formation in an unconfined barrier-island aquifer. *Journal of the American Water Resources Association*, 35(1), 1–22, <https://doi.org/10.1111/j.1752-1688.1999.tb05448.x>.
- Crow, H. L., Hunter, J. A., Olson, L. C., Pugin, A., & Russell, H. (2017). Borehole geophysical log signatures and stratigraphic assessment in a glacial basin, southern Ontario. *Canadian Journal of Earth Sciences*, 55, 829–845. <https://doi.org/10.1139/cjes-2017-0016>.
- Day-Lewis, F. D., Johnson, C. D., Paillet, F. L., & Halford, K. J. (2011). A computer program for flow-log analysis of single holes (FLASH). *Groundwater*, 49(6), 926–931. <https://doi.org/10.1111/j.1745-6584.2011.00798.x>.
- Dlubac, K., Knight, R., Song, Y. Q., Bachman, N., Grau, B., Cannia, J., & Williams, J. (2013). Use of NMR logging to obtain estimates of hydraulic conductivity in the High Plains

- aquifer, Nebraska, USA. *Water Resources Research*, 49(4), 1871–1886.
<https://doi.org/10.1002/wrcr.20151>.
- Dunn, K. J., Bergman, D. J., & Latorraca, G. (Eds.).(2002). Nuclear magnetic resonance: Petrophysical and logging applications. *Handbook of Geophysical Exploration: Seismic Exploration*, 32, 1–293. <https://www.sciencedirect.com/handbook/handbook-of-geophysical-exploration-seismic-exploration/vol/32/suppl/C>.
- Eckhardt, D. A., Williams, J. H., & Anderson, J. A. (2011). *Geophysical, stratigraphic, and flow-zone logs of selected wells in Cayuga County, New York, 2001–2011* (Open-File Report 2011-1319). US Geological Survey. <https://pubs.usgs.gov/of/2011/1319>.
- Fitterman, D. V., & Prinos, S. T. (2011). *Results of time-domain electromagnetic soundings in Miami-Dade and southern Broward Counties, Florida*. (Open-File Report 2011-1299). US Geological Survey. <https://pubs.usgs.gov/of/2011/1299/>.
- Halford, K. J. (2009). *AnalyzeHOLE – An integrated wellbore flow analysis tool* (Techniques and Methods 4-F2). US Geological Survey. <https://pubs.usgs.gov/tm/tm4f2/>.
- Hammond, E. C., & Bell, C. F. (1995). *Hydrogeologic and water-quality data for the explosive experimental area, Naval Surface Warfare Center, Dahlgren Site, Dahlgren, Virginia* (Open-File Report 95-386). US Geological Survey. <https://pubs.usgs.gov/of/1995/0386/report.pdf>.
- Hanson, R. T., & Nishikawa, T. (1996). Combined use of flowmeter and time-drawdown data to estimate hydraulic conductivities in layered aquifer systems. *Ground Water*, 34(1), 84–94. <https://doi.org/10.1111/j.1745-6584.1996.tb01868.x>.
- Hearst, J. R., & Nelson, P. H. (1985). *Well logging for physical properties*. McGraw-Hill.
- Hess, A. E. (1986). Identifying hydraulically conductive fractures with a slow-velocity borehole flowmeter. *Canadian Geotechnical Journal*, 23(1), 69–78.
<https://doi.org/10.1139/t86-008>.
- Izbicki, J. A., Christensen, A. H., & Hanson, R. T. (1999). *United States Geological Survey combine well-bore flow and depth-dependent water sampler* (Fact Sheet 196-99). US Geological Survey. <https://pubs.usgs.gov/fs/1999/fs19699/>.
- Izbicki, J. A., Christensen, A. H., Newhouse, M. W., & Hanson, R. T. (2005). Temporal changes in the vertical distribution of flow and chloride in deep wells. *Ground Water*, 43(4), 531–544. <https://doi.org/10.1111/j.1745-6584.2005.0032.x>.
- Johnson, C. D., Mondazzi, R. A., & Joesten, P. K. (2011). *Borehole geophysical investigation of a formerly used defense site, Machiasport, Maine, 2003–2006* (Scientific Investigations, Report 2009-5120). US Geological Survey. <http://pubs.usgs.gov/sir/2009/5120/>.
- Jorgensen, D. G., & Petricola, M. (1993). *Petrophysical analysis of geophysical logs, National Drilling Company – U.S. Geological Survey ground-water research project for Abu Dhabi Emirate, United Arab Emirates*. US Geological Survey. <http://doi.org/10.3133/ofr9385>.
- Keys, W. S. (1990). *Borehole geophysics applied to ground-water investigations* (Techniques of Water-Resources Investigations 02-E2). US Geological Survey. <https://doi.org/10.3133/twri02E2>.

- Knight, R., David, O., Walsh, D. O., Butler, Jr., J. J., Grunewald, E. E., Gaisheng, L., Parsekian, A. D., Edward, C., Reboulet, E. C., Knobbe, S., & Barrows, M. (2015). NMR logging to estimate hydraulic conductivity in unconsolidated aquifers. *Ground Water*, 54(1), 104–114. <https://doi.org/10.1111/gwat.12324>.
- Lindenbach, E. J. (2016). Improving investigations with drill parameter recorder technology. In *Proceedings of the Rocky Mountain Geo-Conference 2016: Geotechnical Practice Publication #10* (pp. 51–59). American Society of Civil Engineers. <https://doi.org/10.1061/9780784480250.005>.
- Maurer, J., & Knight, R. (2016). Models and methods for predicting hydraulic conductivity in near-surface unconsolidated sediments using nuclear magnetic resonance. *Geophysics*, 81(5), D503–D518. <https://doi.org/10.1190/geo2015-0515.1>.
- Maurice, L., Barker, J. A., Atkinson, T. C., Williams, A. T., & Smart, P. L. (2011). A tracer methodology for identifying ambient flows in boreholes. *Groundwater*, 49(2), 227–238. <https://doi.org/10.1111/j.1745-6584.2010.00708.x>.
- McCall, W., Christy, T. M., Pipp, D., Terkelsen, M., Christensen, A., Weber, K., & Engelsen, P. (2014). Field application of the combined membrane-interface probe and hydraulic profiling tool (MiHPT). *Groundwater Monitoring & Remediation*, 34(2), 85–95. <https://doi.org/10.1111/gwmr.12051>.
- Molz, F. J., & Young, S. C. (1993). Development and application of borehole flowmeters for environmental assessment. *The Log Analyst*, 34(1), 13–23.
- Newhouse, M. W., Izbicki, J. A., Smith, G. A. (2005). Comparison of velocity-log data collected using impeller and electromagnetic flowmeters. *Groundwater*, 43(3), 291–461. <https://doi.org/10.1111/j.1745-6584.2005.0030.x>.
- Paillet, F. L. (1991). Graphical overlay applications in geotechnical log analysis. In *Proceedings of the 4th International MGLS/KEGS Symposium on Borehole Geophysics for Minerals, Geotechnical and Groundwater Applications* (pp. 249–265). Society of Professional Well Log Analysts, Minerals and Geotechnical Logging Society.
- Paillet, F. L. (1998). Flow modeling and permeability estimation using borehole flow logs in heterogeneous fractured formations. *Water Resources Research*, 34(5), 997–1010. <https://doi.org/10.1029/98WR00268>.
- Paillet, F. L. (2000). A field technique for estimating aquifer parameters using flow log data: *Groundwater*, 38(4), 510–521. <https://doi.org/10.1111/j.1745-6584.2000.tb00243.x>.
- Paillet, F. L. (2001) Hydraulic head applications of flow logs in the study of heterogeneous aquifers. *Groundwater*, 39(5), 667–675. <https://doi.org/10.1111/j.1745-6584.2001.tb02356.x>.
- Paillet, F. L. (2004). Borehole flowmeter applications in irregular and large-diameter boreholes. *Journal of Applied Geophysics*, 55(1), 39–59. <https://doi.org/10.1016/j.jappgeo.2003.06.004>.
- Paillet, F. L. (2012). A mass-balance code for the quantitative interpretation of fluid column profiles in ground-water studies. *Computers & Geosciences*, 45, 221–228. <https://doi.org/10.1016/j.cageo.2011.11.016>.

- Paillet, F. L., & Cheng, C. H. (1991). *Acoustic waves in boreholes*. CRC Press.
- Paillet, F. L., & Crowder, R. E. (1996). A generalized approach for the interpretation of geophysical well logs in ground water studies—Theory and application. *Groundwater*, 34(5), 883–898. <https://doi.org/10.1111/j.1745-6584.1996.tb02083.x>↗.
- Paillet, F. L., & Ellefsen, K. J. (2005). Downhole applications of geophysics. In D. K. Butler, (Ed.), *Near-surface geophysics* (pp. 439–472). Society of Exploration Geophysics. <https://doi.org/10.1190/1.9781560801719.ch12>↗.
- Paillet, F. L., Hite, L., & Carlson, M. (1999). Integrating surface and borehole geophysics in ground water studies—An example using electromagnetic soundings in south Florida. *Journal of Environmental and Engineering Geophysics*, 4(1), 45–55. <https://doi.org/10.4133/JEEG4.1.45>↗.
- Paillet, F. L., Lundy, J., Tipping, R., Runkel, A., Reeves, L., & Green, J. (2000a). *Hydrogeologic characterization of six sites in southeastern Minnesota using borehole flowmeters and other geophysical logs*. Water-Resources Investigations Report 2000–4142). US Geological Survey. <https://doi.org/10.3133/wri004142>↗.
- Paillet, F. L., & Ollila, P. W. (1994). *Identification, characterization, and analysis of hydraulically conductive fractures in granitic basement rocks, Millville, Massachusetts* (Water-Resources Investigations Report 94-4185). U.S. Geological Survey. <https://doi.org/10.3133/wri944185>↗.
- Paillet, F. L., Senay, Y., Mukhopadhyay, A., & Szekely, F. (2000b). Flow metering of drainage wells in Kuwait City, Kuwait. *Journal of Hydrology*, 234(3-4), 208-227. [https://doi.org/10.1016/S0022-1694\(00\)00261-4](https://doi.org/10.1016/S0022-1694(00)00261-4)↗.
- Paillet, F. L., Williams, J. H., Urik, J., Lukes, J., Kobr, M., & Mares, S. (2012). Cross-borehole flow analysis to characterize fracture connections in the Melechov Granite, Bohemian-Moravian Highland, Czech Republic. *Hydrogeology Journal*, 20(1), 143–154. <https://doi.org/10.1007/s10040-011-0787-1>↗.
- Pehme, P. E., Greenhouse, J. P., & Parker, B. L. (2007). The active line source temperature logging technique and its application in fractured rock hydrogeology. *Journal of Environmental and Engineering Geophysics*, 12(4), 307–322. <http://dx.doi.org/10.2113/JEEG12.4.307>↗.
- Pehme, P. E., Parker, B. L., Cherry, J. A., & Greenhouse, J. P. (2010). Improved resolution of ambient flow through fractured rock with temperature logs. *Groundwater*, 28(2), 191–211. <https://doi.org/10.1111/j.1745-6584.2009.00639.x>↗.
- Pehme, P. E. (2012). *New approaches to the collection and interpretation of high sensitivity temperature logs for detection of groundwater flow in fractured rock*. [Doctoral dissertation,, University of Waterloo]. UWSpace. <https://uwspace.uwaterloo.ca/handle/10012/6859>↗.
- Reynolds, R. J., Anderson, J. A., & Williams, J. H. (2015). *Geophysical log analysis of selected test and residential wells at the Shenandoah Road National Superfund Site, East Fishkill, Dutchess County, New York* (Scientific Investigations Report 2014-5228). US Geological Survey. <http://dx.doi.org/10.3133/sir20145228>↗.

- Rider, M. H., & Kennedy, M. (2011). *The geological interpretation of well logs* (3rd Ed.). Rider-French Consulting Limited.
- Risser, D. W., Williams, J. H., Hand, K. L., Behr, R., & Markowski, A. K. (2013). *Geohydrologic and water-quality characterization of a fractured-bedrock test hole in an area of Marcellus shale gas development, Bradford County, Pennsylvania* (Open-File Report OFMI 13-01.1). Pennsylvania Geological Survey. http://elibrary.dcnr.pa.gov/GetDocument?docId=1751415&DocName=OFMI13-01_Geohydro-WtrQltyCharac_FrxBedrxTestHole_BradfordCo.
- Risser, D. W., Williams, J. H., & Bierly, A. D. (2021). *Geohydrologic and water-quality characterization of a fractured-bedrock test hole in an area of Marcellus shale gas development, Sullivan County, Pennsylvania* (Open-File Report OFMI 21-02). Pennsylvania Geological Survey. http://elibrary.dcnr.pa.gov/GetDocument?docId=3642801&DocName=OFMI21-02_Geohydro-WtrQltyCharac_FrxBedrxTestHole_SullivanCo.
- Rivard, C., Bordeleau, G., Lavoie, D., Lefebvre, R., Ladevèze, P., Duchesne, M. J., Séjourné, S., Crow, H., Pinet, V. N., Brake, V., Bouchedda, A., Gloaguen, E., Ahad, J. M. E., Malet, X., Aznar, J. C., & Malo, M. (2019). Assessing potential impacts of shale gas development on shallow aquifers through upward fluid migration-A multi-disciplinary approach applied to the Utica Shale in eastern Canada. *Marine and Petroleum Geology*, 100, 466–483 <https://doi.org/10.1016/j.marpetgeo.2018.11.004>.
- Robertson, P. K. (1990). Soil classification using the cone penetration test. *Canadian Geotechnical Journal*, 27(1), 151–158. <https://doi.org/10.1139/t90-014>.
- Rutledge, A. T. (1991). *An axisymmetric finite-difference flow model to simulate drawdown in and around a pumped well* (Water-Resources Investigations Report 90-4098). US Geological Survey. <http://doi.org/10.3133/wri904098>.
- Schubert, C. E. (2010). *Analysis of the shallow groundwater flow system at Fire Island National Seashore, Suffolk County, New York* (Scientific Investigations Report 2009-5259). US Geological Survey. <http://pubs.usgs.gov/sir/2009/5259/>.
- Schulmeister, M. K., Butler Jr., J. J., Healey, J. M., Zheng, L., Wysocki, D. A., & McCall, G. W. (2003). Direct-push electrical conductivity logging for high-resolution hydrostratigraphic characterization. *Ground Water Monitoring & Remediation*, 23(3), 52–62. [Direct Zoom to Article](#).
- Spurlin, M. S., Barker, B. W., Cross, B. D., & Divine, C. E. (2019). Nuclear magnetic resonance logging-Example applications of an emerging tool for environmental investigations. *Remediation*, 29(2), 63–73. <https://doi.org/10.1002/rem.21590>.
- Stumm, F., & Como, M. D. (2017). Delineation of saltwater intrusion through use of electromagnetic-conduction logging: A case study in southern Manhattan Island, New York. *Water*, 9(9), 631. <https://doi.org/10.3390/w9090631>.
- Taylor, K. C., Hess, J. W., & Mazzela, A. (1989). Field evaluation of a slim-hole borehole induction tool. *Groundwater Monitoring Review*, 9(1), 100–104. <https://doi.org/10.1111/j.1745-6592.1989.tb01125.x>.

- Tsang, C. F., Hufschmied, P., & Frank, H. V. (1990). Determination of fracture inflow parameters from a borehole fluid conductivity method. *Water Resources Research*, 26(6), 561–578. <https://doi.org/10.1029/WR026i004p00561>.
- US Geological Survey (USGS). (2021a). *GeoLog Locator*. [https://txdata.usgs.gov/GeoLogArchiver/odata/Logs\(31765\)/LogFile](https://txdata.usgs.gov/GeoLogArchiver/odata/Logs(31765)/LogFile).
- US Geological Survey (USGS). (2021b). *GeoLog Locator*. [https://txdata.usgs.gov/GeoLogArchiver/odata/Logs\(34202\)/LogFile](https://txdata.usgs.gov/GeoLogArchiver/odata/Logs(34202)/LogFile).
- US Nuclear Regulatory Commission (USNRC). (2013). Part 39-Licenses and radiation safety requirements for well logging. In *NRC Regulations Title 10, Code of Federal Regulations*. USNRC. <https://www.nrc.gov/reading-rm/doc-collections/cfr/part039/full-text.html>.
- Walsh, D., Turner, P., Grunewald, E., Zhang, H., Butler, J. J., Reboulet, E., Knobbe, S., Christy, T., Lane, J. W., Johnson, C. D., Munday, T., & Fitzpatrick, A. (2013). A small-diameter NMR logging tool for ground-water investigations. *Groundwater*, 51(6), 914–926. <https://doi.org/10.1111/gwat.12024>.
- West, L. J., & Odling, N. E. (2007). Characterization of a multi-layer aquifer using open well dilution tests. *Groundwater*, 45(1), 74–84. <https://doi.org/10.1111/j.1745-6584.2006.00262.x>.
- White, J. E. (1983). *Underground sound. Application of seismic waves (Methods in Geochemistry & Geophysics, 18)*. Elsevier. <http://dx.doi.org/10.1190/1.9781560802471>.
- Williams, J. H. (2008). *Flow-log analysis for hydraulic characterization of selected test wells at the Indian Point Energy Center, Buchanan, New York* (Open-File Report 2008-1123). US Geological Survey. <http://doi.org/10.3133/ofr20081123>.
- Williams, J. H., Lapham, W. W., & Barringer, T. H., (1993). Application of electromagnetic logging to contamination investigations in glacial sand-and-gravel aquifers. *Ground Water Monitoring and Remediation Review*, 13(3), 129–138. <https://doi.org/10.1111/j.1745-6592.1993.tb00082.x>.
- Williams, J. H., & Johnson, C. D., (2004). Acoustic and optical borehole-wall imaging for fractured-rock aquifer studies. *Journal of Applied Geophysics*, 55(1–2), 151–159. <https://doi.org/10.1016/j.jappgeo.2003.06.009>.
- Williams, J. H., Lacombe, P. J., Johnson, C. D., & Paillet, F. L., (2007). Cross-borehole flow tests and insights into hydraulic connections in fractured mudstone and sandstone. In *Symposium on the Application of Geophysics to Engineering and Environmental Problems, Denver, Colorado*. Environmental and Engineering Geophysical Society. <https://doi.org/10.3997/2214-4609-pdb.179.01140-1152>.
- Williams, J. H., Risser, D. W., & Dodge, C. H. (2015) *Geohydrologic and water-quality characterization of a fractured-bedrock test hole in an area of Marcellus shale gas development, Tioga County, Pennsylvania* (Open-File Report OFMI 15-24). Pennsylvania Geological Survey. <https://maps.dcnr.pa.gov/publications/Default.aspx?id=852>.
- Winterer, E. (2012). Pelagic realms. In *Regional Geology and Tectonics: Principles of Geologic Analysis*, 538–551. <https://doi.org/10.1016/B978-0-444-53042-4.00019-4>.

- Young, S. C., & Pearson, H. S. (1995). The electromagnetic borehole flowmeter-Description and applications. *Ground Water Monitoring & Remediation*, 15(4), 138–146.
- Young, S. C., Julian, H. E., Pearson, H. S., Molz, F. J., & Boman, G. K. (1998). *Application of the electromagnetic borehole flowmeter* (EPA/600/R-98/058). US Environmental Protection Agency. https://frtr.gov/pdf/boreholeflowmeter_2.pdf.
- Zemanek, J., Glenn, E. E., Norton, L. J., & Caldwell, R. J. (1970). Formation evaluation by inspection with the borehole televiewer. *Geophysics*, 35(2), 254–269. <https://doi.org/10.1190/1.1440089>.
- Zoback, M. L., & Zoback, M. (1980). State of stress in the conterminous United States. *Journal of Geophysical Research*, 85(B11), 6113–6156. <https://doi.org/10.1029/JB085iB11p06113>.

9 Boxes

Box 1 - Cone Penetration Testing for Geotechnical Investigations

The Cone Penetration Test (CPT) method is widely used to identify conditions in the upper 30 m (100 ft) of the subsurface. Sensors on the cone measure tip resistance and sleeve friction as the cone is pushed into the ground. Tip resistance (Q_t) is determined by the force required to push the tip of the cone. Sleeve friction (F_s) is determined by the force required to push the sleeve through the soil. Both are measured in tons per square foot (tsf), kilogram force per square centimeter (kgf/cm^2), or bar units. The friction ratio (Fr) is the ratio between sleeve friction and tip resistance expressed as a percentage.

Soil behavior type (SBT) can be inferred from the CPT log measurements by using standard engineering correlation charts like those shown in Figure Box 1-1. Identification of sensitive fine-grained soils that are susceptible to liquefaction is important for geotechnical investigations of earthquake and landslide hazards.

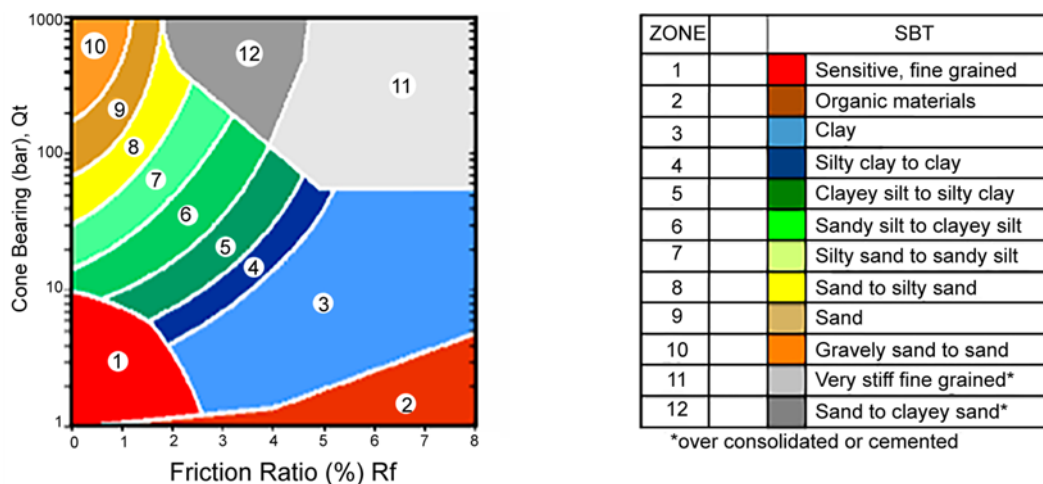


Figure Box 1-1 - Classification of soil behavior types (SBT) based on cone penetration testing (CPT) (Robertson, 1990).

[Return to where text linked to Box 1](#)

Box 2 - Nuclear Randomness and Filtering of Gamma Log Data

Gamma logs provide a record of total gamma radiation detected in a borehole and are useful over a wide range of borehole conditions. Although the petroleum industry has adopted the American Petroleum Institute (API) gamma ray unit, in groundwater studies, gamma logs most commonly are expressed in counts per second (cps).

The statistical nature of gamma emissions must be considered when collecting and interpreting gamma logs. A short time window for gamma pulse counting can introduce error into the log data due to nuclear statistical variation. The standard error (E) associated with a recorded gamma count of N is given as Equation Box 2-1.

$$E = \frac{\sqrt{N}}{N} \quad (\text{Equation Box 2-1})$$

Since the measured count at a depth station (i.e., location of a measurement from the reference point) depends on the time the probe is within about 30 cm (1 ft) of that nominal depth, the total counts from a formation characterized by average gamma activity of N_0 in cps is given by Equation Box 2-2, assuming the probe receives gammas originating from within 15 cm above and below the detector.

$$N = 36N_0/V \quad (\text{Equation Box 2-2})$$

where:

V = logging speed in m/min (meters per minute)

N_0 = formation emission rate (counts per second)

Given a formation emission rate (N_0) of 100 cps and a logging speed (V) of 10 m/min yields a measurement (N) of 360 effective counts for a standard fluctuation error (E) of about 5 percent. This error is acceptable in many applications in most geologic formations. However, some formations such as basalts, gabbros, clay-free carbonates, and clay-free sandstones may yield counts as low as 10 cps and logging rates need to be greatly reduced to obtain meaningful logs that faithfully indicate stratigraphy based on the counts expressed by Equation Box 2-2. Depending on project setting and objective—such as collecting high-resolution gamma logs in shallow boreholes for lithologic identification—logging rates may be reduced to less than 2 m/min.

The simplest way to verify that a gamma log has acceptable nuclear statistics is to check for repeatability. An example is given in Figure Box 2-1 where repeat logs are compared for a shallow borehole in alluvial sediments. Some differences in the distribution of counts on the logs are apparent, but the two logs clearly indicate a similar stratigraphy that could be used to identify depth intervals with low gamma activity associated with permeable sediments. However, there is a significant depth discrepancy between the two logs. This resulted from a failure to re-set the reference point before running the repeat log.

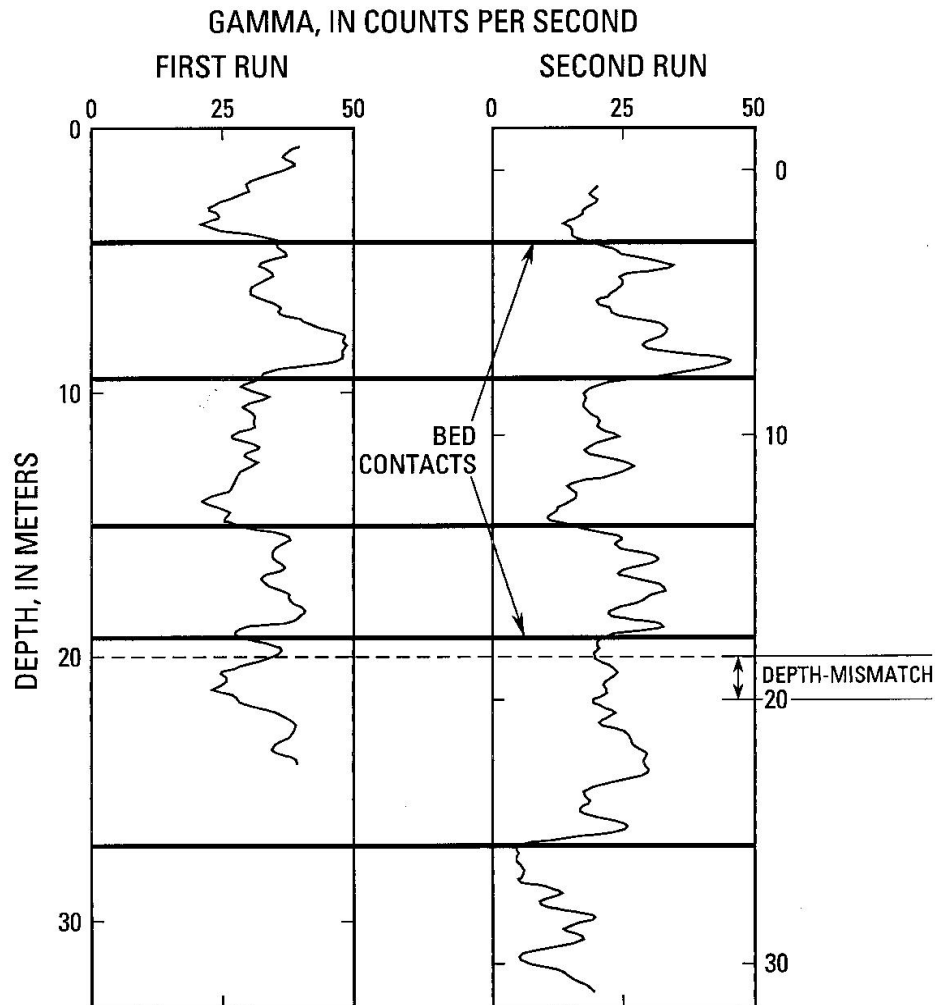


Figure Box 2-1 - Repeated gamma logs collected at 10 m/min from a borehole in an alluvial aquifer showing the ability to identify stratigraphic contacts despite the effects of nuclear statistical variation. Depth adjustment was needed because the reference point was not reset for the repeated log.

A common depth discrepancy is inconsistent establishment of the log measuring point, for example, the rotary table or Kelly bushing, top of casing, or land surface. Depth discrepancies need to be resolved before logs are interpreted. Software used for log analysis typically have depth shift capability that can be used for depth alignment purposes.

Random variation or *dither* in gamma logs can be removed by filtering, most commonly by averaging measured values with those at multiple adjacent depths. Since the gamma detector receives counts from about 30 cm (1 ft) above and below the nominal measurement station, a spatial filter of that length can be applied without losing any information about the formation being investigated. Longer spatial filters will affect the detailed lithologic information contained in the log but are commonly applied for display purposes. Log analysis software typically applies filtering for display only, while retaining the raw gamma counts.

[Return to where text linked to Box 2.1](#)

Box 3 - Use of Gamma Logs for Defining Lithology and Stratigraphy

Gamma logs are one of the simplest geophysical logs to collect but remain one of the most useful for defining lithology and stratigraphy of aquifer systems. As shown in Figure Box 3-1, lithologic contacts on gamma and other nuclear logs are picked at one-half of the maximum amplitude of a given bed.

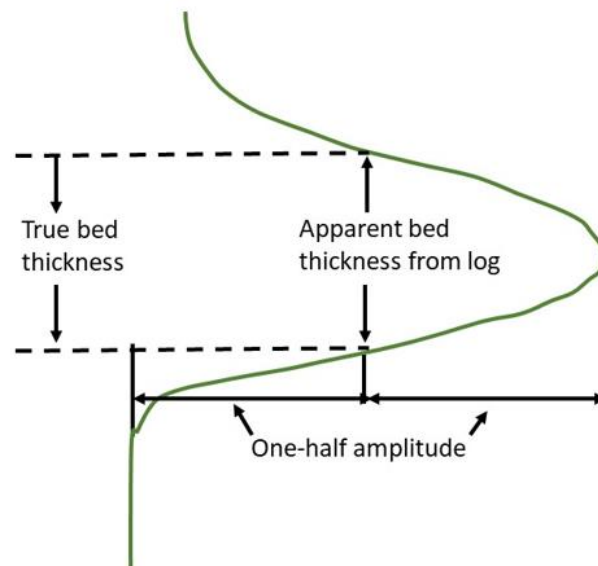


Figure Box 3-1 - Lithologic contacts on gamma logs and other nuclear logs are picked at one-half of the maximum amplitude of a given bed.

An example of the way in which a gamma log can be used to identify the depth contacts in a known stratigraphic sequence is shown in Figure Box 3-2 where the gamma log is correlated with the classic series of sedimentary formations on the south rim of the Grand Canyon in the southwestern United States. The depth of the contact between the Supai Formation and the underlying Redwall Limestone and other displayed contacts are defined by the depth where the log reaches the midpoint between the average gamma activity within each formation.

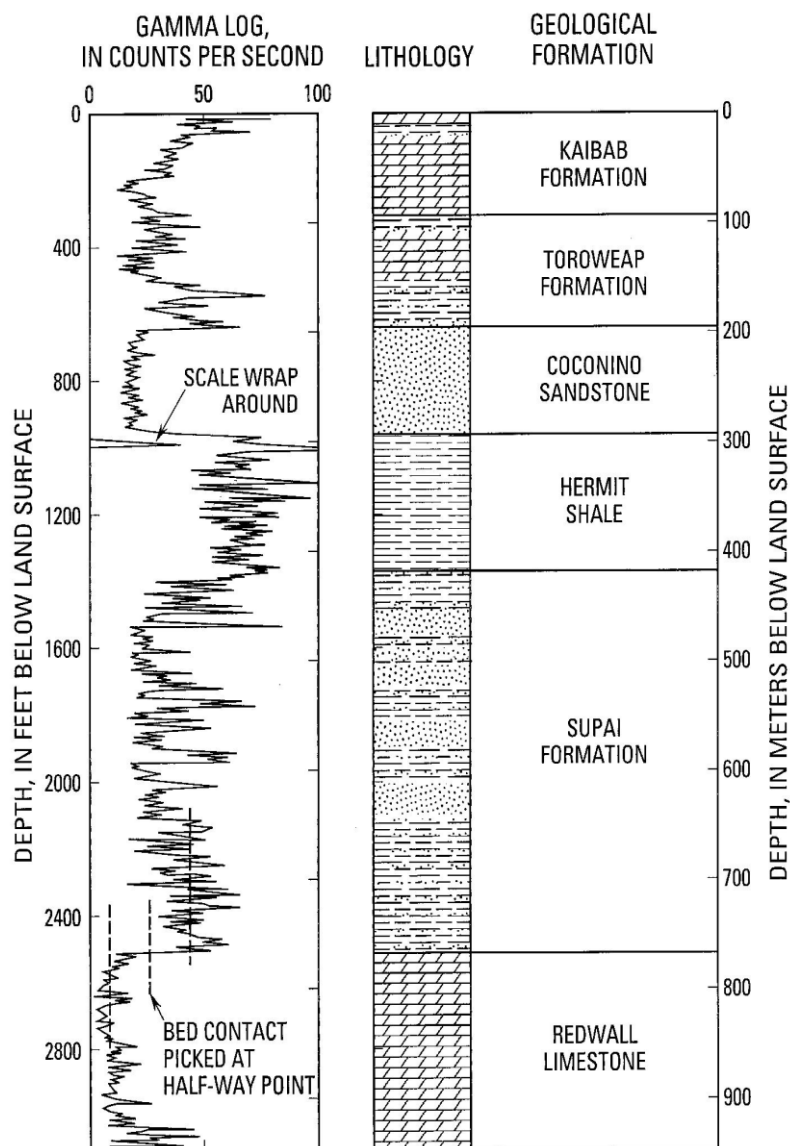


Figure Box 3-2 - Gamma log correlated with the sedimentary sequence for the south rim of the Grand Canyon, USA, showing how the shifts in gamma activity are associated with stratigraphic contacts.

Because there can be large differences among individual gamma readings, the display scale is sometimes adjusted to best display bed contacts, with excursions to large values represented as *wrap arounds* such as the one shown near the top of the Hermit Shale. These wrap arounds are common on paper logs collected with older analog systems before the advent of digital systems.

[Return to where text linked to Box 3](#) ↑

Box 4 - Use of Gamma Logs for Monitoring-Well Completion in Unconsolidated Aquifers

Gamma logs are commonly used to identify permeable intervals in unconsolidated aquifers where well screened will be placed for groundwater quality monitoring. Using the common assumption that gamma activity is associated with the *CF* at a given depth and that permeability is inversely related to the amount of clay, the gamma log can be interpreted to identify permeable intervals (low gamma activity) separated by confining beds (high gamma activity). Figure Box 4-1 shows an example of such a gamma log and its alignment with a drilling report commonly called a driller's log. The local geology consists of glaciofluvial sediments overlain by till. The driller's log provides a description of the sediments but only a rough estimate of the depths at which sediment properties change.

In contrast, the gamma log provides precise depth information but only gives gamma emission rate that has no unique relation to geology. Thus, interpretation of the two logs together provides information not available from either log on its own. In this case, the gamma log indicates the precise depth intervals where permeable intervals intersect the borehole.

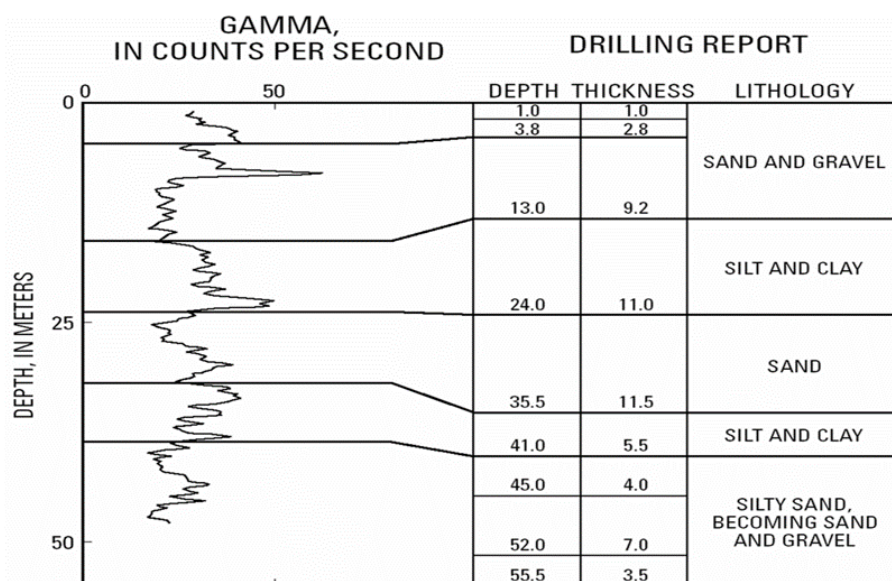


Figure Box 4-1 - Gamma log correlated with sediment description given by the driller's log for a borehole in glaciofluvial sediments overlain by till; the gamma peak near 23 m is interpreted as the base of the fine-grained material, thus a likely depth for placement of the top of the screen.

Note the prominent gamma high at about 9 m in depth in Figure Box 4-1. This might be interpreted as a thin clay-rich bed, but local geology indicates that the *sand and gravel* surrounding the upper part of the borehole is till. This local gamma *spike* probably represents a small boulder derived from unweathered granite containing a substantial component of gamma-emitting potassium-40 (^{40}K), demonstrating that higher gamma counts cannot be unambiguously assigned to clay mineral fraction.

[Return to where text linked to Box 4 ↑](#)

Box 5 - Geophysical Log Analysis of an Appalachian Basin Borehole

The following case study is summarized from Risser and others (2021). This case study presents the integrated analysis of drilling, construction, petrophysical, image, fluid property, and flow logs from a borehole that penetrated fractured clastic rock with fresh and saline water zones. In the Appalachian basin, the Marcellus, Utica, and upper Devonian shale formations are undergoing development by horizontal drilling and high-volume hydraulic fracturing at depths of greater than 1,200 m (4,000 ft) bls (below land surface). Fractured-bedrock aquifers overlying the Appalachian shale plays include those of Mississippian age as well as upper Devonian and Pennsylvanian age. In north-central Pennsylvania, USA, Marcellus gas drillers report zones of major water gains and losses in the uppermost Huntley Mountain Formation of Mississippian age. Consequently, protection of freshwater aquifers from saline water and methane migration during shale-gas development is an issue of paramount concern (Rivard et al., 2019). Characterization of the depth to the base of freshwater and the top of shallow gas and saline water is critical for proper design of programs for cementing surface and intermediate casing in gas and oil wells.

Box 5.1 Data Collected at the Site

In response to the migration issue, several major energy companies are collecting driller and petrophysical logs in the shallow interval of one topset well at each multiple well pad site. Geophysical logs were collected by the USGS and a private contractor in a 430 m (1,400 ft) deep test well on a synclinal ridge in east-central Sullivan County, Pennsylvania, USA. Since there were no known historic or current gas-well development in the area, it was believed the geohydrology and water quality that was characterized at the borehole site were representative of natural background conditions.

Petrophysical logs collected by the energy companies and the USGS collected image, flow, and fluid logs from the borehole site. Depth-dependent water quality samples were collected from the borehole for field and laboratory analysis including methane isotopic composition. A straddle-packer system was also used to hydraulically test and sample discrete intervals in the borehole. The data are shown in Figure Box 5-1 and explanation of the abbreviations used in the figure are provided in Table Box 5-1.

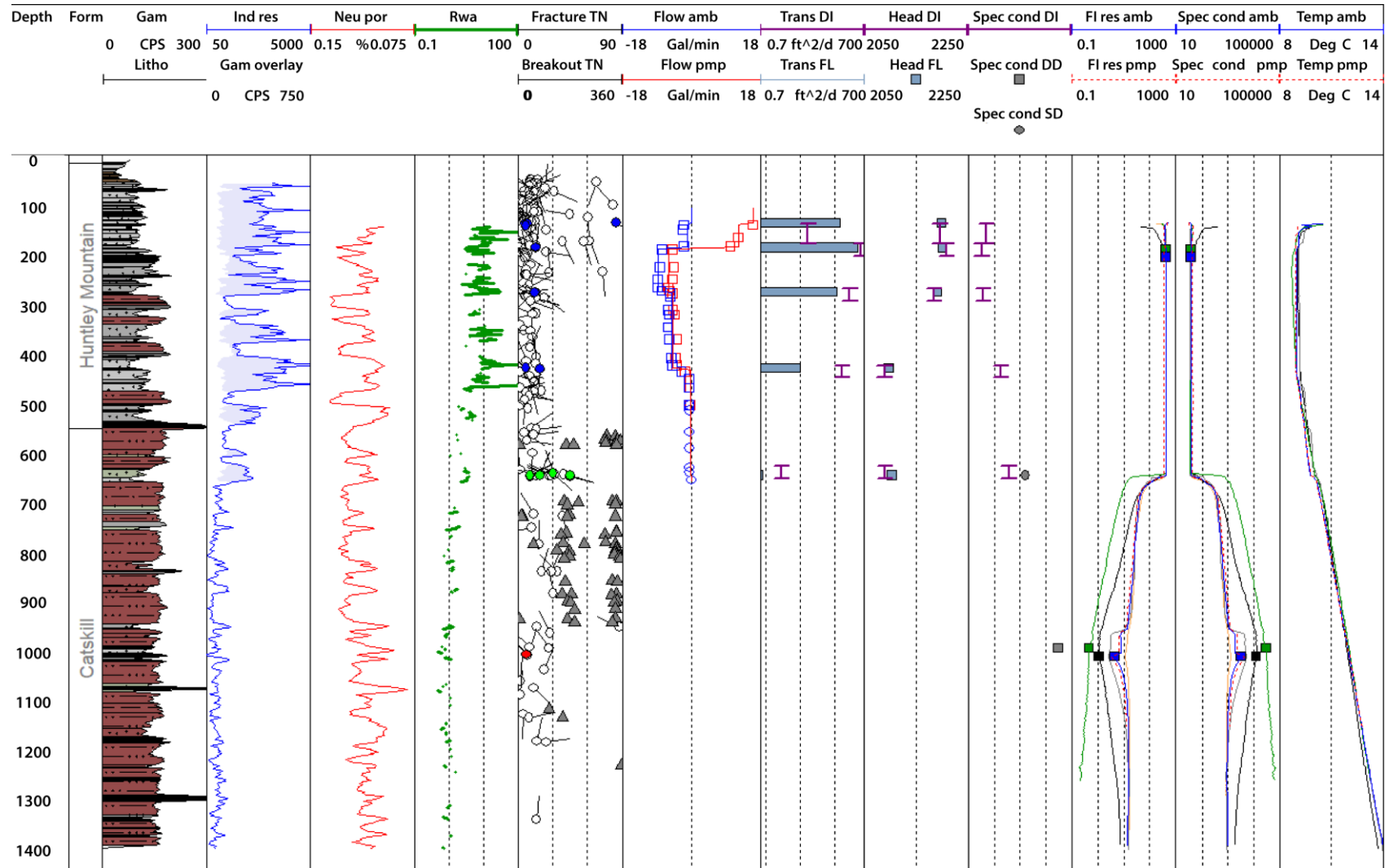


Figure Box 5-1 - Logs of geologic formations, gamma, lithology, induction resistivity, neutron porosity, and ambient and pumped flow, temperature, and fluid resistivity with flow zone transmissivity and hydraulic head from flow log analysis and discrete interval hydraulic test analysis of a fractured bedrock borehole.

Table Box 5-1 - Explanation of abbreviations used in Figure Box 5-1.

Abbreviation	Full content
Depth	Depth below land surface, in feet
Form	Geological Formation
GAM CPS	Gama in cps
Litho	Lithology
Ind res Ohm-m	Induction resistivity in ohm-m
Gam overly CPS	Gamma in cps with shading indicating greater resistivity relative to gamma
Neu por percentage	Neutron porosity in percent
Rwa Ohm-m	Estimated formation water resistivity in ohm-m
Fracture TN	Fracture location and orientation with tadpole body indicates dip angle in degrees and tail indicates the direction of dip in degrees relative to True Geographic North (blue indicates freshwater zone, green indicates transitional zone, and red indicates saline water zone)
Breakout TN	Breakout location and orientation relative to True Geographic North (gray triangle)
Flow amb Gal/min	Ambient flow in gallons per minute (blue square)
Flow pmp Gal/min	Pumped flow in gallons per minute (red square)
Trans DI ft 2/d	Transmissivity estimated from flow-log analysis in square feet per day (gray bar)
Head DI ft asl	Measured hydraulic head for discrete interval in feet above sea level (purple segment)
Head FL ft asl	Estimated hydraulic head from flow-log analysis in feet above sea level (gray square)
Spec cond DI	Specific conductance of discrete-interval water sample in microsiemens per centimeter at 25 °C (purple segment)
Spec cond DD	Specific conductance of depth-dependent water sample in microsiemens per centimeter at 25 °C (gray square)
Spec cond SD	Specific conductance of water discharged to surface while drilling in microsiemens per centimeter at 25 °C (gray circle)
FI res amb	Ambient fluid resistivity in ohm-m with corresponding depth-dependent sample (blue, black, and green squares)
FI res pmp	Pumped fluid resistivity in ohm-m
Spec cond amb and Spec cond pmp	Ambient specific conductance in microsiemens per centimeter at 25 °C with corresponding depth-dependent sample (blue, black, and green squares)
Temp amb, Deg C	Ambient temperature in °C
Temp pmp, Deg C	Pumped temperature in °C

Transmissivity of the entire borehole as well as for discrete intervals were estimated from short-term, specific-capacity tests analyzed using the method of Bradbury and Rothschild (1985). The transmissivity and hydraulic head of the flow zones were estimated using the analytical method of Day-Lewis and others (2011).

Box 5.2 Data Analysis

The log analyses and specific-capacity tests of discrete intervals showed similar trends. Partial dewatering of the shallowest flow zone occurred between the open-hole logging and discrete-interval testing, as reflected by the declining open-hole water levels and the observed decrease in cascading water. At least in part, this accounted for the difference between the transmissivity estimates for the shallow zone. Wellbore leakage past the upper packer during the two deeper hydraulic tests accounted, at least in part, for the differences between the transmissivity estimates for the deeper zones.

Analysis of the driller's log and petrophysical logs collected by the Pennsylvania Geological Survey indicated that the borehole penetrated sandstones and shales of the Huntley Mountain and Catskill Formations with the contact between the formations at 166 m (545 ft) bls. The acoustic televiewer log displayed a decrease in fracturing in the Catskill as compared to the Huntley Mountain Formation. Breakouts, which are formed by spalling of bedrock fragments from the borehole wall parallel to the direction of minimum horizontal stress, were commonly observed on the acoustic televiewer log in the Catskill red shales.

The distribution and orientation of the breakouts were like those delineated in two other deep boreholes on synclinal ridges in the region (Risser et al., 2013; Williams et al., 2015). Breakout orientation indicated that the direction of maximum horizontal stress was at an azimuth of about 75 degrees, which is consistent with regional estimates presented by Zoback and Zoback (1980).

Box 5.3 The Huntley Mountain Formation Flow Zones

Flow zones penetrated by the borehole in the Huntley Mountain Formation are described in Table Box 5-2.

Table Box 5-2 – The Huntley Mountain Formation borehole flow zones.

Flow zone 130-135 ft bls	<ul style="list-style-type: none"> ● Associated with several bedding-related fractures and a steeply dipping fracture in interbedded sandstone and carbonaceous shale. ● The zone produced about 1 gal/min (3.78 L/min) of downflow under ambient (non-pumping) conditions. Some of the downflow was cascading. ● The water level in the open hole during the study fluctuated across this fracture zone, which probably caused the yield from the zone to vary.
Flow zone 180 ft bls	<ul style="list-style-type: none"> ● Large sub-horizontal fractured zone in sandstone, produced 100 gal/min (380 L/min) during air-hammer drilling, by far the most of all the penetrated zones. ● The zone produced more than 7 gal/min (26.49 L/min) of downflow under ambient (non-pumping) conditions. ● The zone produced more than 12 gal/min (45.42 L/min) of upflow along with about 6 gal/min (22.71 L/min) of downflow when the open test hole was pumped at 16.2 gal/min (61.32 L/min).
Flow zone 267-275 ft bls	<ul style="list-style-type: none"> ● Associated with bedding-related fractures in sandstone above a contact with red shale. ● The zone received about 3 gal/min (11.35 L/min) of the downflow under ambient open-hole conditions, which was reduced to < 1 gal/min (3.78 L/min) when the borehole was being pumped at 16.2 gal/min (61.32 L/min).
Flow zone 425 ft bls	<ul style="list-style-type: none"> ● Associated with two bedding-related fractures in sandstone. ● The flow zone received about 4.8 gal/min (18.1 L/min) of the downflow under ambient open-hole conditions. Hydraulic heads that were 100 ft (30.5 m) lower than the composite head of the well. ● Estimated transmissivity values that were more than one and two orders of magnitude less than that of the 180 ft (54.9 m) zone. ● Specific conductance of water 180 $\mu\text{S}/\text{cm}$ at 25° C (). ● The rates of outflow were only slightly reduced when the borehole was pumped.

Box 5.4 The Catskill Formation Flow Zones

Flow zones penetrated by the borehole in the Catskill Formation are described in Table Box 5-3.

Table Box 5-3 - The Catskill Formation borehole flow zones.	
Flow zone 637-644 ft bls	<ul style="list-style-type: none"> ● Associated with multiple bedding-related and higher angle fractures in green sandstone. ● The zone received about 0.4 gal/min (1.5 L/min) of the downflow under ambient open-hole conditions. ● The rates of outflow to these two zones were only slightly reduced when the borehole was pumped. ● Estimated hydraulic head of the zone was 100 ft (≈ 30.5 m) lower than the composite head of the well. ● The zone had estimated transmissivity values that were more than one and two orders of magnitude less than that of the 180 ft (54.9 m) zone. ● The specific conductance of the water sampled during discrete-interval testing was not believed to be representative as it continuously increased during pumping reaching a maximum value of 380 $\mu\text{S}/\text{cm}$ at 25° C. ● The specific conductance of the blown yield, which is believed to be representative, was 1,650 $\mu\text{S}/\text{cm}$ at 25° C. Based on this specific conductance, the water quality of the zone would be considered transitional between the freshwater zones above and the saline-water zone below. ● No flow was detected by the heat-pulse flowmeter below the zone. ● The temperature gradient below the zone to the bottom of the well approached the geothermal gradient (approximately 0.56° C per 100 ft (30.5 m)), which indicated there was minimal fracture transmissivity in this interval.
Flow zone 1,002 ft bls	<ul style="list-style-type: none"> ● A bedding fracture at 1,003 ft (305.7 m) bls was associated with a very small inflow of saline water under ambient open-hole conditions. ● The saline-water inflow appeared on the optical-televiewer log as streaks of reddish iron-oxide staining extending below several distinct points along the bedding-related fracture. ● The iron-oxide staining of the most prominent streak also extended above the fracture. ● The specific conductance of this saline inflow was greater than 30,000 $\mu\text{S}/\text{cm}$ at 25° C (77° F) as indicated by depth-dependent sampling. The time series of fluid resistivity and specific conductance logs collected over several months indicated apparent downward and upward flow of the saline water. The slow downward movement of the saline water would be the result of the contrast in density between the saline water and the freshwater used by the driller to flush the test hole. ● The slow upward movement of saline water suggests an upward hydraulic gradient between the very low transmissivity saline-water zone and the transitional zone at 637 to 644 ft (194.2-196.3 m) bls. The saline inflow contained thermogenic methane at a concentration of more than 90 mg/L.

Box 5.5 Case Study: Formation Water Salinity in the Huntley Mountain and Catskill Formations

Formation water resistivity (R_w) was estimated for the Huntley Mountain and Catskill sandstone intervals. At this site sandstone intervals were interpreted to be present where gamma values were < 80 cps based on application of Archie's Equation (Archie,

1942). Archie's Law is an empirical relation that describes formation water resistivity in terms of the true formation resistivity, porosity, and the cementation factor as shown in Equation Box 5-1.

$$R_w = R_t \emptyset^m \quad (\text{Equation Box 5-1})$$

where:

R_w = formation water resistivity, typically in ohm-m ($\text{MLT}^{-3}\text{I}^{-2}$, i.e., dimensions in mass, length, time, and electric current)

R_t = true formation resistivity, typically in ohm-m ($\text{MLT}^{-3}\text{I}^{-2}$)

\emptyset = porosity (dimensionless)

m = cementation factor (dimensionless)

Values of true formation resistivity were derived from the induction resistivity log. Values of porosity were derived from the neutron porosity log, which is affected not only by porosity but also by clay content. A cementation factor of 2.0, which is typical for consolidated sandstone, was assumed (Jorgensen & Petricola, 1993 Rider & Kennedy, 2011).

The application of Archie's Equation to estimate water quality is complicated by the variable clay content, presence of very fresh formation water in shallower intervals, low primary porosity, and the discrete fractured nature of the bedrock. Due to particle-surface conduction, Archie's Equation becomes invalid in a low-clay sandstone when fluid resistivity is greater than about 10 ohm-meters (Hearst & Nelson, 1985). Increasing clay content increases surface conduction and lowers this threshold.

The estimated formation water resistivities for the selected sandstone intervals above 500 ft (152.4 m) bls were, generally, greater than 5 ohm-m. Between 450 to 800 ft (137.2 to 243.8 m) bls, the estimated formation water resistivities generally ranged from 1 to 5 ohm-m. Below 800 ft (243.8 m) bls, the estimated formation water resistivities generally were 1 ohm-m or less. A formation water resistivity of < 1 ohm-m at the ambient formation temperature of 12° C (53.6° F) at a depth of 1,000 ft (304.8 m) bls, corresponds to a specific conductance of more than 12,500 $\mu\text{S}/\text{cm}$ at 25° C. The apparent transition from fresh to saline formation water between 500 and 800 ft (152.4 and 234.8 m) bls that was estimated using this petrophysical approach is consistent with the fracture zones at 425 ft (129.5 m), 637 to 644 ft (194.2 to 196.3 m), and 1,003 ft (305.7 m) bls being fresh-, transitional-, and saline-water bearing, respectively.

[Return to where the text linked to Box 5 ↑](#)

Box 6 - Use of Gamma, Electric, and Induction Logs for Defining Lithology and Salinity

In many aquifer studies, the interpretation of the log data involves both lithology and the quality of the water saturating the formation. Electric and induction-conductivity logs respond to both clay content of the formation and dissolved solids content of the pore water, and therefore are commonly collected and interpreted along with gamma logs to separate these two effects. A simple example of the application of electric and gamma logs for the delineation of saltwater intrusion in a coastal sedimentary aquifer in Egypt (Paillet, 1991; Paillet & Crowder, 1996) is presented in Figure Box 6-1.

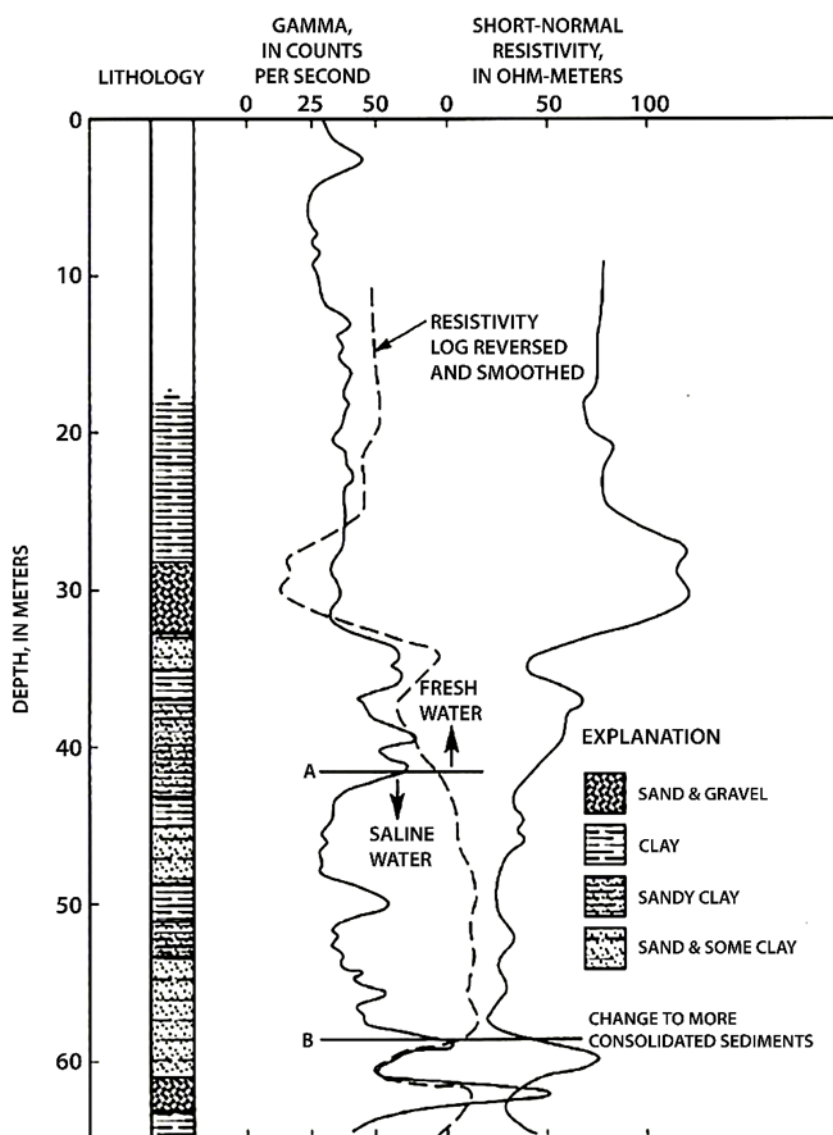


Figure Box 6-1 - Comparison of lithology, gamma and short normal resistivity logs collected from a mud-filled borehole in coastal sediments; departure of the trends in gamma and resistivity logs show where increased salinity affects log response (Paillet, 1991).

Normal-resistivity log data collected in a mud-filled borehole responded to both salinity and clay content in the unconsolidated aquifer. The effects of salinity associated with saltwater intrusion and presence of clay-rich zones were separated by using the gamma log as a clay indicator. To aid in the analysis, the resistivity log was reversed and overlaid on the gamma log and its amplitude was adjusted to match the variation in the gamma log trace. The two logs deflected in a similar way as they responded to changes in the CF, departing below 34 m (111.55 ft) where increased salinity caused the log traces to separate. The two logs started to track each other again at 58 m (190 ft) where the borehole penetrated more consolidated sediments with decreased porosity.

[Return to where the text linked to Box 6 ↴](#)

Box 7 - Use of Flow Logs for Hydraulic Property Analysis

In some cases, flow logs are made under only a single hydraulic condition, which is typically ambient flow. In these cases, the flow logs can be used to identify the *hydraulically active* zones within a borehole under the measured conditions. No other interpretation is possible. In fact, inflow and outflow rates under ambient conditions can be misleading. The water level in an open borehole represents the transmissivity-weighted average of the water levels in the individual zones penetrated by the borehole. The zone with the lowest transmissivity controls (limits) flow between borehole intervals. Thus, the ambient hydraulic condition minimizes the hydraulic gradient driving flow into or out of the borehole in the most permeable zones. This causes the flow to/from the most transmissive zones to appear no different from the inflow or outflow from one or more of the other zones. Thus, under ambient flow conditions, relatively low transmissivity zones have negligible effect on the borehole water level, but a major or even dominant effect on the measured ambient borehole flow (Paillet et al., 2000a).

Flow logs that can be used for quantitative hydraulic property analysis are collected under quasi-steady-state ambient and stressed conditions. As shown in Figure Box 7-1, flow measurements are interpreted with other geophysical logs to identify the distribution of and flow between permeable zones under the two different hydraulic conditions.

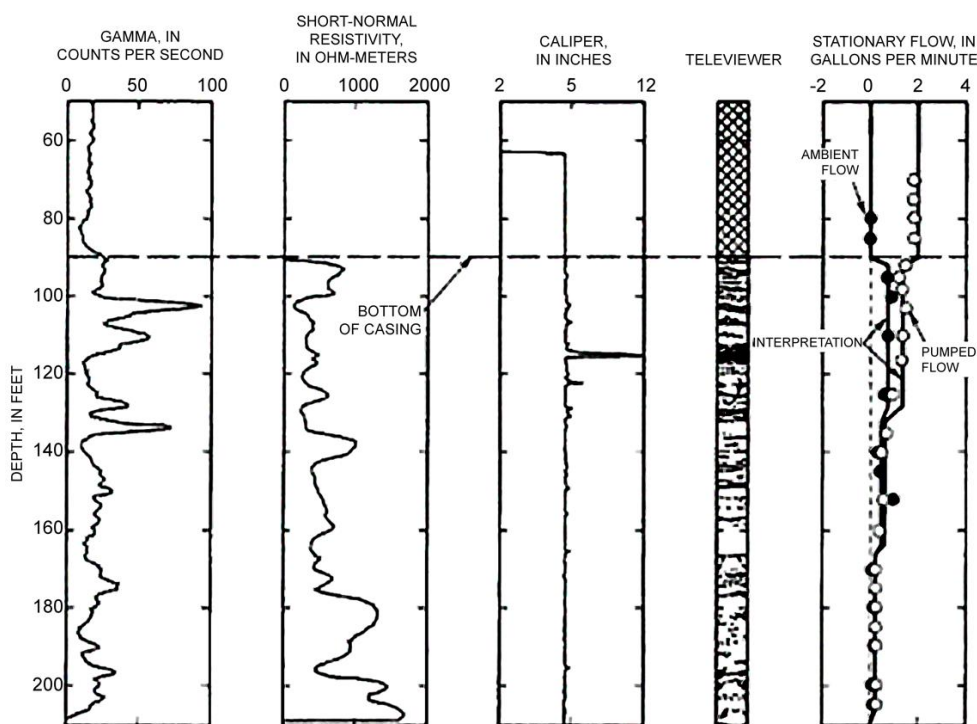


Figure Box 7-1 - Stationary flow measurements under ambient and pumped conditions interpreted with other geophysical data from an open borehole in a carbonate-bedrock aquifer at the Rochester site, southeastern Minnesota, USA (Paillet et al., 2000a). Scale conversions: 60 ft \cong 18 m, 200 ft \cong 61 m, 2 inches \cong 5 cm, 2 inches \cong 30.5 cm, -2 gal/min \cong -8 L/min, 4 gal/min = 15 L/min.

Given a set of flow logs collected under two different hydraulic conditions, the proportion method can be used to estimate the relative transmissivity of flow zones penetrated by the borehole. Ambient hydraulic-head differences between the flow zones are eliminated from the analysis by subtracting the flows from the two logs according to Equation Box 7-1 and Equation Box 7-2.

$$Q_k^0 = Q_k^b - Q_k^a \quad (\text{Equation Box 7-1})$$

where:

Q_k^a = measured inflow for the zone k obtained under ambient flow condition a (ambient)

Q_k^b = measured inflow for the zone k obtained under flow condition b (pumping or injection)

Q_k^0 = measured inflow for the zone k

$$\frac{T_k}{\sum T_k} = \frac{Q_k^0}{\sum Q_k^0} \quad (\text{Equation Box 7-2})$$

where:

T_k = relative transmissivity for zone k

Outflow is expressed as negative inflow. The relative transmissivity for zone k is then expressed as the ratio of Q_k^0 for zone k and the sum of Q_k^0 for each of the zones (Paillet, 1998). Flow-interpretation using the proportion method is shown in Table Box 7-1 for four boreholes open to fractured and solutioned carbonate bedrock.

Table Box 7-1 - Flow-log interpretation using the proportion method for open boreholes in carbonate-bedrock aquifers at selected sites, southeastern Minnesota, USA (modified from Paillet et al., 2000a). Condition A is ambient flow and condition B is injected flow. Scale conversion: 1 gal/min \cong 4 L/min.

Depth Interval (m)	Depth Interval (ft)	Zone ¹ Type	Condition A (gal/m)	Condition B (gal/m)	Difference (gal/m)	Percent of Overall Borehole Transmissivity
Savage Site - Observation well #593579						
			Ambient	Injection		
177.39–178.61	582–586	a or b	-1.2	-2.8	1.6	18
184.40–195.07	605–640	a	1.2	-6.2	7.4	82
Total			0	-9.	9.0	100
Faribault Site - Observation well #625327						
			Pumping	Ambient		
14.63	48	b	5.8	5.0	0.8	40
24.38	80	c	1.0	0.9	0.1	5
35.05	115	e	2.0	2.1	-0.1	-5
52.43	172	e	-4.5	-5.4	0.9	45
55.47	182	e	-1.8	0.0	-1.8	-90
63.40	208	b	-0.5	-2.6	2.1	105
68.28	224	e	0.0	0.0	0.0	0
Total			2.0	0.0	2.0	100
Rochester site - Observation well #485610						
			Pumping	Ambient		
26.52–28.04	87–92	b	0.55	-0.80	1.35	68
39.32–39.93	129–131	b and d	0.85	0.30	0.55	28
50.9	167	b	0.40	0.35	0.05	2
62.48–64.01	205–210	e	0.20	0.15	0.05	2
Total			2.0	0.00	2.00	100
Austin site - Observation well #613746						
			Pumping	Ambient		
24.99–26.52	82–87	f	4.20	2.35	1.85	93
28.04–30.48	92–100	c or e	-2.20	-2.35	0.15	7
Total			2.00	0.00	2.00	100

¹Zone Type:

a: Permeable bed without fractures or bedding planes.

b: Bedding plane or set of planes with possible minor solution enlargements.

c: Bedding plane or set of planes with significant enlargement by solutioning.

d: Fracture or set of fractures, possibly enlarged by solutioning.

e: Paleokarst horizon characterized by irregular solution openings.

f: Cavernous zone possibly developed on bedding planes or paleokarst horizon.

[Return to where the text linked to Box 7 ↑](#)

Box 8 - Relating Gamma Log and Core Porosity

The issues involved in relating geophysical logs with other borehole measurements are illustrated by the comparison of a gamma log from a borehole in a sandstone aquifer with a set of core porosity measurements obtained from the same borehole. Gamma-log response is commonly attributed to the clay fraction (CF) in the approximately 30-cm (1-ft) diameter sample volume of the gamma detector. The presence of clay effectively reduces the porosity of sandstone so it is expected that gamma counts on the log might be inversely related to core sample porosity. A section of gamma log from a sandstone aquifer and a list of discrete core porosity data obtained using plugs taken from core samples is shown in Figure Box 8-1. The relation between core and gamma values shows poor correlation and would indicate that gamma activity is not a good indicator of core porosity contrary to the initial assumption. This occurs for two reasons that are typical of such correlation attempts:

- 1) a depth discrepancy exists between nominal depths given for log and core, and
- 2) there is a difference in the volume sampled by the two different measurements as shown in Figure Box 8-1.

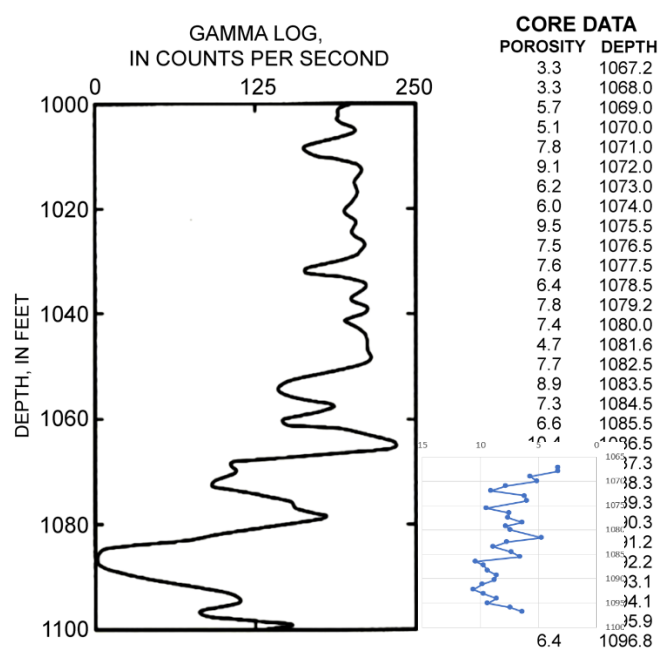


Figure Box 8-1 - Gamma log collected from a borehole in a sandstone aquifer and a set of discrete core porosity measurements obtained from plugs removed from a core taken from the same borehole (Paillet & Crowder, 1996). Scale conversions: 1,000 ft \cong 305 m; 1,100 ft \cong 335 m.

[Return to where text linked to Box 8](#)

10 Exercise Solutions

Solution Exercise 1

Data for this exercise, is provided in a spreadsheet within a [zip file that can be downloaded from the web page for this book](#)[↗]. The zip file is named *Geophysical-Logging-for-Hydrogeology-Exercise_Spreadsheets.zip*. The solution is provided in the spreadsheet named

GPloggingExercise1_CPT_SBT_Solution.xlsx

in the worksheet named

[*Answer*].

An example of how you can combine the Direct Push logs, computed friction ratio, and soil behavior type (SBT) is shown in the worksheet [*Extra-CPT_SBT_litho*].

[Return to Exercise 1](#) ↗

[Return to where text linked to Exercise 1](#) ↗

Solution Exercise 2

Data for this exercise, is provided in a spreadsheet within a [zip file that can be downloaded from the web page for this book](#)[↗]. The zip file is named *Geophysical-Logging-for-Hydrogeology-Exercise_Spreadsheets.zip*. The solution is provided in the spreadsheet named

GPloggingExercise2_GammaFilter_Solution.xlsx

in the worksheet named

[*Answer-Gamma&FilterPlots*].

Your raw gamma and filtered gamma plots should look something like these plots. If your plots do not look like this, check the formula used in column C to apply a filter. Try different ranges in your averaging filter. For a more advanced filter, you can use the AVERAGEIF function in Excel to omit the ≈9999.0 values that indicate missing values with =Averageif(range to average, ">0").

[Return to Exercise 2](#) ↗

[Return to where text linked to Exercise 2](#) ↗

Solution Exercise 3

Data for this exercise, is provided in a spreadsheet within a [zip file that can be downloaded from the web page for this book](#)[↗]. The zip file is named *Geophysical-Logging-for-Hydrogeology-Exercise_Spreadsheets.zip*.

The solution is provided in the spreadsheet named

GPloggingExercise3_GammaLithoStrat_Solution.xlsx

in the worksheet named

[Answer-StratPick_GeolLog].

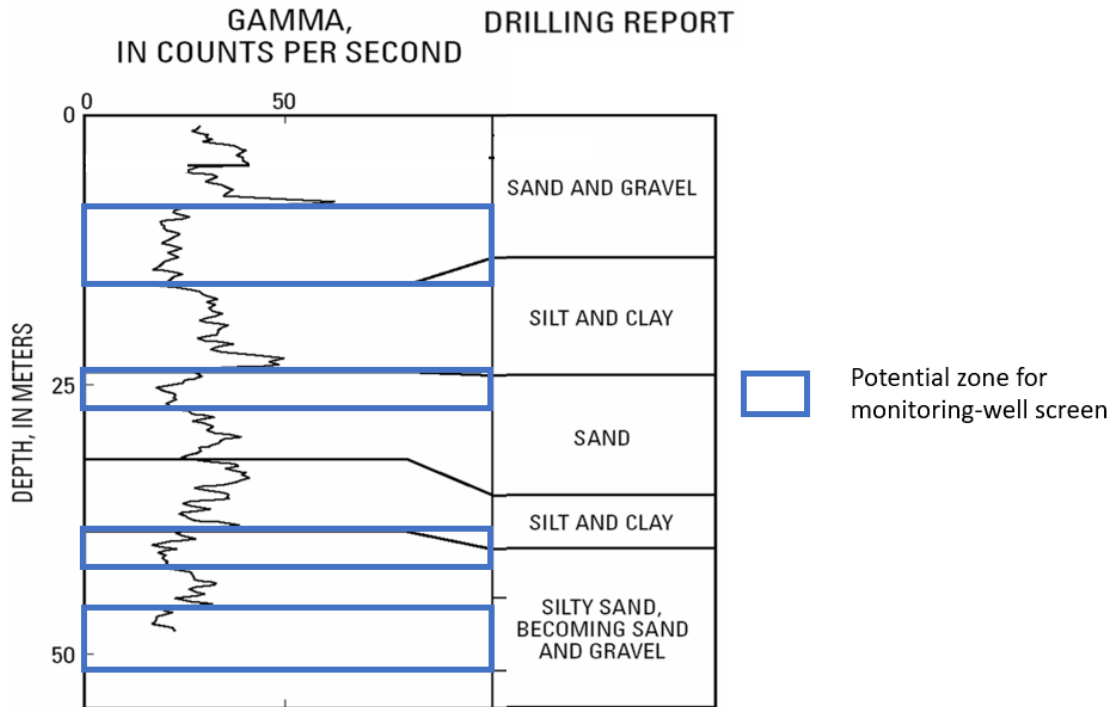
Although there are multiple ways to do this in Excel, the easiest way is to make a graphical comparison. The goal was to determine the top and the bottom of the confining unit. After you plotted the gamma data and delineated the confining unit based on gamma alone, your results should look like the plot shown in *[Answer-StratPick_GeolLog]* with the top at ≈ 600 ft (≈ 182.9 m) and the bottom at ≈ 800 ft (≈ 243.8 m). The next step was to compare your interpretation to the geologist log. Did your interpretation of the gamma log match the geologist's log?

[Return to Exercise 3](#)[↗]

[Return to where text linked to Exercise 3](#)[↗]

Solution Exercise 4

Potential zones to be fitted with well screen for a nested monitoring well installation are indicated with blue rectangles in the diagram below.



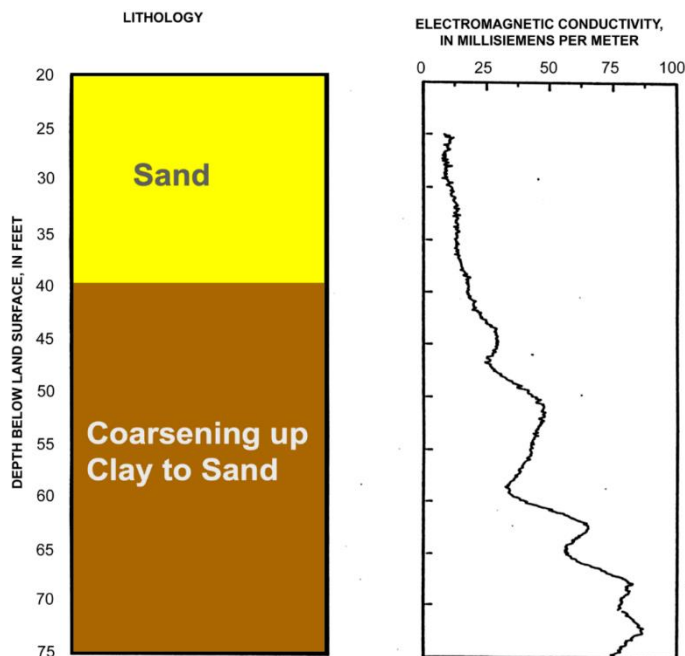
Gamma and driller logs with blue rectangles indicating appropriate zones for screens in a nested monitoring well.

[Return to Exercise 4](#) ↑

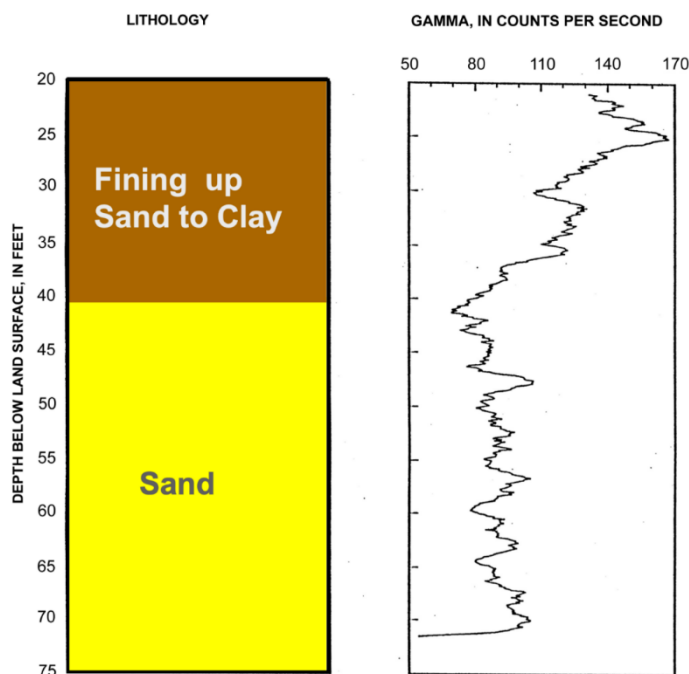
[Return to where text linked to Exercise 4](#) ↑

Solution Exercise 5

- a) Your interpreted lithologic logs should look like the colored lithology on the left side of these diagrams.

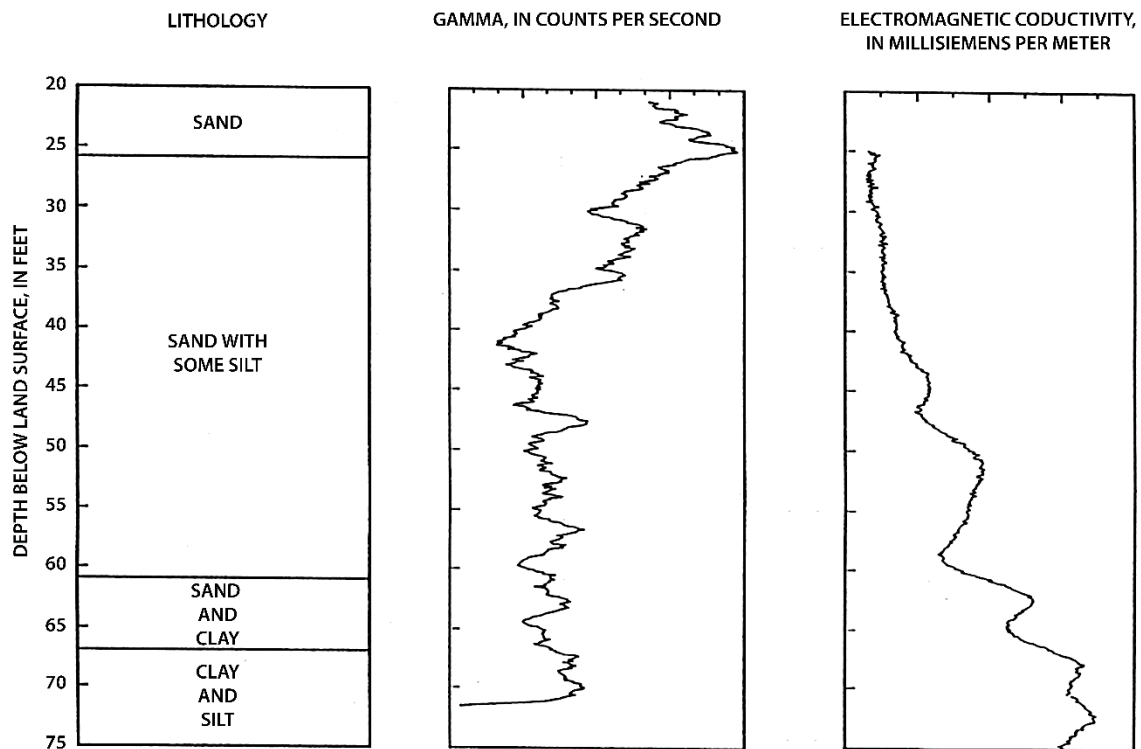


Electromagnetic-conductivity log and interpreted lithology of a monitoring well at the Explosive Experimental Area, Naval Surface Warfare Center, Dahlgren Site, Dahlgren, Virginia, USA. For the depth scale, 20 ft \approx 6 m and 75 ft \approx 23 m.



Gamma log and interpreted lithology of a monitoring well at the Explosive Experimental Area, Naval Surface Warfare Center, Dahlgren Site, Dahlgren, Virginia, USA. For the depth scale, 20 ft \approx 6 m and 75 ft \approx 23 m.

- b) Assuming that the gamma log is significantly affected by the presence of glauconite, the electromagnetic conductivity log is given more weight so the logs are interpreted to indicate a coarsening upward sequence from clay to sand as shown in this diagram.



Lithologic, gamma, and electromagnetic-conductivity logs of a monitoring well at the Explosive Experimental Area, Naval Surface Warfare Center, Dahlgren Site, Dahlgren, Virginia, USA with interpretation heavily weighted on the electromagnetic-conductivity logs because the gamma log is assumed to be impacted by the presence of glauconite. For the depth scale, 20 ft \cong 6 m and 75 ft \cong 23 m.

To confirm the alternate interpretation, the lithologic log based on split-spoon sampling during drilling is presented in this table, confirming the interpretation in (b).

Lithologic log of observation wells at the Explosive Experimental Area, Naval Surface Warfare Center, Dahlgren, Virginia, USA (From Hammond and Bell (1995) at [USGS](#) ⁷).

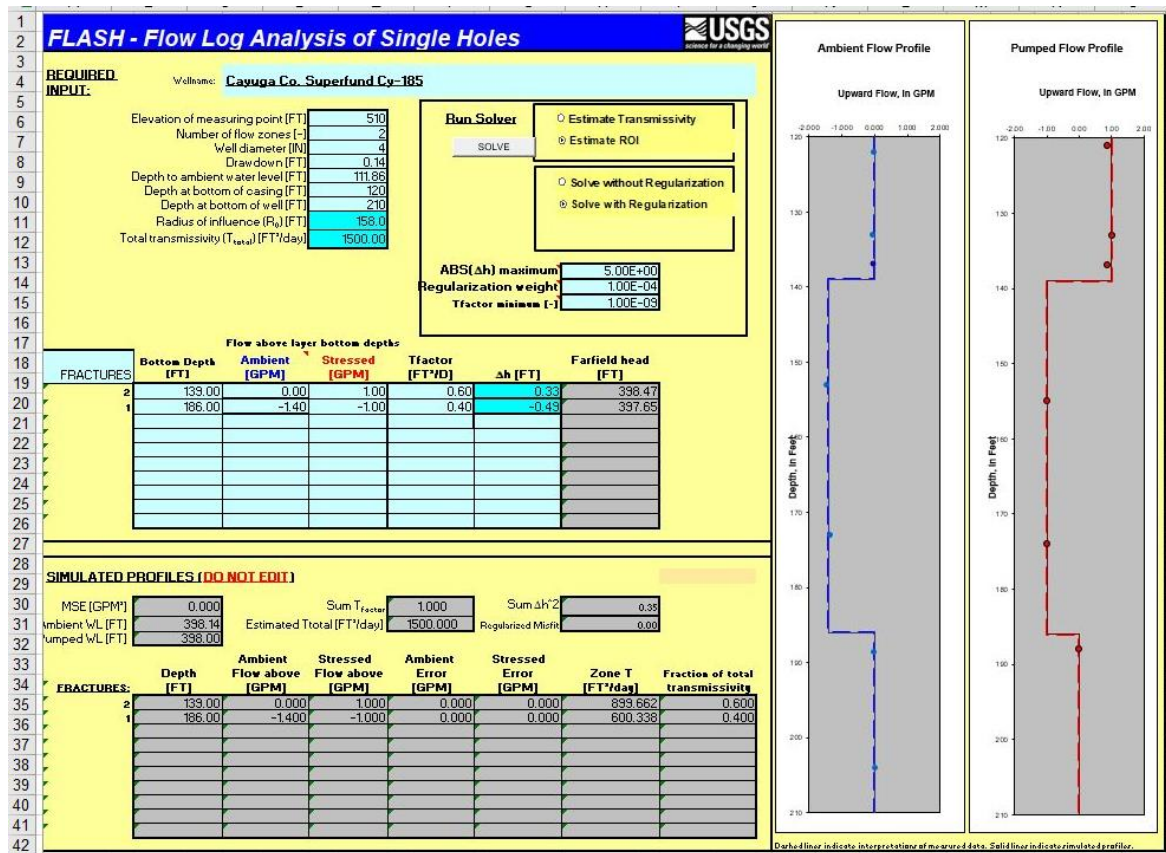
Depth (ft) 1 ft \approx 0.3 m	Description Well EEA-M5 (54Q63).
18.5	Sand, greenish-black (5GY 2/1), fine-to very-fine-grained, micaceous, very glauconitic.
20–22	Sand, dark-greenish-gray (5GY 4/1). very-fine-to fine-grained, micaceous, glauconitic. Contains shell fragments. Contains quartz pebble (75 mm) at 21.5 ft (from above?).
25–27	Silty sand, dark-greenish-gray (5GY 4/1) to greenish-black (5GY 2/1), fine-grained, micaceous, glauconitic. Contains abundant bivalve fragments and whole shells (<i>Macrocallista</i> , <i>Cubitostrea</i>), some shells articulated.
30–32	Silty sand, dark-greenish-gray (SGY 4/1), fine-grained, micaceous, glauconitic. Contains bivalve fragments and whole shells (<i>Macrocallista</i> , <i>Cubitostrea</i>). Massively bedded.
35–37	Silty sand, dark-greenish-gray (5GY 4/1), fine-grained, micaceous, glauconitic. Contains bivalve fragments and whole shells (<i>Macrocallista</i> , <i>Cubitostrea</i>). Massively bedded.
40–42	Silty sand, dark-greenish-gray (5GY 4/1) to greenish-black (5GY 2/1), medium-to fine-grained, micaceous, very glauconitic. Contains bivalves (<i>Macrocallista</i> , <i>Venericardia</i> , <i>Cubitostrea</i>). Massively bedded.
45–47	Silty sand, greenish-gray (5GY4/1) to greenish-black (5GY 2/1) very-fine-to medium-grained, micaceous, very glauconitic. Massively bedded. Sparsely fossiliferous (<i>Macrocallista</i> , <i>Venericardia</i>).
50–52	Silty sand, greenish-black (5GY 2/1), fine-grained, micaceous, very glauconitic. Massively bedded. Sparsely fossiliferous (<i>Venericardia</i>), shells chalky. Contains 3" diameter carbonate concretion at 51.7 ft.
55–57	Silty sand, greenish-black (5GY 2/1), fine-to very-fine-grained, micaceous, very glauconitic. Bioturbated. Moderately fossiliferous (<i>Venericardia</i> , <i>Macrocallista</i>).
60–62	Silty sand, dark-greenish-gray (5GY4/1), fine-to very-fine-grained, micaceous, glauconitic. Bioturbated. Sparsely fossiliferous (<i>Venericardia</i>).
65–67	Clayey silty sand, dark-greenish-gray (SGY 4/1) to greenish-black (5GY 2/1), fine-grained, micaceous, glauconitic. Bioturbated. Contains plant material. Fossiliferous (<i>Venericardia</i> , <i>Cubitostrea</i>).
70–72	Sandy silty clay, dark-greenish-gray (5GY 4/1), micaceous, glauconitic. Sand is very-fine-grained. Sparsely fossiliferous. Contains plant stem.
75–77	Silty sandy clay, dark-greenish-gray (5GY 4/1), micaceous, glauconitic. Sand is very-fine-grained. Contains sparse chalky shell fragments.

[Return to Exercise 5](#) [↑]

[Return to where text linked to Exercise 5](#) [↑]

Solution Exercise 6

The [FLASH] solution to the flow-log analysis exercise is presented below.



The model-estimated transmissivity for the 133-foot zone is 900 ft²/d and that for the 186-foot zone is 600 ft²/d. The model-estimated hydraulic head of the 133-foot zone is 0.82 feet higher than that of the 186-foot zone. The 186-foot zone did not contribute any water to the pumped sample when pumped at 1 gallon per minute.

[Return to Exercise 6](#) ↑

[Return to where text linked to Exercise 6](#) ↑

Solution Exercise 7

Data for this exercise, is provided in a spreadsheet within a [zip file that can be downloaded from the web page for this book](#)[↗]. The zip file is named *Geophysical-Logging-for-Hydrogeology-Exercise_Spreadsheets.zip*.

The solution is provided in the spreadsheet named

GPloggingExercise7_GammaCore_Solution.xlsx

in the worksheet named

[Answer-Plot&DepthAdj&Regression].

Part 1: Plot the Data

You should have graphed the two logs and seen a depth discrepancy. The depth of interest is from 1,060 to 1,100 ft (323.1 to 335.3 m), so only that section of the log needs to be plotted.

Part 2: Perform a Depth Matching

In this part of Exercise 7, you had to estimate the depth discrepancy and correct the depth of the core porosity. You could do this graphically or with a formula. Here we created a table with the original depth and the adjusted depth along with the porosity and gamma data and use a variable so that we can do a trial-and-error shift of the data. Once you determine the depth shift, you need to create a table with the shifted porosity data, so that porosity and gamma are paired so they can be plotted on the same graph on the same line to calculate the regression line.

Part 3: Plot Depth Adjusted Data and Perform Regression

Yes, we think this regression makes sense. The low gamma counts in a sandstone coincide with higher porosity; higher gamma counts in a sandstone coincide with low porosity.

[Return to Exercise 7](#)[↑]

[Return to where text linked to Exercise 7](#)[↑]

11 Notations

a	=	Ambient flow conditions
b	=	Pumping or injection flow conditions
CF	=	clay fraction
E	=	Standard error
G	=	Gamma value
G_1	=	Minimum gamma endpoint (clean)
G_2	=	Maximum gamma endpoint (clay)
k	=	Zone
m	=	Cementation factor (dimensionless)
N	=	Gamma count
N_0	=	Average gamma activity
\emptyset	=	Porosity
Q_k^0	=	Measured inflow for the zone k
Q_k^a	=	Measured inflow for zone k obtained under ambient flow condition a
Q_k^b	=	Measured inflow for zone k obtained under stressed flow condition b (pumping or injection)
$SQRT(N)$	=	Square root of N
T_k	=	Relative transmissivity for zone k
R_t	=	True formation resistivity typically in ohm-m ($ML^3T^{-3}A^{-2}$)
R_w	=	Formation water resistivity typically in ohm-m ($ML^3T^{-3}A^{-2}$)
V	=	Logging rate typically in meters per minute (LT^{-1})

12 About the Authors



John H. Williams is a groundwater and borehole-geophysical specialist with the USGS. He has a Bachelor of Arts in Geology from Colgate University, and a Master of Sciences in Geosciences from Pennsylvania State University. Since joining the USGS in 1980, John has applied borehole geophysical methods to a wide range of groundwater investigations in cooperation with the Environmental Protection Agency, Nuclear Regulatory Commission, Army Corp of Engineers, and state geological surveys and water agencies. His recent research focused on the application of borehole geophysics to the characterization of deep groundwater in the northern Appalachian shale-gas basin. He has taught regional and national courses on borehole geophysics for the USGS and its partners, and international workshops for government water agencies in the United Arab Emirates, Iraq, Kurdistan, and India.



Frederick L. Paillet is Adjunct Professor of Geosciences at the University of Arkansas and Emeritus Research Scientist with the USGS National Research Program (NRP). He received a Bachelor of Science in Mechanical and Aerospace Sciences from the University of Rochester in 1968, and then completed his Doctor of Philosophy in the same department specializing in Geophysical Fluid Dynamics in 1974. After two years as Hydrogeologist at Wright State University in Dayton, Ohio, he joined the USGS Water Resources Division NRP in Denver as a Geophysicist in 1978. At that time, he began a long-term project in the characterization of the hydrogeology of fractured crystalline rocks for applications in radioactive waste repository design and extraction of geothermal energy from fractured bedrock reservoirs. This included development of downhole acoustic imaging and borehole seismic methods.

After serving as Visiting Scientist at the Massachusetts Institute of Technology (MIT) Earth Resources Laboratory for the 1982–1983 academic year, he returned to become Chief of the USGS Borehole Geophysics Research Project. While directing a broad program of the application of well logging to ground water studies, his own research concentrated on the use of downhole hydraulic measurements to characterize multi-zone karst and bedrock aquifers using flowmeters and fluid-column logs without the need for cumbersome straddle-packer equipment. He also investigated methods to integrate surface and borehole geophysics, and to evaluate the effects of hydraulic fracture methods used to

augment water production from bedrock wells. These methods were tested at sites in North America, Europe, the Middle East, and Australia. This work resulted in the development of computer codes for the evaluation of borehole production tests, cross-borehole flowmeter experiments, and fluid column solute tracing methods. The codes have been made available as requested by numerous users of geophysical data.

Please consider signing up to the GW-Project mailing list to stay informed about new book releases, events, and ways to participate in the GW-Project. When you sign up to our email list, it helps us build a global groundwater community. [Sign up](#)[↗].



Modifications to Original Release

Changes from the Original Version to Version 2

Original Version: November 7, 2023, Version 2: November 8, 2023

Page numbers refer to the original PDF.

Page iii, corrected copyright page

Changes from Version 2 to Version 3

Version 2: November 8, 2023, Version 3: January 19, 2024

Page numbers refer to the Version 2 PDF.

page ii, added page requesting support of the Groundwater Project

page ii, now page iii, updated version number and date

page iii, now page iv, added "Any use of trade, firm, or product names is for descriptive purposes only and does not imply endorsement by the U.S. Government."